Characterisation of a 4-Amino-3-Hydroxybenzoate 2,3-Dioxygenase from *Bordetella* sp. 10d, a protein with cupin-fold

Masterarbeit

Zur Erlangung des akademischen Grades einer

„Diplomingenieurin“

Studienrichtung

Biotechnologie

an der

Technischen Universität Graz

Verfasserin

Claudia Pany, BSc

Betreuer

DI Dr Steiner

Univ.-Prof. DI Dr techn. Schwab

Graz, 2014

EIDESSTATTLICHE ERKLÄRUNG

Ich erkläre an Eides statt, dass ich die vorliegende Arbeit selbstständig verfasst, andere als die angegebenen Quellen/Hilfsmittel nicht benutzt, und die den benutzten Quellen wörtlich und inhaltlich entnommene Stellen als solche kenntlich gemacht habe.

....

Datum Unterschrift

STATUORY DECLARATION

I declare that I have authored this thesis independently, that I have not used other than the declared sources/resources, and that I have explicitly marked all material which has been quoted either literally or by content from the used sources.

....

date signature

ACKNOWLEDGMENT (DANKSAGUNG)

Mein besonderer Dank gilt Prof. Helmut Schwab, für die Aufnahme in seine Arbeitsgruppe, die Betreuung und die Begutachtung dieser Diplomarbeit sowie die wertvollen Hinweise und das Vertrauen in meine Arbeit.

Bei Frau Dr. Steiner bedanke ich mich für die Überprüfung der Sequenzen, designen der Primer sowie die Übernahme der Begutachtung dieser Diplomarbeit.

Ein weiterer Dank gilt PhD Ivan Hajnal, der mir bei inhaltlichen und methodischen Fragen immer mit Rat und Tat zur Seite stand.

Außerdem möchte ich mich bei Julia Midl für ihre Unterstützung bei der Herstellung von *E. coli* TOP10F' Zellen und der guten Zusammenarbeit bedanken.

Ebenso möchte ich mich bei den Arbeitskollegen im 4. Stock für die herzliche Aufnahme, die Hilfsbereitschaft und die angenehme Atmosphäre bedanken.

Des Weiteren danke ich meiner Familie und Freunden - besonders Angelika, Claudia, und Regina – für die Unterstützung und die Geduld.

KURZFASSUNG

Diese Diplomarbeit wurde im Rahmen eines Forschungsprojektes an der TU Graz durchgeführt. Das Ziel der Arbeit war es eine 4-Amino-3-Hydroxybenzoate 2,3-Dioxygenase (4A3HBA23DA) von *Bordetella* sp. 10d, ein Protein mit Cupin Faltung zu charakterisieren. Der Schwerpunkt lag einerseits auf der Charakterisierung des Cupin13 (4A3HBA23DA) und andererseits auf der Untersuchung von verschiedenen Cupin13 Varianten. Dafür, wurde das synthetische Cupin13 Gen in verschiedene Expressionsvektoren umkloniert. Darüber hinaus wurde das pET26-Cupin13 Konstrukt (Wildtyp), sowie die modifizierten Proteine mit Hilfe von biochemischen Techniken analysiert. Des Weiteren, wurde die Enzymaktivität des Wildtyps mit den veränderten Proteinvarianten verglichen. Zusätzlich wurden auch ganze intakte *E. coli* BL21-Gold (DE3) Zellen auf ihre Aktivität getestet.

Mutationen wurden in das vermutete aktive Zentrum (Cupin13-Q60A, -Q60F, -S62A, -S62Q, -R144I) sowie in die darin befindliche Metallbindestelle (Cupin13-H52A, -N54A, -E58A, -H97A) eingefügt. Das Cupin13-H52A Protein wurde durch die Mutation nicht mehr produziert. Des Weiteren, verfügen nur fünf der elf Enzymvarianten (Cupin13-Q60A, -Q60F, -S62A, -S62Q, -R144I) über eine nachweisbare Aktivität und davon wurden die drei besten Enzyme weiter getestet (Cupin13-Q60A, -S62A, -R144I). Es wurde nachgewiesen, dass Cupin13-S62A eine höhere Aktivität im Vergleich zum Wildtyp aufweist. Die maximale Enzymaktivität vom Cupin13 Protein (pET26-Cupin13 Konstrukt) wurde detektiert als es in Gegenwart von 100 µM Eisen (II) Sulfat exprimiert wurde.

ABSTRACT

This master thesis was part of a research project at the TU Graz. The major aim of this thesis was the characterisation of a 4-amino-3-hydroxybenzoate 2,3-dioxygenase (4A3HBA23DA) from *Bordetella* sp. 10d, a protein with a cupin fold. The main focus was on the one hand to characterise Cupin13 (4A3HBA23DA) and on the other hand to test several Cupin13 variants. For that, the purchased synthetic Cupin13 was recloned in various expression vectors. Furthermore, the pET26-Cupin13 construct (wild type) as well as the modified proteins were analysed by protein biochemical techniques. Additionally, the enzyme activity of the wild type was compared with the modified enzyme variants. Additionally, whole intact *E. coli* BL21-Gold (DE3) cells were tested on their activity.

Mutations were integrated in the presumed active site (Cupin13-Q60A, -Q60F, -S62A, -S62Q, -R144I) as well as in the putative metal binding site (Cupin13-H52A, -N54A, -E58A, -H97A). The Cupin13-H52A protein was not expressed due to the mutation. Furthermore, of eleven Cupin13 proteins containing mutations only five were active (Cupin13-Q60A, -Q60F, -S62A, -S62Q, -R144I). Thereof the best enzymes (Cupin13-Q60A, -S62A, -R144I) were tested, which resulted in a higher activity of the Cupin13-S62A (in the presence or absence of 100 µM $FeSO_4$) compared to the wild type. The maximal enzyme activity was detected for Cupin13 protein (pET26-Cupin13 construct), when it was expressed in the presence of 100 µM ferrous sulphate.

CONTENTS

FIGURES

SCHEMES

EQUATIONS

TABLES

ABBREVIATIONS

General	
1,2-GD	Gentisate 1,2-dioxygenase
2,3-HPCD	Homoprotocatechuate 2,3-dioxygenase
2,3-PCD	Protocatechuate 2,3-dioxygenase
3-HAD	3-Hydroxyanthranilate 3,4-dioxygenase
3,4-PCD	Protocatechuate 3,4-dioxygenase
4,5-PCD	Protocatechuate 4,5-dioxygenase
4A3HBA	4-Amino-3-hydroxybenzoic acid
4A3HBA23DA	4-Amino-3-hydroxybenzoate 2,3-dioxygenase
5-Hydroxy-trp	5-Hydroxy-tryptophan
Amp^R	Ampicillin resistance
BLAST	Basic local alignment search tool
C12O	Catechol 1,2-dioxygenase
C23O	Catechol 2,3-dioxygenase
cfu	Colony forming unit
conc.	Concentration
dATP	Deoxyadenosine triphosphate
dCTP	Deoxycytidine triphosphate
ddH_2O	Bi-distilled water
dGTP	Deoxyguanosine triphosphate
dHbm	ddH_2O-HEPES buffer mix
DMSO	Dimethyl sulfoxide
dNTP mix	Deoxynucleotide triphosphate mix
D-Trp	D-Tryptophan
DTT	1,4-Dithiothreitol
dTTP	Deoxythymidine triphosphate
EDTA	Ethylenediaminetetraacetic acid
EtBr	Ethidium bromide
EtOH abs.	Ethanol absolutely
g	Gram (weight) or gravitation (centrifugation)
h	Hours
HEPES	4-(2-Hydroxyethyl)-1-piperazineethanesulfonic acid

HGD	Homogentisate dioxygenase
His-tag	Histidine-tag
HMSA	2-Hydroxymuconic semialdehyde
HOD	1H-3-hydroxy-4-oxoquinaldine 2,4-dioxygenase
HQD	Hydroquinone dioxygenase
IDO	Indoleamine 2,3-dioxygenase
IDT	Integrated DNA Technologies
IPTG	Isopropyl-β-D-1-thiogalactopyranoside
Kan^R	Kanamycin resistance
kb	Kilobase pairs
k_{cat}	Turnover number
kDa	Kilodalton
K_m	Michaelis constant
L	Litre
LB-Agar/-Medium	Lysogeny Broth-Agar/-Medium
L-Trp	L-Tryptophan
MES	2-(N-morpholino)ethanesulfonic acid
min	Minutes
mL	Millilitre
mM	Millimolar
ms	Millisecond
N_2 gas	Nitrogen gas
NAD^+	Nicotinamide adenine dinucleotide
NCBI	National Center for Biotechnology Information
n.d.	Not determinable
Ni-agarose beads	Nickel agarose beads
ng	Nanogram
no.	Number
PCR	Polymerase Chain Reaction
pmol	Picomol
QOD	1H-3-hydroxy-4-oxoquinoline 2,4-dioxygenase
R^2	Coefficient of determination
s	Second
SBP-tag	Streptavidin-binding peptide-tag
SDS-PAGE	Sodium dodecyl sulphate polyacrylamide gel

	electrophoresis
SOC	Super optimal broth with catabolite repression
supern.	Supernatant
Syn	Synthetic
TAE-buffer	Tris-acetate-EDTA buffer
TCA	Tricarboxylic acid cycle
TDO	Tryptophan 2,3-dioxygenase
Trafo	Transformation
Tris	Tris(hydroxymethyl)aminomethane
U	Unit
V	Voltage
v_{max}	Maximum velocity
µg	Microgram
µL	Microlitre

1. INTRODUCTION

Soil contains different nutrients, carbon sources, aromatic compounds, aromatic amino acids, such as L-phenylalanine, L-tyrosine, and L-tryptophan, which are essential and utilised by bacteria [1]. In the environment the aromatic compounds exist as plant materials for example lignin or as pollutants from man-made sources like oils, paints, pesticides, detergents [1–3]. The latter are dangerous environmental contaminants respectively toxic for higher organisms [4]. Aromatics are chemically stable and can be defined as organic molecules that include one or more aromatic rings [5–9]. Furthermore, the aromatic compounds can be used as carbon and energy source and additionally, microorganisms such as the soil bacteria *Rhodococcus, Pseudomonas* or *Acinetobacter* possess the ability to degrade them under anaerobic as well as aerobic conditions [1,5–8,10]. Principally, microorganisms use different catabolic pathways to degrade each type of aromatic compounds [11]. The usual bacterial aromatic degradation process is oxidative and includes monooxygenase hydroxylation and dioxygenase reactions [1].

1.1 Dioxygenases

Dioxygenases are enzymes, which frequently require a metal cofactor such as iron(II) or iron(III) and possess the ability to cleave natural and synthetic aromatic compounds [12,13]. Moreover, different dioxygenases exist for example non-heme-, heme-, cofactor-independent and non-ring cleaving dioxygenases, which are all described in the following chapters 1.1.1–1.1.4.

1.1.1 Non-heme dioxygenases

The major class of dioxygenases are the non-heme dioxygenases, which can be divided, due to the cleavage site, in three classes [11,13].

1.1.1.1 Classes

Class I: intradiol dioxygenases (ring cleaving enzymes)

Class II: extradiol dioxygenases (ring cleaving enzymes)

- **Type 1:** vicinal oxygen chelate superfamily
- **Type 2:** enzymes consisting of one or two various subunits, superfamily unknown
- **Type 3:** cupin superfamily

Class III: dioxygenases (ring cleaving enzymes)

There are a few differences and interestingly, some similarities between the classes. For example, the first and second class require two hydroxyl-groups in ortho-orientation to each other and exists in catechol and protocatechuate [13]. The difference between these two classes is that intradiol dioxygenases utilise non-heme Fe(III) to oxidise the aromatic ring between the two hydroxyl-groups (ortho cleavage), whereas the extradiol dioxygenases use non-heme Fe(II) to cleave the aromatic ring next to one of the two hydroxyl-groups (meta cleavage) [4,11,13–16]. Another difference is that intradiol enzymes include a 2-His-2-Tyr metal-binding motif and extradiol enzymes contain a 2-His-1-carboxylate metal-binding motif [13,17,18]. The 2-His-1-carboxylate metal binding motif was not only detected in extradiol dioxygenases, but also in various types of enzymes, which bind Fe(II) [19].

However, there are a few extradiol dioxygenases, which do not require Fe(II), but need the presence of Mn(II) such as homoprotocatechuate 2,3-dioxygenase of *Arthrobacter globiformis*, Ni(II) (acireductone dioxygenase) or Cu(II) (quercetin 2,3-dioxygenase of *Aspergillus* [1,11,20–23].

In addition, the class II includes three types, which represent three evolutionarily independent families [11].

The first type of extradiol dioxygenases belongs to the vicinal oxygen chelate superfamily and contains two copies of a module comprising of four β strands as well as one α helix (with the sequence βαβββ) [10,11]. Members of this superfamily can be subdivided in a non-dioxygenase- and dioxygenase-group [24]. The isomerase e.g. glyoxalase I and the methylmalonyl-CoA epimerase belong to the non-dioxygenase group [11,24]. The 2,3-dihydroxybiphenyl 1,2-dioxygenase, catechol 2,3-dioxygenase and homoprotocatechuate 2,3-dioxygenase are members of the dioxygenase group [23].

The second type of extradiol dioxygenases includes enzymes, which are all multimers and comprise of one or two different subunit types (e.g. 2,3-dihydroxyphenylpropionate 1,2-dioxygenase) [11].

The third type of extradiol dioxygenase (e.g. gentisate 1,2-dioxygenase, salicylate 1,2-dioxygenase and 3-hydroxyanthranilate dioxygenase) belongs to the cupin superfamily [11,13,25]. Members of the cupin superfamily have very low levels of sequence identity, a highly conserved structure and comprise proteins, which bind various sugars [25,26]. Moreover, this family has both enzymatic- and non-enzymatic members [27]. For example the stress-related proteins, the transcription regulators and the plant seed storage proteins belong to the non-enzymatic proteins, while the dioxygenases (e.g. 4-

amino-3-hydroxybenzoate 2,3-dioxygenase, gentisate 1,2-dioxygenase, 3-hydroxyanthranilate 3,4-dioxygenase) are enzymatic proteins [10,25,27].

The members of the cupin superfamily can be divided into single domain (monocupin), a two-domain (bicupin) or a multi-domain (multicupin) structure(s), depending on the number of cupin domains in their structure [26,28,29]. Monocupins occur in the majority of cupin proteins and are either monomeric (e.g. phosphomannose isomerases and dioxygenases), dimeric (e.g. auxin-binding proteins) or oligomeric (e.g. germin and germin-like proteins, present in plants) [29,30].

Bicupins contain two domains (e.g. seed storage proteins of higher plants), that are structurally similar, but the similarity of the sequence can be very low [25,29].

There are some proteins, which have multiple copies (>2) of cupin domains for example an *Arabidopsis* protein, that contains four 2-oxoglutarate-Fe(II) domains [31].

Cupins were found in archaea, bacteria as well as in eukaryotes [10,29]. A β-barrel fold is named “cupin” (due to the Latin term for small barrel), which was detected in the members of this superfamily [10,13,26,28].

Cupin domains comprise two highly conserved sequence motifs and each include two β-strands [11,13,28]. Motif 1 is composed of $G(X)_5$**H**X**H**$(X)_{3,4}$**E**$(X)_6G$, while motif 2 includes $G(X)_5PXG(X)_2$**H**$(X)_3N$ and both motifs are separated with a variable intermotif sequence (less conserved loop) ranging from 11 residues in several bacterial enzymes up to more than 50 residues in some storage proteins [10,11,25,26,30]. X is any amino acid and the important residues in the metal’s first coordination shell are emphasised in bold and yellow [32]. The residues (two histidines and one glutamate) in motif 1, together with the residue (conserved histidine) in motif 2, work as ligands for the binding of a divalent metal ion (form one functional metal-binding site) [10,13]. This metal-binding site was detected in several cupin structures, such as oxalate decarboxylase, acireductone dioxygenase, germin and flavonol 2,4-dioxygenases [13]. However, there are some cupin subfamilies, which do not possess all four conserved metal-binding residues [10]. For example the glutamate residue in motif 1 is surrogated by a cysteine in mammalian cysteine dioxygenases and by a glycine in bacterial thiol dioxygenases [10,33,34].

Another difference in the classes concerns the position of the hydroxyl-groups [11]. Class I as well as class II (both are ring cleaving enzymes) need two hydroxyl-groups at the ortho-position to each other for example catechol and protocatechuate [11]. While class III use two hydroxyl groups in para-orientation (for example in the intermediates gentisate and hydroquinone (1,4-dihydroxy-benzene) [13,15,35].

However, there are a few enzymes (also belonging to class III), which possess the ability to cleave aromatic compounds with a single hydroxyl-group in ortho-position by the side of a carboxylate residue, for example in 5-nitrosalicylate, salicylate and 1-hydroxy-2-naphthoate [13,14]. Moreover, the enzymes in both classes (II and III) possess catalytically active Fe(II) ions in their active centres [13].

1.1.1.2 Intermediates

Catechol (1,2-dihydroxybenzene; can be used in synthetic flavours) belongs to the intermediates in aerobic catabolism of aromatic compounds and is one of four "major intermediates" [11,36,37]. The other three ones are protocatechuate, gentisate and hydroquinone [4,11,15]. Additionally, other intermediates for the ring cleavage reaction exist, such as homoprotocatechuate and homogentisate [11].

1.1.1.2.1 Catechol

The key step of degradation is the cleavage of the catecholic structure via catechol dioxygenases [12,38]. These enzymes require molecular oxygen for the catalysis of the aromatic ring, therefore a suitable concentration of oxygen has to be present [38]. Two types of oxidative-ring cleavage can be identified [1]. Catechol can be cleaved either in the ortho-cleavage pathway (intradiol dioxygenase) or meta cleavage pathway (extradiol dioxygenase) [1]. The ortho-cleavage pathway includes a catechol 1,2-dioxygenase (C12O, intradiol dioxygenase), which catalyses the cleavage of catechol and forms cis,cis-muconic acid, which consequently is cyclised to muconolactone; this reaction is followed by an isomerisation and ring opening, which results in the formation of β-ketoadipate [1,4,11,39].

In contrast, the meta-cleavage pathway contains a catechol 2,3-dioxygenase (C23O, extradiol dioxygenase), that cleaves catechol to produce 2-hydroxymuconaldehyde [1,11,12,39,40]. The final products of both pathways can enter the tricarboxylic acid cycle [41,42].

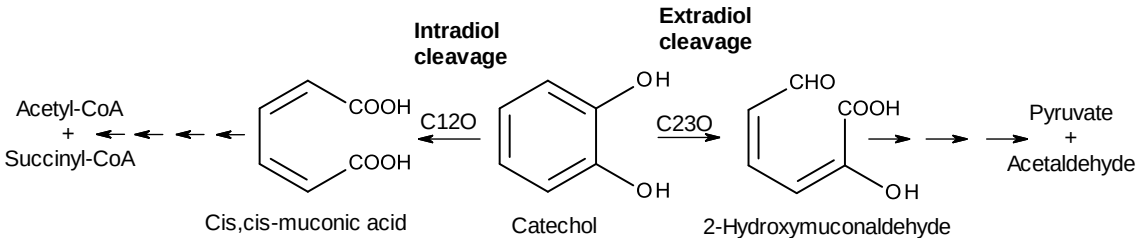

Scheme 1: Catechol conversion
Catechol can be converted by the enzyme catechol 1,2-dioxygenase (C12O) into cis,cis-muconic acid and by the catechol 2,3-dioxygenase (C23O) into 2-hydroxymuconaldehyde. This Scheme was created by using the program Accelrys Draw 4.1.

1.1.1.2.2 Protocatechuate

Another “major intermediate” is protocatechuate, which exists e.g. in the degradation of aromatic compounds, hydroxybenzoates, vanillyl alcohols and of the plant biopolymer lignin [11,43]. Protocatechuate can be cleaved either through intradiol cleavage (protocatechuate 3,4-dioxygenase) or extradiol cleavage (protocatechuate 4,5-dioxygenase as well as protocatechuate 2,3-dioxygenase) [4,11,12,43,44].

The degradation pathway of protocatechuate can be performed by a protocatechuate 3,4-dioxygenase (3,4-PCD, ortho-cleavage) to produce 3-carboxy-cis,cis-muconate. This product is converted via 3-carboxy-cis,cis-muconate cycloisomerase into 4-carboxymuconolactone [4,12,45]. Afterwards, it is cleaved by 4-carboxymuconolactone decarboxylase into β-ketoadipate enol-lactone [45]. Subsequently, this chemical compound is hydrolysed by a β-ketoadipate enol-lactone hydrolase into β-ketoadipate, as a consequence, this is converted by a β-ketoadipate succinyl-CoA transferase into β-ketoadipyl-CoA, which is finally cleaved by a β-ketoadipyl-CoA thiolase to produce succinyl-CoA and acetyl-CoA [45].

In contrast to protocatechuate 3,4-cleavage pathway, protocatechuate is converted by protocatechuate 4,5-dioxygenase (4,5-PCD) to 4-carboxy-2-hydroxymuconate-6-semialdehyde, then non-enzymatically transformed into an intramolecular hemiacetal and afterwards, it is oxidised (via 4-carboxy-2-hydroxymuconate-6-semialdehyde dehydrogenase) to 2-pyrone-4,6-dicarboxylate [46]. This product is hydrolysed (by 2-pyrone-4,6-dicarboxylate hydrolase) to obtain the keto and enol form of 4-oxalomesaconate (both are in equilibrium) [46]. The compound 4-oxalomesaconate is transformed (via 4-oxalomesaconate hydratase) into 4-carboxy-4-hydroxy-2-oxoadipate [46]. At the end, 4-carboxy-4-hydroxy-2-oxoadipate is cleaved (by 4-carboxy-4-hydroxy-2-oxoadipate aldolase) to receive pyruvate and oxaloacetate [46].

The protocatechuate 2,3-cleavage pathway proceeds via protocatechuate 2,3-dioxygenase (2,3-PCD) [47]. Protocatechuate is cleaved via 2,3-PCD to produce 5-carboxy-2-hydroxymuconate-6-semialdehyde [47]. The 5-carboxy-2-hydroxymuconate-6-semialdehyde is then decarboxylated to 2-hydroxymuconate-6-semialdehyde, which is ultimately converted to acetaldehyde and pyruvate [47].

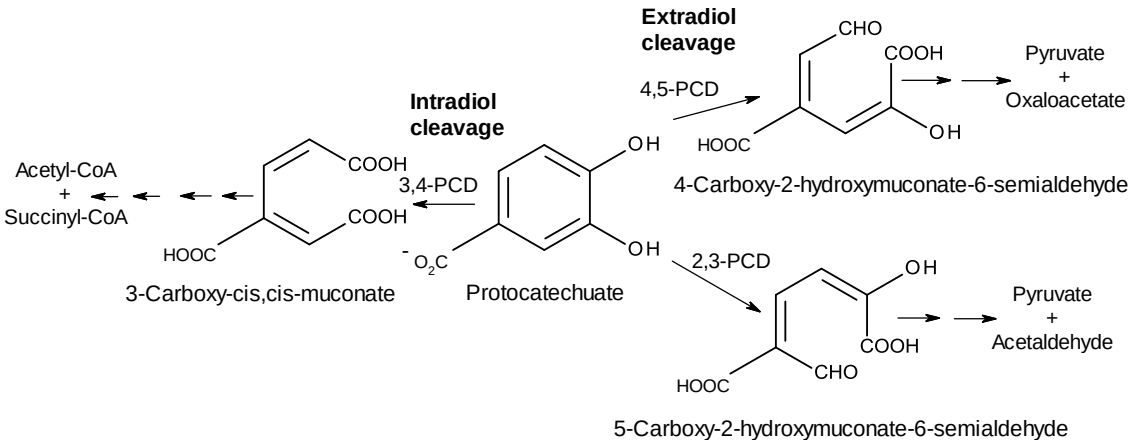

Scheme 2: Cleavage of protocatechuate
Protocatechuate can be converted via intradiol cleavage (protocatechuate 3,4-dioxygenase, 3,4-PCD) or extradiol cleavage (protocatechuate 4,5-dioxygenase, 4,5-PCD or protocatechuate 2,3-dioxygenase, 2,3-PCD). This Scheme was created by using the program Accelrys Draw 4.1.

1.1.1.2.3 Gentisate

Gentisate (2,5-dihydroxybenzoate) is one of the “major intermediates” and is produced during the catabolism of various phenolic compounds, like 3-hydroxybenzoate, salicylate, m-cresol or polycyclic aromatic hydrocarbons such as naphthalene and phenanthrene [10,43]. Gentisate 1,2-dioxygenases (1,2-GD, extradiol cleavage type) belong to the cupin family (is a bicupin) and possess the same ability such as salicylate 1,2-dioxygenase and 1-hydroxy-2-naphthoate dioxygenase to cleave their substrates between the adjacent carbon atoms, carrying a carboxylate and a hydroxyl substituent [10,13,15].

The gentisate pathway proceeds via a gentisate 1,2-dioxygenase, which converts gentisate to maleylpyruvate [43,45,48,49]. Afterwards, this product is then isomerised (by glutathione-dependent maleylpyruvate isomerase) to fumarylpyruvate and subsequently, it is hydrolysed (via fumarylpyruvate hydrolysed) to fumarate and pyruvate, which are intermediates of the tricarboxylic acid cycle [43,45,49].

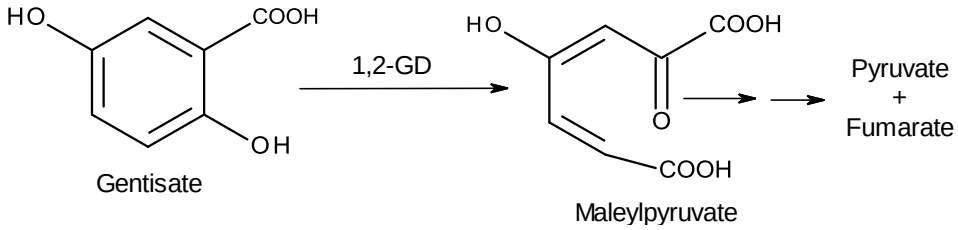

Scheme 3: Cleavage of gentisate
Gentisate is converted by gentisate 1,2-dioxygenase (1,2-GD) to maleylpyruvate [43,45,49]. This Scheme was created by using the program Accelrys Draw 4.1.

1.1.1.2.4 Hydroquinone

The last "major" intermediate is hydroquinone, which is produced in the degradation process of e.g. the following compounds 4-aminophenol, 4-hydroxyacetophenone, 4-nitrophenol and γ-hexachlorocyclohexane [50]. Hydroquinone dioxygenases (HQD, extradiol cleavage type) belong to the non-heme containing Fe(II)-dependent dioxygenases [51]. The hydroquinone is cleaved by a hydroquinone dioxygenase (extradiol-cleavage type) to produce γ-hydroxymuconic semialdehyde [52]. This product is oxidised to maleyl acetic acid and afterwards reduced to β-ketoadipic acid [52].

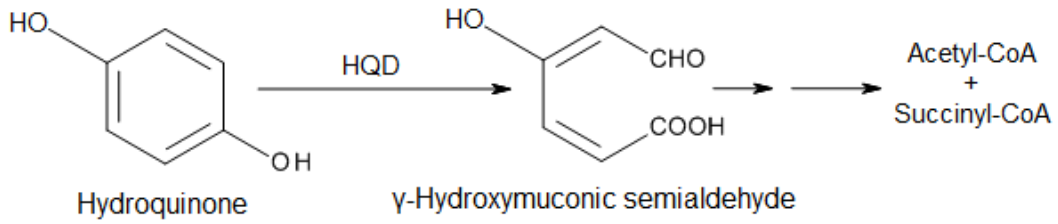

Scheme 4: Cleavage of hydroquinone
Hydroquinone is converted by hydroquinone dioxygenase (HQD) to γ-hydroxymuconic semialdehyde. This Scheme was created by using the program Accelrys Draw 4.1.

Other important intermediates for ring-cleavage reactions are homoprotocatechuate and homogentisate.

1.1.1.2.5 Homoprotocatechuate

Homoprotocatechuate 2,3-dioxygenases (2,3-HPCD, extradiol cleavage type) transform the aromatic ring of homoprotocatechuate (3,4-dihydroxyphenyl acetate) and produce muconic semialdehyde [3,53]. Additionally, these enzymes have Fe(II) ions and rarely Mn(II) ions in the centre of the active site [53].

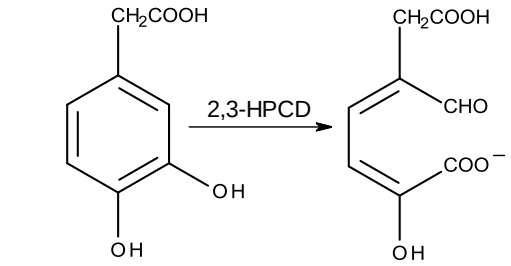

Homoprotocatechuate Muconic semialdehyde

Scheme 5: Homoprotocatechuate conversion
Homoprotocatechuate is cleaved by homoprotocatechuate 2,3-dioxygenase to produce muconic semialdehyde. This Scheme was created by using the program Accelrys Draw 4.1.

1.1.1.2.6 Homogentisate

Homogentisate exists in the catabolism of tyrosine and phenylalanine [11,43]. These amino acids are cleaved to 4-hydroxyphenylpyruvate and afterwards, converted into homogentisate via 4-hydroxyphenylpyruvate dioxygenase (non-heme Fe(II)-dependent) [43]. Homogentisate dioxygenase (HGD) is an extradiol dioxygenase and belongs to the cupin superfamily [1,11,43]. This enzyme cleaves the aromatic ring between the acetyl substituent and the proximal hydroxyl group [1,11,43]. The product is maleylacetoacetate, which is converted (via maleylacetoacetate isomerase) into fumarylacetoacetate [1,11,43]. Afterwards, this fumarylacetoacetate is hydrolysed (by fumarylacetoacetate hydrolase) to fumarate and acetoacetate [1,11,43].

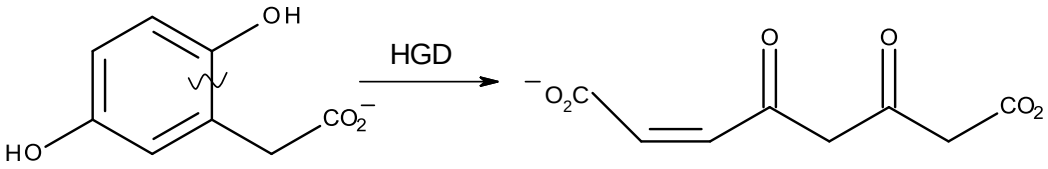

Homogentisate Maleylacetocacetate

Scheme 6: Cleavage of homogentisate
Homogentisate is converted by homogentisate dioxygenase (HGD) into maleylacetoacetate. This Scheme was created by using the program Accelrys Draw 4.1.

Less dioxygenases possess the ability to cleave aromatic compounds with a single hydroxyl group such as salicylic acid, 2-aminophenol, 3-hydroxyanthranilic acid and 4-amino-3-hydroxybenzoic acid (4A3HBA) [54].

1.1.1.3 2-Aminophenol 1,6-dioxygenase

The most dioxygenases cleave aromatic compounds with two hydroxyl groups in the benzene ring. However, there are a few dioxygenases, which can cleave aromatic compounds with one hydroxyl group such as 2-aminophenol [55]. Bacteria use the 2-aminophenol (substrate) as carbon and nitrogen source for their growth [56]. The

benzene ring of 2-aminophenol is cleaved via 2-aminopehnol 1,6-dioxygenase (a heterotetramer) to 2-aminomuconic 6-semialdehyde [57]. This enzyme cleaves (with the cofactor Fe^{2+}) the ring of 2-aminophenol as well as its methyl- or chloro-derivatives, however, no carboxyl-group substituted 2-aminophenols [55,57]. The 2-aminomuconic 6-semialdehyde can be converted either non-enzymatically or enzymatically. Due to the instable substrate, the first possibility is a non-enzymatically conversion to picolinic acid in vitro [45,56,58]. The second opportunity contains the enzymatically conversion of 2-aminomuconic 6-semialdehyde in the presence of NAD^+ via 2-aminomuconate 6-semialdehyde dehydrogenase to yield 2-aminomuconate [58].

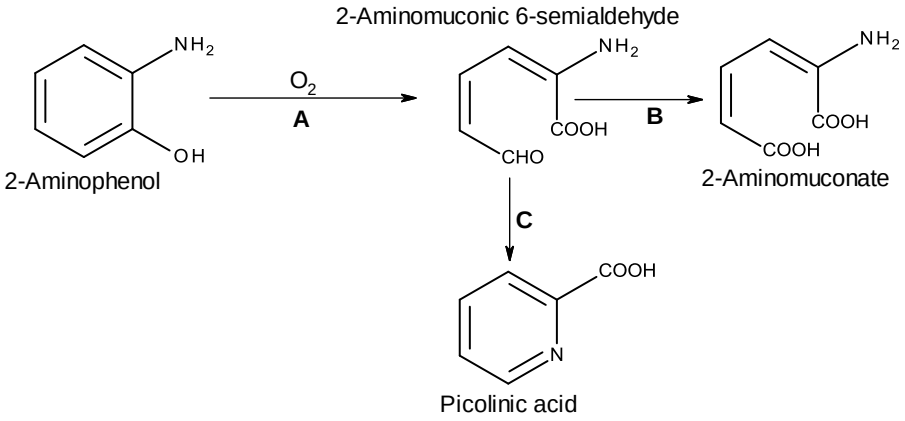

Scheme 7: Process of 2-aminophenol metabolism in Pseudomonas sp. strain AP-3
The benzene ring of 2-aminophenol is catalysed via **(A)** 2-aminophenol 1,6-dioxygenase in 2-aminomuconic 6-semialdehyde and afterwards by **(B)** 2-aminomuconate 6-semialdehyde dehydrogenase into 2-aminomuconate [56]. However, 2-aminomuconic 6-semialdehyde is instable and therefore converted **(C)** non enzymatically to picolinic acid in vitro or enzymatically via **(B)** 2-aminomuconate 6-semialdehyde dehydrogenase into 2-aminomuconate [56,59]. This Scheme was created by using the program Accelrys Draw 4.1.

1.1.1.4 3-Hydroxyanthranilate 3,4-dioxygenase

The 3-hydroxyanthranilate 3,4-dioxygenase (3-HAD) belongs to the non-heme Fe(II) dependent extradiol dioxygenase of the cupin superfamily [59,60]. For example the 3-HAD (a homodimer) of *Ralstonia metallidurans* has iron binding residues, which contain two histidine- and one glutamate residue [59]. Another example is 3-HAD (a homodimer) of *Saccharomyces cerevisiae* [60]. This enzyme is a member of the cupin superfamily [60].

The 3-HAD possesses the ability to cleave the 3-hydroxyanthranilate (HAA), which results in a 2-amino-3-carboxymuconic semialdehyde [59].

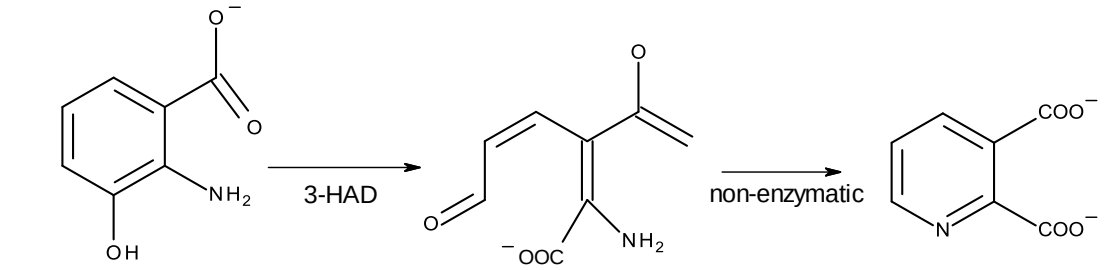

3-Hydroxyanthranilate 2-Amino-3-carboxymuconic semialdehyde Quinolinate

Scheme 8: Cleavage of 3-hydroxyanthranilate by 3-hydroxyanthranilate 3,4-dioxygenase The 3-hydroxyanthranilate is cleaved by 3-hydroxyanthranilate 3,4-dioxygenase (3-HAD) to 2-amino-3-carboxymuconic semialdehyde, which can be converted to quinolinate by a non-enzymatic reaction [59,60]. This Scheme was created by using the program Accelrys Draw 4.1.

1.1.1.5 4-Amino-3-hydroxybenzoate 2,3-dioxygenase

The last example of dioxygenases, which possesses the ability to cleave aromatic compounds with a single hydroxyl group, is the enzyme 4-amino-3-hydroxybenzoate 2,3-dioxygenase (4A3HBA23DA) [54]. This enzyme was produced of a soil bacterium *Bordetella* sp. 10d, which grew well in the basal medium with 4-amino-3-hydroxybenzoic acid (4A3HBA) and yeast extract [54,55,61]. *Bordetella* sp. 10d utilises the 4A3HBA as nitrogen, carbon and energy source [54,55,61]. The yeast extract supplies growth factors and vitamins [55]. The 4A3HBA23DA belongs to the meta-cleavage dioxygenases and cleaves the 4A3HBA between the C_2 and C_3 of the ring (while one mol of O_2 per mol of substrate was consumed) to produce the 2-amino-5-carboxymuconic 6-semialdehyde [54,55,61]. Furthermore, the 4A3HBA23DA (is a homodimer with a subunit size of 21 kDa) only uses the 4A3HBA as substrate [55]. This enzyme completely inhibited by the addition of 1 mM $HgCl_2$, 1 mM $ZnSO_4$, 1 mM $CuSO_4$, 1 mM $CoCl_2$ while 1 mM $FeSO_4$ as well as 1 mM $Fe(NH_4)_2(SO_4)_2$ slightly increased the activity which indicated that this enzyme needs Fe^{2+} [55,56].

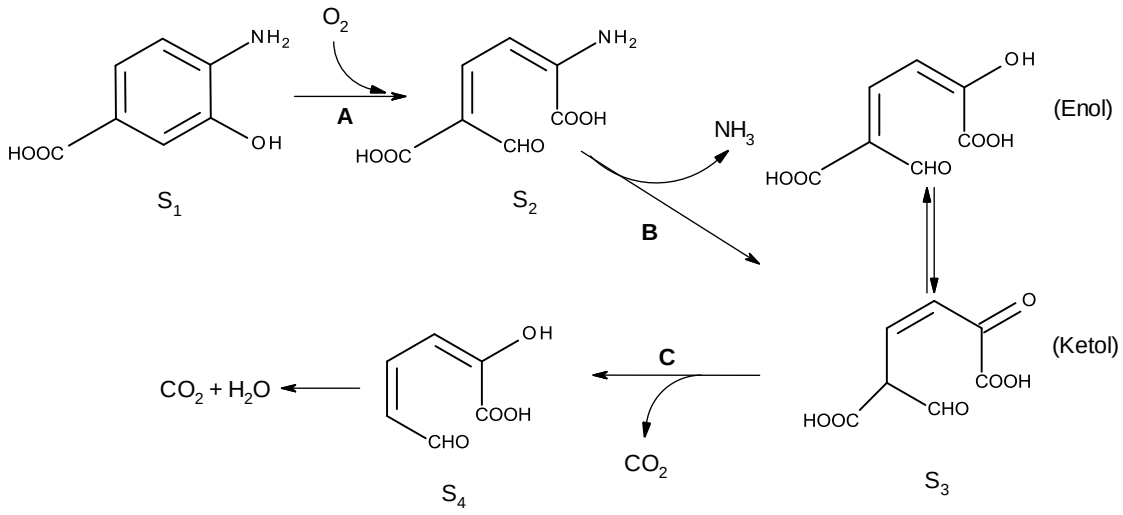

Scheme 9: Process of 4-amino-3-hydroxybenzoic acid degradation in *Bordetella* sp. strain 10d
4-Amino-3-hydroxybenzoic acid (S_1) is cleaved by **(A)** 4-amino-3-hydroxybenzoate 2,3-dioxygenase to produce 2-amino-5-carboxymuconic 6-semialdehyde (S_2) in *Bordetella* sp. strain 10d. Afterwards, this intermediate is deaminated via **(B)** 2-amino-5-carboxymuconic 6-semialdehyde deaminase to 2-hydroxy-5-carboxymuconic 6-semialdehyde (S_3). Subsequently, this intermediate is converted by a **(C)** non-enzymatic decarboxylation step to 2-hydroxymuconic 6-semialdehyde (S_4) [56,61]. This Scheme was created by using the program Accelrys Draw 4.1.

Up to this point, different non-heme dioxygenases were described, but there are also some dioxygenases, which need a heme or do not require a cofactor or do not cleave benzene.

1.1.2 Heme-containing dioxygenases

Indoleamine 2,3-dioxygenase (IDO) and tryptophan 2,3-dioxygenase (TDO) are heme-containing enzymes [62]. These dioxygenases possess the ability to cleave the pyrrole ring of L-tryptophan (L-Trp) and add both oxygen atoms of a dioxygen molecule to produce *N*-formylkynurenine [62,63]. The oxidative cleavage of Trp is the first and a rate-limiting step in L-Trp catabolism through the kynurenine pathway [62,63]. The IDO belongs to the monomeric enzymes and had a broader substrate specificity (e.g. L-Trp, D-Trp, 5-hydroxy-Trp, tryptamine and serotonin) than TDO, which is a tetramer with a heme cofactor bound at each active site and is highly specific for L-tryptophan [62,64–68].

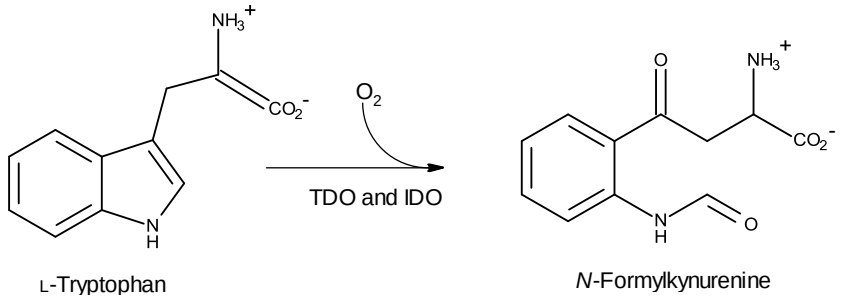

Scheme 10: Oxidation of L-tryptophan by TDO and IDO to *N*-formylkynurenine
The TDO as well as the IDO cleave the pyrrole ring of L-tryptophan and add both oxygen atoms of a dioxygen molecule into the L-tryptophan to produce *N*-formylkynurenine [62,63]. This Scheme was created by using the program Accelrys Draw 4.1.

1.1.3 Cofactor-independent dioxygenases

The majority of dioxygenases use a metal cofactor to assist oxygen activation, but there are a few enzymes that do not require neither metal ion nor organic cofactor [12]. Epoxyquinone dioxygenase is an enzyme that does not need metal ion or organic redox cofactor and converts 2,5-dihydroxyacetanilide to epoxyquinone [12].
Other dioxygenases such as 1H-3-hydroxy-4-oxoquinoline 2,4-dioxygenase (QOD) and 1H-3-hydroxy-4-oxoquinaldine 2,4-dioxygenase (HOD) require neither metal ion nor an organic cofactor [1,12]. These two enzymes belong to the αβ-hydrolase superfamily and include a Ser-His-Asp triad [1,12].

The majority of dioxygenases possess the ability to cleave the benzene ring, but there are also some existing, which do not cleave it and they are listed in 1.1.4.

1.1.4 Non-ring cleaving dioxygenases

For example lipoxygenase belongs to the family of dioxygenases and is a non-heme iron-dependent dioxygenase, which cleaves the polyunsaturated fatty acids into lipid hydroperoxides [12]. The enzyme detected in plants as well as in animals, can convert the linoleic acid (substrate in plants) in lipid hydroperoxides and arachidonic acid (substrate in mammals) into leukotriene (family of physiological regulators) [12].
Another example is the beta-carotene dioxygenase (non-heme iron-dependent dioxygenase), which belongs to the carotenoid cleavage dioxygenase family and is responsible for biosynthesis of the retina in mammals [1,17].
The 9-cis-epoxycarotenoid dioxygenase (a member of the carotenoid cleavage dioxygenase family) possesses the ability to catalyse the oxidative cleavage of epoxy-

carotenoid 9-cis-neoxanthin and moreover, this is a key step in the biosynthesis of plant growth [1].

Another member of the carotenoid cleavage dioxygenase family is apocarotenoid 15,15'-dioxygenase from *Synechocystis* [17]. The non-heme iron(II) cofactor is bound via four histidine residues [1,17].

1.2 Aim of the master thesis

The aim of the thesis was on the one hand to characterise the wild type enzyme 4-amino-3-hydroxybenzoate 2,3-dioxygenase and on the other hand to test several Cupin13 muteins, which were produced by using site directed mutagenesis with polymerase chain reaction (PCR).

As a consequence, the focus was on the comparison of the wild type and modified proteins, which had mutations in the putative active site and therein presumed metal binding site. Furthermore, it was the objective to analyse the wild type and modified protein by sodium dodecyl sulphate polyacrylamide (SDS) gel electrophoresis and Bradford protein assay after recloning the synthetic gene of 4-amino-3-hydroxybenzoate 2,3-dioxygenase in selected expression vectors. Moreover, this study aimed on the improvement of the enzyme assay based on Takenaka et al. and the modification of this assay for a smaller reaction volume. Another objective of the thesis was to compare the enzyme activity of the wild type with the modified enzymes and additionally, whole intact *E. coli* BL21-Gold (DE3) cells were tested.

2. MATERIAL AND METHODS

2.1 Material

Table 1: Chemicals and reagents

Component	Manufacturer
1,4-Dithiothreitol	Carl Roth
4-Amino-3-hydroxybenzoic acid	Aldrich
Acetic acid	Carl Roth
Aqua bidest.	Fresenius Kabi
Bovine serum albumin acetylated stock (Exp 2/13)	Promega
Bradford 5x	Bio-Rad
Coomassie Brilliant Blue G250	Fluka
Copper(II)sulphate pentahydrate	Fluka
Dimethyl sulfoxide	Carl Roth
Disodium hydrogen phosphate	Carl Roth
Ethanol absolutely	E. Merck
EDTA buffer	Serva
Ferrous sulphate heptahydrate	E. Merck
Glucose-Monohydrate	Carl Roth
HEPES	Carl Roth
Hydrochloric acid	Carl Roth
Imidazole	Aldrich
Isopropyl-β-D-1-thiogalactopyranoside	Carl Roth
LB-Agar Lennox	Carl Roth
LB-Medium	Carl Roth
Magnesium chloride	E. Merck
Magnesium sulphate	Carl Roth
Nickel(II) sulphate hexahydrate	Carl Roth
Potassium chloride	Carl Roth
Sodium dihydrogen phosphate monohydrate	E. Merck
Sodium chloride	Carl Roth
Tris	Carl Roth

Tryptone/Peptone from casein	Carl Roth
Urea	Carl Roth
Yeast extract	Carl Roth

Table 2: dNTP mix

Component	Manufacturer
Deoxyadenosine triphosphate	Fermentas
Deoxycytidine triphosphate	Fermentas
Deoxyguanosine triphosphate	Fermentas
Deoxythymidine triphosphate	Fermentas

Table 3: Gelelectrophoresis

Component	Manufacturer
Agarose	Biozym
Ethidium bromide	Sigma
LDS sample buffer 4x NuPAGE	Invitrogen
Loading dye 6x	Fermentas
MES buffer 20x	Invitrogen
NuPAGE 4-12% Bis-Tris-Gel 1.00 mmx15well	Invitrogen
NuPAGE 4-12% Bis-Tris-Gel 1.00 mmx10well	Intvitrogen

Table 4: Standard marker

Component	Manufacturer
O'Gene Ruler 1 kb Plus DNA Ladder	Fermentas
Page Ruler^{TM} Prestained Protein Ladder	Fermentas

Table 5: Antibiotics

Component	Manufacturer
Ampicillin sodium salt	Carl Roth
Kanamycin sulphate	Carl Roth

Table 6: Enzymes

Component	Manufacturer
Benzonase	E. Merck
*Eco*RV or *Eco*32I	Fermentas
*Hind*III	Fermentas
Hot Star *Taq* Plus DNA Polymerase	Quiagen
Lysozyme from chicken egg white protein	Sigma-Aldrich
*Nco*I	Fermentas
*Nde*I	Fermentas
*Pag*I	Fermentas
Phusion DNA polymerase	Finnzyme
T4 DNA ligase	Promega

Table 7: Primers
Oligonucleotides were designed by Dr. Steiner and manufactured by "Integrated DNA Technologies" (IDT) company.

Name	Nucleotide sequence 5' → 3'
SynCupin13_fw	AATCATCATGATCATCCTGGAAAACTTCAAAATCG
SynCupin13_rev	AATCAAAGCTTTTAATCGCGACCCGGTG
Cupin13-H52A_fw	CGTGAATATCGTAGCGAATTTGCAATTAACGCCAGCTATGAAATC
Cupin13-H52A_rev	GATTTCATAGCTGGCGTTAATTGCAAATTCGCTACGATATTCACG
Cupin13-N54A_fw	CGTAGCGAATTTCATATTGCAGCCAGCTATGAAATCCAG
Cupin13-N54A_rev	CTGGATTTCATAGCTGGCTGCAATATGAAATTCGCTACG
Cupin13-E58A_fw	CATATTAACGCCAGCTATGCAATCCAGTATAGCCTGAAAG
Cupin13-E58A_rev	CTTTCAGGCTATACTGGATTGCATAGCTGGCGTTAATATG
Cupin13-H97A_fw	CTCCGTTTCTGCCGGCAAGTCCGCGTTTTG
Cupin13-H97A_rev	CAAAACGCGGACTTGCCGGCAGAAACGGAG
Cupin13-Q60A_fw	CGCCAGCTATGAAATCGCATATAGCCTGAAAGGTGC
Cupin13-Q60A_rev	GCACCTTTCAGGCTATATGCGATTTCATAGCTGGCG
Cupin13-Q60F_fw	CGCCAGCTATGAAATCTTTTATAGCCTGAAAGGTGC
Cupin13-Q60F_rev	GCACCTTTCAGGCTATAAAAGATTTCATAGCTGGCG

Cupin13-S62A_fw	CAGCTATGAAATCCAGTATGCACTGAAAGGTGCACAGGATC
Cupin13-S62A_rev	GATCCTGTGCACCTTTCAGTGCATACTGGATTTCATAGCTG
Cupin13-S62Q_fw	CAGCTATGAAATCCAGTATCAGCTGAAAGGTGCACAGGATC
Cupin13-S62Q_rev	GATCCTGTGCACCTTTCAGCTGATACTGGATTTCATAGCTG
Cupin13-F101A_fw	CATAGTCCGCGTGCAGCACCGGATAGC
Cupin13-F101A_rev	GCTATCCGGTGCTGCACGCGGACTATG
Cupin13-F101R_fw	CATAGTCCGCGTCGTGCACCGGATAG
Cupin13-F101R_rev	CTATCCGGTGCACGACGCGGACTATG
Cupin13-R144I_fw	CTTCTATGTGGACGATTATATCAAAGATCCGGTTAGCCGTG
Cupin13-R144I_rev	CACGGCTAACCGGATCTTTGATATAATCGTCCACATAGAAG

Table 8: Plasmids and bacterial strains

Component	Resistance	Manufacturer
Escherichia coli BL21-Gold (DE3)		Agilent Technologies
Escherichia coli TOP10F'		Invitrogen
pEHISTEV	Kan^R	[69]
pESBPTEV	Kan^R	in house
pET26b	Kan^R	Novagen
pET28a	Kan^R	Novagen
pMA_Cupin13	Amp^R	Geneart/Life technologies
pMS470Δ8	Amp^R	[70]
pUC19 DNA [10 pg/µL]	Amp^R	Invitrogen

Table 9: Kit's

Name	Manufacturer
Gene JET™ Plasmid Miniprep	Fermentas
Wizard® SV Gel and PCR Clean-Up System	Promega

Table 10: Equipment

Instrument/Disposable	Manufacturer
Balance	Kern&Sohn
Biofuge pico	Heraeus
Bunsen burner Labogaz 206	Campingaz
Centrifuge 5810R	Eppendorf
Centrifuge Biofuge pico	Heraeus
Centrifuge Avanti J-20XP	Beckmann Coulter™
Cuvette Polystyrene 10x4x45 mm	Greiner bio-one
DU 800 Spectrophotometer	Beckmann Coulter™
Electrophoreses Xcell SureLock ™	Invitrogen
Electrophoreses PowerPac Basic Powersupply	Bio-Rad
Electroporation cuvettes 50x2 mm	Cellprojects
Electroporation Micro Pulser	Bio-Rad
Reaction tubes (1.5, 15, 50 mL)	Greiner bio-one
G: Box HR16	Syngene
Incubator	Binder
Laminar EN12469	Clean Air
Membrane filter 0.025 µm	Merck Millipore
Mini twist	Select bio products
Multichannel pipettes Proline 50-1200 µL	Biohit
Nalgene Cryoware Cryogenic Vials	Thermo Scientific
Nanodrop 2000c Spectrophotometer	Thermo Scientific
Pasteur pipette 230 mm	Carl Roth
PCR 2720 Thermal Cycler	Applied Biosystems
PCR tubes 0.2 mL thin walls	Greiner bio-one
PCR tubes strips 0.2 mL with domed cap strips	Peqlab
PD-10 column	GE-Healthcare
Petri dishes	Greiner bio-one
PH-Probe MR3001K	Heidolph
Pipette 3000i™ (10, 20, 200, 1000 µL)	Denville
Pipette (5, 10, 25 mL)	Greiner bio-one
Pipette tips (10, 20, 200, 1000 µL)	Greiner bio-one
Plate reader SynergyMx	BioTek

Precision balance	Sartorius
Quartz cuvettes Suprasil	Hellma
Shaker Certomat® BS-1	Sartorius
Shaker Titramax 1000	Heidolph
Sterile filter 0.45 µm	Whatman
Syringe 20 mL	B. Braun Melsungen
Thermomixer comfort	Eppendorf
Toothpicks	Rauch
Ultrasonic Branson Sonifier 250	Inula
UV-Star Microplate 96-well, F-bottom	Greiner bio-one
Vivaspin	Sartorius
Vortexer Genie2	Scientific Industries

Table 11: Medium and buffer composition

Medium/Buffer	Components	Conc./Volume
0.1 M $NaPO_4$ buffer pH 7.5	$NaH_2PO_4 * H_2O$	0.1 M
	Na_2HPO_4	0.1 M
Sigma-Aldrich Company offers a table for various buffer combinations, which was used for the calculation of the $NaPO_4$ buffer at pH 7.5.		
2x TY medium	Tryptone	16 g
	Yeast extract	10 g
	NaCl	5 g
	ddH_2O	filled up to 1 L
10 % Glycerol	Glycerol	100 g
	ddH_2O	fill up to 1 L
x mM imidazole		
The various concentrations of imidazole were calculated by the mathematical method “Mischkreuz or called Andreaskreuz” for HisTEV-Cupin13 protein purification.		
Buffer A pH 7.4	$NaPO_4$ buffer	20 mM
	NaCl	500 mM
	Imidazole	10 mM

Buffer B pH 7.4	$NaPO_4$ buffer	20 mM
	NaCl	500 mM
	Imidazole	500 mM
Destaining solution	Acetic acid	75 mL
	EtOH absolute	200 mL
	ddH_2O	fill up to 1 L
HEPES buffer with NaCl pH 7.0	HEPES	50 mM
	NaCl	154 mM
MES buffer	MES buffer 20x	50 mL
	ddH_2O	950 mL
SOC medium	Tryptone/Peptone	
	from casein	20 g
	NaCl	0.58 g
	Yeast extract	5 g
	$MgCl_2$	2 g
	KCl	0.18 g
	$MgSO_4$	2.46 g
	Glucose monohydrate	3.46 g
	ddH_2O	1 L
Tris/HCl pH 7.5	Tris	50 mM
	ddH_2O	900 mL
	The pH was adjusted with HCl.	

2.2 Molecular biological methods

The main objective of the master thesis is to characterise the 4-amino-3-hydroxybenzoate 2,3-dioxygenase, which was called Cupin13. A synthetic gene was ordered from Generart/Life Technologies Company and amplified for recloning. Therefore, the synthetic gene was on the one hand used as template for the PCR technique and on the other hand excised from plasmids. The Cupin13 and the respective expression vector were cleaved by restriction enzymes and afterwards, they were ligated by using the T4 DNA ligase. This product was desalted for the transformation in electrocompetent *E. coli* TOP10F' cells and streaked out on LB-agar-plates, which were supplemented with antibiotics. Selected colonies were transferred on another LB-agar-plate with ampicillin or kanamycin. The colonies were screened with the colony PCR technique, if the LB-agar-plate with the vector control had fewer colonies than the LB-agar-plates with the selected ligation ratios of 1:2 and 1:3. However, if no colonies existed on the LB-agar-control-plate, colonies from the LB-agar-plates with 1:3 and 1:2 ligation ratio were chosen and streaked out on a new LB-agar plate for plasmid isolation. The recombinant plasmids were isolated from the *E. coli* TOP10F' cells and as control, these plasmids were digested and subsequently, analysed on an agarose gel. The DNA was sent for sequencing to the LGC genomics Company, and the obtained results were controlled by Dr. Steiner. Moreover, the recombinant plasmids were transferred in electrocompetent *E. coli* BL21-Gold (DE3) cells and thereof, cryo cultures were produced as well as from *E. coli* TOP10F' with recombinant plasmids. The cultures were kept at -20 °C until subsequent use.

2.2.1 PCR and colony PCR

The Cupin13 gene (from the purchased synthetic Cupin13_pMA plasmid) was amplified by polymerase chain reaction (PCR) to get sufficient amounts for the recloning in various expression vectors. Fifty microlitres of PCR mixture contained the following components (Table 12) and were transferred in 0.2 mL thin wall PCR tubes. Ten millimolar dNTP mix consisted of 20 µL of each 100 mM dNTPs and 120 µL ddH_2O.

Table 12: PCR pipetting scheme

Component/Concentration	Stock solution	Volume [µL]
ddH_2O	---	35.5
HF-buffer 5x	---	10.0
dNTPs	10 mM	1.0
SynCupin13_for	10 pmol/µL	1.0
SynCupin13_rev	10 pmol/µL	1.0
Template syn pMA_Cupin13	50 ng/µL	1.0
Phusion DNA Polymerase	2 U/µL	0.5
Total reaction volume		**50.0**

The setting for the PCR was at 98 °C for 5 min for denaturation, afterwards 30 cycles with 95 °C for 30 s for denaturation of the double stranded DNA, 55 °C for 30 s for the annealing of the oligonucleotides, and 72 °C for 60 s for elongation by the Phusion DNA Polymerase. At the end of the 30 cycles the PCR tube was incubated at 72 °C for 7 min (final extension), to ensure that any remaining singe-stranded DNA is fully extended and finally kept on 4 °C.

Colony PCR

The colony PCR technique is an accurate and fast screening method for plasmids to ensure that the desired insert was integrated in the selected plasmid. Ingredients (Table 13) for one sample were pipetted in a 0.2 mL PCR tube stripe with domed cap strips. Additionally, an *E. coli* colony as template was picked with a sterile toothpick from the transformation LB-agar-plate and added in the 0.2 mL PCR tube. A mastermix was prepared for the screening of more colonies and therefore the ingredients were calculated with the number of colonies.

Table 13: Colony PCR pipetting scheme

Component/Concentration	Stock solution	Volume [µL]
Template	---	---
SynCupin13_fw	10 pmol/µL	0.5
SynCupin13_rev	10 pmol/µL	0.5
Hot Star *Taq* Plus DNA Polymerase	5 U/µL	0.125
dNTP mix	10 mM	0.5
PCR buffer 10x	---	2.5
ddH_2O	---	20.8
Total reaction volume		**25.0**

The following setting was used for the colony PCR:

95 °C, 5 min initial denaturation

94 °C, 30 s denaturation
55 °C, 30 s annealing
72 °C, 60 s elongation
} 30 cycles

72 °C, 10 min final extension

2.2.2 Agarose gel electrophoresis and DNA elution

The agarose gel electrophoresis is an effective method of separating DNA fragments by sizes. Due to the phosphate backbone, which is negatively charged, the DNA fragments will migrate (when placed in an electric field) to the positively charged anode. Moreover, the DNA molecules are separated by their size within an agarose gel (based on the uniform mass/charge ratio of DNA). Additionally, the rate of DNA molecule migration through a gel is determined by the following conditions e. g. the size of DNA molecule, DNA conformation, agarose concentration, type of agarose, electrophoresis buffer, presence of ethidium bromide and electrophoresis buffer.

Ingredients for the agarose gel are listed in Table 14. The samples were prepared with loading dye 6x and transferred on an agarose gel.

Table 14: Various usage and size of 1 % agarose gel

Agarose gel	Time/Voltage	Component
Small control gel		
8 slots	30 min/90 V	0.6 g agarose 60 mL TAE-buffer 1 drop of EtBr
Large control gel		
15, 20, 26 slots	45 min/120 V	2.0 g agarose 200 mL TAE-buffer 2 drops of EtBr
Small preparative gel		
8 slots	60 min/75 V	0.6 g agarose 60 mL TAE-buffer 1 drop of EtBr
Large preparative gel		
10 slots	90-120 min/90 V	2.0 g agarose 200 mL TAE-buffer 2 drops of EtBr

The band corresponding to the size of the cupin13 gene (size of 537 bp) was excised from the agarose gel and isolated via "Wizard® SV Gel and PCR Clean-Up System".

Protocol from "Wizard® SV Gel and PCR Clean-Up System"

The protocol was modified in some steps to receive a higher concentration of purified DNA.

Dissolving the gel slice

Membrane binding solution was added until the gel slice was covered and the samples were incubated at 60 °C in a thermomixer until the slice was completely dissolved.

Binding of DNA

A SV minicolumn was inserted into the collection tube, then the dissolved gel mixture was transferred to the minicolumn assembly (incubated at room temperature for one minute) and centrifuged at 16,060 g for one minute and subsequently, the flow through was discarded.

Washing

Five hundred microlitres of membrane wash solution were added (which included ethanol) and centrifuged at 16,060 g for one minute. Afterwards, the flow through was discarded. The wash step was repeated. Subsequently, the collection tube was emptied and the column assembly was re-centrifuged for two minutes.

Elution

The minicolumn was carefully transferred into a clean 1.5 mL reaction tube. Thirty microlitres of nuclease-free H_2O were added to the minicolumn, which was incubated at room temperature for two minutes and subsequently, centrifuged at 16,060 g for one minute. The minicolumn was discarded and the DNA was stored at 4 °C until subsequent use.

2.2.3 Restriction of DNA

The applied restriction enzymes (Table 15) recognised a specific sequence of nucleotides and created cohesive ends in the vectors pET26b, pEHISTEV, pMS470Δ8, pESBPTEV, pMA_Cupin13 and Cupin13 PCR product for recloning. Furthermore, the plasmid maps of pET26b, pMS470Δ8 and pMA_Cupin13 are shown in the Appendix.

Table 15: Restriction enzymes with buffers

Vector/Insert	Quantity for digestion	Restriction enzyme I	Restriction enzyme II	Buffer 10x	Size [bp]
pEHISTEV	2 µg	*Nco*I	*Hind*III	R	5,400
pESBPTEV	2 µg	*Nco*I	*Hind*III	R	5,400
pET26b	2 µg	*Nde*I	*Hind*III	R	5,300
pMS470Δ8	2 µg	*Nde*I	*Hind*III	R	4,500
pMA_Cupin13	3 µg	*Nde*I	*Hind*III	R	537
Cupin13 PCR product	30 µL	*Pag*I	*Hind*III	O and R	537

The expression vectors as well as pMA_Cupin13 were cleaved at 37 °C for 6 h or overnight. Afterwards, the digested components were transferred on a preparative agarose gel (Table 14). The digested pESBPTEV, pEHISTEV, pET26, pMS470 and Cupin13 (from pMA_Cupin13) were isolated as band at 5,400 bp, 5,400 bp, 5,300 bp, 4,500 bp and 537 bp from the preparative agarose gel. Subsequently, they were purified via “Wizard® SV Gel and PCR Clean-Up System”.

The Cupin13 PCR product was digested in two steps at 37 °C, as the restriction enzymes are not active in the same buffer, and intermediately, it was purified via “Wizard® SV Gel and PCR Clean-Up System”. At last, the digested sample was transferred on a preparative agarose gel, where then the band corresponding to the correct size was excised and the DNA was isolated from the agarose gel by “Wizard® SV Gel and PCR Clean-Up System”.

2.2.4 Ligation

The digested products were ligated by the T4 DNA ligase. This enzyme possesses the ability to ligate blunt and cohesive ends as well as to repair single stranded nicks in duplex DNA, RNA or DNA/RNA hybrids.

The ligation mix consisted of 100 ng digested vector (Table 16), the insert (Table 16; amount was calculated with the Equation 1), ligase buffer 10x, 1 µL T4 DNA ligase and ddH_2O. Additionally, two ratios "vector to insert" 1:3 and 1:2 were chosen for the ligation. Furthermore, the digested components were ligated at 22 °C for 6 h or at 16 °C overnight. Afterwards, the enzyme was inactivated at 70 °C for 10 min. Subsequently, the ligation mix was desalted via 0.025 µm membrane filter for 30 min at room temperature. The control ligation included digested vectors without insert.

Equation 1: Insert amount

$$\text{Insert mass [ng]} = \frac{\text{vector mass [ng]} * \text{size insert [kb]} * \text{molar ratio}}{\text{size vector [kb]}}$$

Table 16: Ligation of respective insert into the selected vector

Name of the vector	Name of the insert
pMS470	Cupin13 (isolated from pMA_Cupin13)
pET26	Cupin13 (isolated from pMA_Cupin13)
pEHISTEV	Cupin13 (PCR product)
pESBPTEV	Cupin13 (PCR product)

2.2.5 Transformation in *E. coli*

E. coli TOP10F' cells ensure a stable replication of high copy number plasmids, whereas *E. coli* BL21-Gold (DE3) cells (utilise the T7 RNA polymerase) was used for high yield protein expression due to the induction of isopropyl-β-D-1-thiogalactopyranoside (IPTG).

Moreover, the pMS470-Cupin13 construct, was transformed into *E. coli* TOP10F' cells and after reaching a sufficient cell density the tac promoter was induced by the addition of IPTG for the expression of the desired Cupin13 protein [70].

The difference of the transformation between *E. coli* TOP10F' and *E. coli* BL21-Gold (DE3) cells are listed in Table 17. The corresponding amount of µL plasmid (after ligation/from isolation) was transferred in a cooled electroporation cuvette and 80 µL *E. coli* TOP10F' or BL21-Gold (DE3) cells were added. The electroporation cuvette (containing plasmids and cells) was put in the shocking chamber of the Electroporation

Micro Pulser with the setting of “Ec2”, “Bacteria” and Time “ms”. After electromagnetic pulse, 800 µL SOC medium was immediately added and the mixture was transferred in a new reaction tube. The cells regenerated at 37 °C for 45 min at 700 rpm in a Thermomixer comfort, then 50 or 100 µL were plated out on a LB-agar plate with antibiotic (Table 8) and afterwards, centrifuged for 10 s at 16,060 g. X µL supernatant was removed. Subsequently, x µL “rest” was pipetted on a LB-agar-plate with antibiotic (Table 8), which was streaked out and incubated at 37 °C overnight.

Table 17: Different pipetting schemes for the transformation into various *E. coli* cells

***E. coli* TOP10F' cells For transformation**	**x [µL]**	**Supernatant**	**x [µL]**
Plasmid [1]	1	removed	0
		“rest” was streaked out without pellet	50
Plasmid [2]	10	removed	700
		“rest” with scrape down pellet was streaked out	100
***E. coli* BL21-Gold (DE3) cells For transformation**	**x [µL]**	**Supernatant**	**x [µL]**
Plasmid * [3]	1	removed	750
		“rest” with scrape down pellet was streaked out	50
Plasmid * [4]	1	removed	750
		from 50 µL supernatant was taken which was diluted with 90 µL SOC medium, and thereof was streaked out	10 50

***** from plasmid isolation (Mini preparation); [1] purchased synthetic pMA_Cupin13; [2] after ligation and purification: pESBPTEV-Cupin13, pMS470-Cupin13, pEHISTEV-Cupin13, pET26-Cupin13; [3] pET26-Cupin13; [4] pEHISTEV-Cupin13 and pESBPTEV-Cupin13;

2.2.6 Plasmid isolation

The masterplate is a backup, which was always stored at 4 °C, and used for plates to perform the plasmid isolation from *E. coli* colonies and the colony PCR. After transformation and incubation selected colonies were streaked out on a LB-agar-plate, which was supplemented with antibiotic (Table 8) and called masterplate (Figure 1).

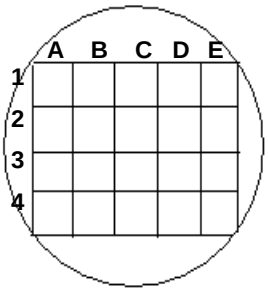

Masterplate with a register painted on the background of the LB-agar-plate.

(A)

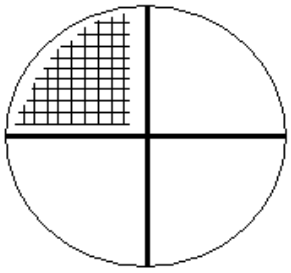

Pattern, shown in one field, for mini preparation.

(B)

Figure 1: (A): Masterplate and (B): pattern for mini preparation

The plasmid was extracted and purified via "Gene JET™ Plasmid Miniprep". Therefore one single colony was chosen, picked with sterile toothpick, streaked out on a LB-agar-plate with antibiotic in one field (Figure 1) and incubated at 37 °C for 6 h or overnight.

Protocol of GeneJET™ Plasmid Miniprep

The protocol was modified in some steps to obtain a higher yield of plasmids. The cells were picked with a sterile toothpick, then resuspended in 250 µL resuspension solution and vortexed.

Resuspend cells, Lyse and Neutralise

Lysis solution (250 µL) was added and the reaction tube was inverted 6 times. Afterwards, neutralisation solution (350 µL) was added and the step above was repeated. Subsequently, the reaction tube with the solutions was centrifuged for 10 min at 16,060 g.

Bind DNA

The supernatant was transferred into the GeneJET™ spin column and afterwards centrifuged for 1 min at 16,060 g.

Wash the column

Five hundred microlitres wash solution were added and centrifuged for 1 min, afterwards, the flow through was discarded and the washing step was repeated. Subsequently, the empty column was centrifuged for 2 min at 16,060 g.

Elute purified DNA

The GeneJET™ spin column was transferred to a new 1.5 mL reaction tube, then fifty microlitres ddH_2O were added to the column, which was incubated 2 min at room temperature and subsequently, centrifuged for 1 min at 16,060 g. The flow through was collected.

Control digestion

After plasmid isolation, the plasmid (2 µL) was digested with the restriction enzymes *Nde*I and *Hind*III (each 0.25 µL) in buffer R (1 µL) and in ddH_2O (6.5 µL) at 37 °C for 2 ½ h. The resulting DNA fragments were controlled on an agarose gel (Table 14).

2.2.7 Determination of DNA concentration

The concentration of purified DNA was determined by one of the two following methods. The first one was the visual comparison between the band of the sample and the bands of standard marker e.g. O'Gene Ruler 1kb Plus DNA Ladder, on the agarose gel in combination with the Equation 2 to determine the concentration of the DNA.

Equation 2: Calculation of the DNA band concentration

$$\text{DNA conc.} = \frac{\text{band of standard marker [ng]}}{\text{sample loaded on agarose gel [µL]}}$$

Second approach was a spectrophotometric analysis by Nanodrop 2000c Spectrophotometer that analysed a 2 µL sample at 260 nm. The computer program "Nano Drop 2000" calculated the DNA concentration. The optical density 1.0 at 260 nm corresponds to 50 ng double stranded DNA per µL. Furthermore, the degree of DNA purity was determined as the ratio 260/280 and should result in ~1.8 for purified DNA [71]. However, if the ratio was lower than 1.8, the sample might be contaminated with protein or other pollutants and if the ratio is higher than 2.0, the sample is possibly contaminated with RNA or denatured DNA [71].

2.2.8 DNA sequencing

The recombinant DNA was sequenced by LGC genomics Company and the obtained sequence was controlled by Dr. Steiner. Afterwards, the plasmids were transformed into electrocompetent *E. coli* BL21-Gold (DE3) cells as described in 2.2.5. Thereof backups (cryo cultures) were created and the added glycerol should prevent cell damages caused by freezing. This reaction mixture contained 1 mL overnight culture and 0.5 mL of a 50 % sterile glycerol solution.

2.2.9 Preparation of LB-agar-plates

The antibiotic ampicillin [100 mg/mL stock] was used for pMS470Δ8, pMA_Cupin13 and pUC19, whereas kanamycin [40 mg/mL stock] was applied for pEHISTEV, pESBPTEV, pET26b and pET28a. Ampicillin plates contained LB-agar Lennox (autoclaved [35 g/L]) and 0.1 mg/mL ampicillin [100 mg/mL stock], while kanamycin plates included LB-agar Lennox (autoclaved [35 g/L] and 0.04 mg/mL kanamycin [40 mg/mL stock]. LB-agar-plates, which were supplemented with antibiotic (Table 8) were created for masterplates, plates for transformation and plates for plasmid isolation alternatively, stored at 4 °C until subsequent use.

2.2.10 Electrocompetent *E. coli* TOP10F' cells

Electrocompetent *E. coli* TOP10F' cells were produced for the transformation, therefore the following components (listed in Table 18) were autoclaved for the precultures and main cultures. Two millilitres of a 1 M HEPES buffer were added to two litres ddH_2O and yield in 1 mM ddH_2O-HEPES buffer mix (dHbm). The production of electrocompetent *E. coli* TOP10F' cells took one day.

Table 18: Ingredients for *E. coli* TOP10F' cells production

Component	Volume [L]
ddH_2O	2.0
10 % glycerol	1.0
2x TY medium in 2 L flask (main culture)	0.4
2x TY medium in 0.1 L flask (preculture)	0.05
HEPES buffer 1 M pH 7	0.002
SOC medium	1.0
Bottles, tubes: 500 mL and 1.5 mL	

Two selected single colonies were picked from a LB-agar-plate, which was prepared by J. Midl, with a sterile inoculation loop and were used for the inoculation of two precultures. The negative control includes 2x TY medium and was shaken at the same conditions as the precultures. Incubation started at 37 °C with 160 rpm overnight. The 1.5 mL reaction tubes, 10 % glycerol and ddH_2O were autoclaved and afterwards kept at 4 °C until subsequent use.

The main culture was inoculated by the addition of 4 mL preculture and was incubated at 37 °C until an OD_{600} of 0.6 was obtained, which was measured by using the DU 800

Spectrophotometer. Afterwards, the main culture was cooled at 4 °C for 60 min and was centrifuged at 3,000 g for 10 min. The supernatant was removed and the pellet was dissolved on ice with 5 mL 1 mM dHbm.

Two dissolved pellets (each had 5 mL of 1 mM dHbm) were pooled and filled up to 125 mL of a 1 mM dHbm solution. Then they were centrifuged at 4 °C for 10 min at 4,000 g and the supernatant was discarded. Five millilitres of 1 mM dHbm solution were added to the pellets, which were dissolved. Two dissolved pellets (each had 5 mL 1 mM dHbm) were pooled and filled up to 340 mL with 10 % glycerol. The centrifugation settings were 20 min at 4 °C and 4,500 g. Then the supernatant was removed. Ten millilitres of the 10 % glycerol solution were added to the pellet, which was dissolved, subsequently, this tube was filled up with 10 % glycerol. The centrifugation was performed for 15 min at 4 °C and 5,000 g and afterwards, the supernatant was discarded. The pellet was dissolved in 2 mL 10 % glycerol. Subsequently, it was distributed as 160 µL in 1.5 mL reaction tubes and stored at -70 °C.

Test transformation

The electrocompetent *E. coli* TOP10F' cells were tested for their transformation efficiency as well as to detect potential contamination.

Therefore electrocompetent *E. coli* TOP10F' cells were thawed on ice, at the same time one microlitre test-vector pUC19 was transferred in an electroporation cuvette, then 80 µL electrocompetent *E. coli* TOP10F' cells were added and cooled for 1 min on ice. The electroporation cuvette (containing pUC19 plasmids and cells) was put in the shocking chamber of the Electroporation Micro Pulser with the setting of "Ec2", "Bacteria" and Time "ms". After electromagnetic pulse 800 µL SOC medium were immediately added to the electroporation cuvette and the mixture was transferred in a new 1.5 mL reaction tube. The cells were regenerated at 37 °C for 45 min and 600 rpm in Thermomixer. Fifty microlitres and 100 µL were plated out on LB-agar-plates, which were supplemented with ampicillin and incubated at 37 °C overnight.

As control, the electrocompetent *E. coli* TOP10F' cells, were streaked out (40 µL) on a LB-agar-plate with ampicillin and (40 µL) on one with kanamycin. Viable cells can be estimated via colony forming units (cfu). Therefore the colonies on the transformation plates were counted and applied for the calculation (Equation 3).

Equation 3: Rate of transformation [cfu/µg]

$$\frac{\text{transformants}}{\mu g \text{ plasmid DNA}} = \frac{\text{number of colonies}}{x\ \mu g \text{ transferred DNA}} * \frac{10^6 \text{ pg}}{\mu g} * \frac{x\ \mu L \text{ total transformant volume}}{x\ \mu L \text{ streaked out}}$$

Number of colonies ..... counted colonies on the plate

10^6 pg/µg ..... conversion factor from picogram (pg) to microgram (µg)

Total transformant volume ..... 880 µL (consisted of 80 µL competent cells plus 800 µL SOC-Medium)

Transformants ..... number of transformants

X µL streaked out ..... x µL cells were plated out on LB-agar-plate

2.3. Biochemical methods

The biochemical methods were used to determine the protein expression by using analytical methods such as SDS gel electrophoresis and Bradford protein assay. Furthermore, the enzyme assay developed by Takenaka et al. was modified for a smaller reaction volume. The enzyme activity was tested with the substrate 4-amino-3-hydroxybenzoic acid, additionally, the activity of whole intact *E. coli* BL21-Gold (DE3) cells was determined.

2.3.1 Expression in cell flasks

The pET26-Cupin13 and pEHISTEV-Cupin13 construct in *E. coli* BL21-Gold (DE3) cells were applied for the protein expression in LB-medium with antibiotic (Table 8). A preculture (6 mL LB-medium with antibiotic) was inoculated from a cryo culture or selected *E. coli* colony. Afterwards, the preculture was incubated at 37 °C 150 rpm overnight. The main culture (400 mL LB-medium with antibiotic) was inoculated with 4 mL preculture and incubated at 37 °C until a ~0.8 OD_{600} was obtained. Optional the corresponding amount of 10 µM $FeSO_4$, $CuSO_4$, $MnCl_2$ or $NiSO_4$ was pipetted in the main culture before 0.1 mM IPTG were added to start the expression of the recombinant protein. The inoculated main culture with 0.1 mM IPTG was incubated at 25 °C for 20 h. The cells were harvested at 4 °C for 15 min at 3,024 g and afterwards, stored at -20 °C until subsequent use. Cells were dissolved in cold 50 mM Tris/HCl buffer at pH 7.5 and disrupted in the Ultrasonic Branson Sonifier 250 (setting for the sonication was 6 min, 80 % duty cycle, 70 % output). After 3 min the process was paused, due to the increasing temperature of the liquid, which had to be cold, because otherwise the protein would be denatured. The supernatant was separated from the unbroken cells, membranes and inclusion bodies by centrifugation at 4 °C for 60 min at 50,000 g. Afterwards, it was filtrated by sterile filter (0.45 µm) and thereof, one millilitre was transferred in a reaction tube for various subsequent tests, while the rest of the protein was transferred in a reaction tube (where the headspace was purged with gaseous nitrogen) and kept at 4 °C to minimise the inactivation of the enzyme.

2.3.2 Expression level analysis

The electrophoretic separation of proteins correlatets to their molecular weight and was performed via SDS-PAGE (sodium dodecyl sulphate polyacrylamide gel

electrophoresis). The soluble part (supernatant of broken and centrifuged *E. coli* cells) was diluted in a ratio of 1:10 with 50 mM Tris/HCl buffer pH 7.5 and separated by SDS-PAGE.

A small part of the pellet (insoluble fraction) was transferred in a reaction tube and weighed. For each mg of transferred pellet a 10x volume of 6 M urea solution was added, e.g. 200 µL 6 M urea solution were added to 20 mg pellet. Afterwards, the samples were shortly mixed (Vortexer Genie2) and then centrifuged for 30 s at 16,060 g. The supernatant was diluted in a ratio of 1:10 with 50 mM Tris/HCl buffer pH 7.5 for SDS-PAGE gel.

SDS-PAGE

Thirty microlitres of the respective sample were mixed with 4x LDS sample buffer, then boiled for 10 min at 96 °C, and subsequently, centrifuged for a minute. A NuPAGE 4-12 % Bis- Tris-Gel was covered with MES buffer and afterwards, the coloured samples were loaded in the wells of the gel. The electrophoresis was performed at 200 V for 35 min. After this, the gel was dyed with Coomassie Brilliant Blue G250 solution, prepared from J. Midl, and decolourised via destaining solution.

The gel in Coomassie Brilliant Blue G250 solution was heated for a few seconds in the microwave and then remained on the shaking platform (Mini twist) for 15 min at room temperature. For decolourisation the gel was shaken in the destaining solution, which was changed several times, for some minutes at room temperature.

2.3.3 Determination of protein concentration

Bradford protein assay

The total amount of protein was determined with a colorimetric protein assay, which measured the colour change of Coomassie Brilliant Blue G-250 that was bound to the protein. Therefore a calibration curve (Table 19) was prepared at 595 nm using a DU 800 Spectrophotometer. The result should be between 0.1 and 1.0 at Abs_{595}, otherwise the values would be out of the range of the calibration curve and the sample has to be diluted.

Table 19: Calibration curve of BSA assay pipetting scheme

BSA stock with ddH_2O [mg/mL]	BSA stock [µL]	ddH_2O [µL]
2.0	100.0	0
1.5	75.0	25.0
1.0	50.0	50.0
0.75	37.5	62.5
0.5	25.0	75.0
0.2	10.0	90.0
0.1	5.0	95.0

Ten microlitres of pure/diluted sample or ddH_2O (blank) were mixed with 990 µL Bradford 1x, vortexed and subsequently, incubated for 10 min at room temperature in a 1.5 mL reaction tube. Afterwards, the sample was transferred in a polystyrene cuvette and immediately measure at 595 nm using a DU 800 Spectrophotometer. The absorption value was filled in the equation of the calibration curve (Figure 11) and calculated the total amount of protein [mg/mL].

Gel quantification

The expression level of two or more proteins can be compared by SDS-PAGE gel on the condition that the equal amount of protein was loaded. The electrophoretic separation of the proteins is based on their molecular weight. Therefore, ten microlitres of the protein (1 mg/mL) were mixed with 4x LDS sample and ddH_2O. The further steps were performed as described in 2.3.2 in section “SDS-PAGE”. The NuPAGE gel was scanned and consequently, the bands were analysed by G: Box HR16. The amount of Cupin13 was calculated with the Equation 4 and with the measured values from the computer program “Gene Tools”.

Equation 4: Cupin13 determination

$$\text{amount of Cupin13 [\%] in protein} = \frac{\text{band}}{\text{total quantity of bands}} \times 100\ \%$$

band	a band on the SDS-PAGE was scanned from G: Box HR16 and the computer program “Gene tools” calculated the value
total quantity of bands	included the sum of the values (which were calculated by “Gene tools”)

2.3.4 His-tag affinity purification

Highly efficient and simple tools for purifying proteins of crude extracts are affinity tags. An example is the hexahistidine tag (is fused to either the N or C terminus of the target protein), which belongs to the class of epitope affinity tags [72–74]. The His-tag can bind to cobalt or nickel ions, which are immobilised on a support [75]. Additionally, the nickel ions are hexa-coordinated, which means that, four ligand sites are occupied by nitrilotriacetic acid and two ligand sites are available for the histidine binding of a His-tag [76]. These interactions possess a high selectivity and affinity and can be reversed due to the utilisation of ethylenediaminetetraacetic acid (EDTA), a low pH, or imidazole [76]. Moreover, the expression of recombinant His-tagged proteins frequently occurs in *E. coli* based on the easy handling of the culture and the high production yield of target proteins [73].

The purified Cupin13 was produced (by Ni-agarose beads in a PD-10 column) with HisTEV-Cupin13. Therefore *E. coli* cells expressing HisTEV-Cupin13 (4.35 g) were thawed and resuspended with buffer A (Table 11), lysozyme [4 mg lysozyme/g pellet] and benzonase [250 U/µL]. The cells were broken by sonication for 6 min with 80 % duty cycle and 70 % output. However, after 3 min the process was paused (due to the increasing temperature of the liquid) because this heating process would result in a protein denaturation.

At first the supernatant was separated from the unbroken cells by centrifugation for 15 min at 4 °C and 3,024 g, subsequently, separated from inclusion bodies and membranes by centrifugation for 60 min at 4 °C and 50,000 g, after that it was filtered with a 0.45 µm sterile filter. Ni-agarose beads were washed with ddH_2O and afterwards with buffer A, incubated with HisTEV-Cupin13 for 30 min at room temperature and then transferred to the PD-10 column. The flow through was collected and put on ice. HisTEV-Cupin13 was eluted with buffer containing various imidazole concentrations and finally with buffer B (Table 11). The eluates were collected and kept on ice. After that the Ni-agarose beads were cleaned with ddH_2O and finally with 20 % ethanol. The protein at 21 kDa was detected by sodium dodecyl sulphate polyacrylamide gel (SDS-PAGE, in Figure 9). Due to this information the fractions corresponding to lane 7-10 (Figure 9) were pooled, concentrated by using Viva Spin (cut-off of 10,000 Dalton) and centrifuged for 90 min at 10 °C and 3,000 g. Subsequently, this purified concentrated HisTEV-Cupin13 was desalted on a PD-10 desalting column and eluted with $NaPO_4$ buffer pH 7.4. The protein concentration of purified HisTEV-Cupin13 (3.5 mL) was analysed by Nanodrop 2000c

Spectrophotometer and calculated via computer program “NanoDrop 2000”. The extinction coefficient (32,110 M^{-1} cm^{-1}) was calculated by using the computer program ProtParam (from ExPASy Bioinformatics Resource Portal; details are listed in the Appendix). The activity of the purified HisTEV-Cupin13 was tested with the enzyme assay (was developed by Takenaka et al.) and modified for 1 mL total reaction volume, which included 0.167 mM 4A3HBA substrate in 100 mM $NaPO_4$ buffer pH 7.4. The blank consisted of 0.03 mg/mL purified HisTEV-Cupin13 and 100 mM $NaPO_4$ buffer pH 7.4. Furthermore, the control contained 0.167 mM 4A3HBA in 100 mM $NaPO_4$ buffer pH 7.4. The reaction was started by adding 0.03 mg/mL purified HisTEV-Cupin13 and analysed (at room temperature in quartz cuvettes Suprasil) at 294 nm in DU 800 Spectrophotometer. The protein was stored at 4 °C at various conditions and separated in:

- 0.5 mL protein with 1 mM DTT and gaseous N_2
- 0.5 mL protein with N_2 gaseous
- 0.5 mL protein

Additionally, aliquots of 100 µL protein were prepared and kept at -20 °C until subsequent use.

2.4. Enzyme assay activity

The activity of Cupin13 was tested with the substrate 4-amino-3-hydroxybenzoic acid (4A3HBA); therefore the enzyme assay by Takenaka et al. was used. The reaction was started by adding 25 µg/mL purified enzyme solution and the degradation of the substrate was analysed at 294 nm [55]. This enzyme assay was modified for 1 mL total reaction volume and includes 100 mM $NaPO_4$ buffer at pH 7.5, 0.167 mM 4A3HBA substrate and 0.0099 mg/mL pET26-Cupin13. Control consisted of 0.167 mM 4A3HBA substrate and 100 mM $NaPO_4$ buffer at pH 7.5. The conversion of 1 µmol substrate 4A3HBA per min was defined as one unit and analysed at 294 nm in DU 800 Spectrophotometer. Values of the results were calculated with the Beer-Lambert law and Lineweaver Burk to determine K_m, v_{max}, k_{cat} and the specific activity in units/mg protein.

2.4.1 Determination of substrate detection limit and layer thickness

Substrate detection limit

Different 4A3HBA substrate concentrations were analysed to determine the amount of substrate, which can be used before the detection limit of the plate reader was reached, and applied for the determination of the layer thickness (Equation 5).

The plate reader SynergyMx was tested in the range of 0 to 1,000 µM 4A3HBA in 100 mM $NaPO_4$ buffer pH 7.5 at room temperature and a wavelength of 294 nm. The blank consisted of 100 mM $NaPO_4$ buffer pH 7.5.

Layer thickness

The layer thickness was required for the determination of kinetic parameters and was therefore calculated with the Beer-Lambert-law (Equation 5). The value of lg (I_0/I) was determined by the plate reader SynergyMx and resulted in "A" (extinction absorbance).

Equation 5: Calculation of the layer thickness

$$A = \varepsilon * c * d$$

$$d = \frac{A}{\varepsilon * c}$$

c ..... 4A3HBA substrate concentration

ε ..... extinction coefficient from 4A3HBA with 7.53 mM^{-1} cm^{-1} [55]

A ..... extinction absorbance

d ..... calculated layer thickness

2.4.2 Activity determination of whole intact cells

The activity of whole intact *E. coli* BL21-Gold (DE3) cells (including pET26-Cupin13 plasmids) was tested, while the enzyme activity was monitored during the substrate (4A3HBA) conversion. Therefore, the measurement was performed at 294 nm and room temperature in the plate reader SynergyMx. Whole intact cells with and without $FeSO_4$ (production described in 2.3.1 until the step "sonication") were compared and the assay contained 1,000 µM 4A3HBA in 100 mM $NaPO_4$ buffer pH 7.5 in UV-Star Microplate 96-well with F-bottom. The reaction was started by the addition of the respective amount of cells.

2.5 Site directed mutagenesis

After various examinations of the Cupin13, Dr. Steiner used the computer program BLAST search and she performed a multiple sequence alignment. Due to the resulted information mutations were integrated in the putative metal binding site (which is part of the active site) as well as in the presumed active site by site directed mutagenesis with overlap extension PCR technique. Therefore, three separate PCR-reactions are required. First, the PCR products were confirmed on an agarose gel and subsequently, transferred on a preparative agarose gel to ensure that the template was completely removed. Afterwards, the DNA was isolated by "Wizard® SV Gel and PCR Clean-Up System" and the purified PCR products were used for the next PCR reaction. The cohesive ends of the digested PCR products (containing the mutations) were ligated with the digested pET28a-vector by using the T4 DNA ligase. After transformation in *E. coli* TOP10F' cells the colonies were selected for a backup on LB-agar plates (masterplate). The Cupin13 mutants were screened after colony PCR (2.2.1) and the isolated plasmids were examined by control digestion. The DNA sequencing and production of backups were performed as described in 2.2.8.

Site directed mutagenesis with overlap extension PCR technique

Cupin13 mutants were produced by using site directed mutagenesis with overlap extension PCR technique. This method requires three PCR steps, two primers including the desired mutation and two flanking primers (Figure 2). Additionally, it is important that the created fragments can overlap (as this ability is required in the third PCR step) and that the mutagenesis primers are complementary to each other.

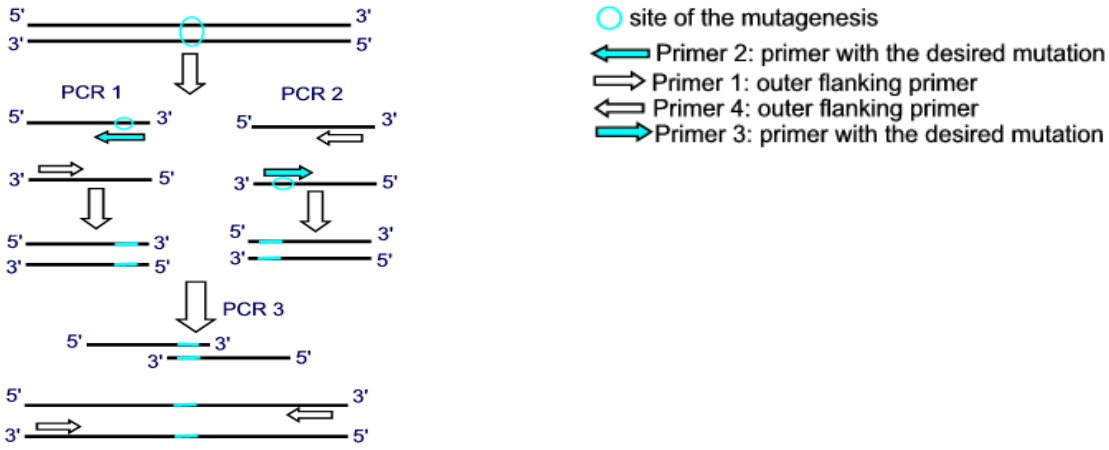

Figure 2: Site directed mutagenesis with overlap extension PCR technique

The ds DNA, oligos (primers 1-4) and site of mutagenesis are represented as line, small arrows and cyan circle. Furthermore, the PCR 1 and 2 are separated PCR reaction, where the desired

mutation is inserted in the DNA. Afterwards, the PCR products of PCR 1 and 2 are purified by e.g. agarose gel electrophoresis. Subsequently, the PCR products (used as templates) can be applied for the third PCR step, where the outer flanking primers indicate the start of the polymerase for amplification of the whole fragment with desired mutation site [77]. This figure was drawn in Microsoft PhotoDraw V2.

Dr. Steiner designed the primers, which were completely complementary to each other and included the desired mutations (Table 7).
In the first and second PCR reaction two moieties of interested section were produced and fit together in the third PCR reaction, where the two halves anneal in the range of complementarity to obtain the complete length of product. The dNTP concentration is described in 2.2.1 and the PCR ingredients, for one mutation, are listed in Table 20 and Table 21.

Table 20: PCR pipetting scheme for PCR product_fw and _rev

Component/Concentration	Stock solution	Volume [µL]
ddH_2O	---	35.5
HF-buffer 5x	---	10.0
dNTPs	10 mM	1.0
Primer_for/rev	10 pmol/µL	1.0
SynCupin13_rev/for	10 pmol/µL	1.0
Template pET26-Cupin13	20 ng/µL	1.0
Phusion DNA Polymerase	2 U/µL	0.5
Total reaction volume		**50.0**

Table 21: 3. PCR pipetting scheme for final PCR product

Component/Concentration	Stock solution	Volume [µL]
ddH_2O	---	31.5
HF-buffer 5x	---	10.0
dNTPs	10 mM	1.0
PCR product_fw	---	2.5
PCR product_rev	---	2.5
SynCup13_for	10 pmol/µL	1.0
SynCup13_rev	10 pmol/µL	1.0
Phusion DNA Polymerase	2 U/µL	0.5
Total reaction volume		**50.0**

The settings for the three PCR reactions are described in detail in the section 2.2.1.

Restriction of DNA

PET28a (received from PhD Hajnal) is a plasmid that includes T7 expression regions and is used for expression of Cupin13 mutants by the addition of IPTG. Two microgram pET28a-vector (kanamycin resistance) was digested with the restriction enzymes *Nco*I and *Hind*III at 37 °C overnight, whereas the Cupin13 mutants were digested using the restriction enzymes *Pag*I and *Hind*III (as the outer primers synCupin13_fw and synCupin13_rev include these restriction sites). Further steps were performed as described in 2.2.3.

Ligation, transformation in *E. coli* cells and sequencing

The digested Cupin13 mutants and pET28a were ligated via T4 DNA ligase (2.2.4) then prepared for the transformation in electrocompetent *E. coli* TOP10F' cells (2.2.5). After plasmid isolation and colony PCR (2.2.6 and 2.2.1), the Cupin13 mutants were additionally tested via cleavage (*Hind*III and *Eco*RV or *Eco*32I) at 37 °C for 2 ½ h, as after the ligation the restriction sites of *Nco*I and *Pag*I no longer existed. Further steps were done as listed in 2.2.7 and 2.2.8.

Table 22: Control digestion of pET28-Cupin13 mutants pipetting scheme

Component	Stock solution	Volume [µL]
pET28-Cupin13 mutant	---	2.0
*Hind*III	10 U/µL	0.25
*Eco*RV *or Eco*32I	10 U/µL	0.25
Buffer R 10x *	---	1.0
ddH_2O	---	0.5
Total reaction volume		**10.0**

* depends on end volume

Analysis of protein expression and activity

The protein analysis of Cupin13 mutants are described in the section 2.3.1 – 2.3.3. Furthermore, the activity of the Cupin13 mutants during the degradation of 4A3HBA in 100 mM $NaPO_4$ buffer at pH 7.5 in UV-Star Microplate 96-well, F-bottom were monitored at (room temperature) a wavelength of 294 nm by using the plate reader SynergyMx. The reaction was started by adding the corresponding concentration of mg/mL Cupin13 mutant.

3. RESULTS

Dr. Steiner used the computer program BLAST search (Basic Local Alignment Search Tool) from the NCBI database (National Center for Biotechnology Information) on the selected 4A3HBA23DA enzyme, because only few information of the enzyme was already published. Consequently, only some enzyme characterisation studies such as the one of Takenaka et al. [55] and Murakami et al. [54], but no mutagenesis study of the enzyme was performed. The computer program BLAST search resulted in a high sequence similarity (more than 50 % query cover) of the 4A3HBA23DA enzyme with the 3-hydroxyantranilic acid dioxygenase superfamily (listed in Table 23). Furthermore, the details of the alignment between the 4A3HBA23DA and the proteins (Table 23) are listed in the Appendix.

Table 23: Result of the BLAST search

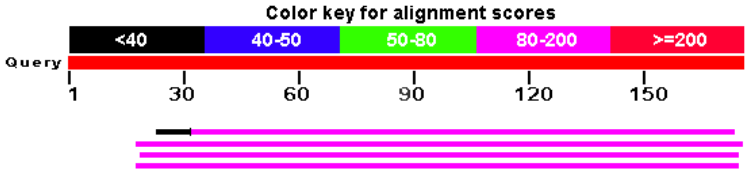

Description	Max score	Total score	Query cover [%]	E value	Ident [%]
3-Hydroxyanthranilate 3,4-dioxygenase [*Dyella ginsengisoli*]	99.0	112	85	$2*10^{-30}$	35
3-Hydroxyanthranilate 3,4-dioxygenase [*Kangiella koreensis* DSM 16069]	92.0	92.0	89	$6*10^{-28}$	34
3-Hydroxyanthranilate 3,4-dioxygenase [*Achromobacter xylosoxidans* A8]	85.5	85.5	88	$2*10^{-25}$	30
3-Hydroxyanthranilate 3,4-dioxygenase [*Cupriavidus basilensis*]	86.3	86.3	89	$9*10^{-26}$	32

Afterwards a multiple sequence alignment (MSA) of the dioxygenases, which had the highest sequence similarity according to the BLAST search result, was performed by using the computer program CLUSTAL Omega from EMBL-EBI. The result of the multiple sequence alignment (Table 23) exhibits that some high conserved groups (marked with colons) as well as weak conserved groups (denoted with full stops) exist. Additionally, the protein sequence of the first 43 residues of 4A3HBA23DA has no

identities with those of 3-HAD's, although conserved residues can be seen between the 3-hydroxyanthranilate 3,4-dioxygenases (3-HAD's). Two histidyl residues (on the position 52 and 97; green frames), which are necessary for the catalytic activity of the 4A3HBA23DA [54], are conserved in the 3-hydroxyanthranilate 3,4-dioxygenases (Figure 3). Due to the conserved residues in the 4A3HBA23DA and the 3-HAD's, the following mutations phenylalanine and glutamine were integrated on the positions 60 (contains glutamine) and 62 (contains serine; black frames in Figure 3).

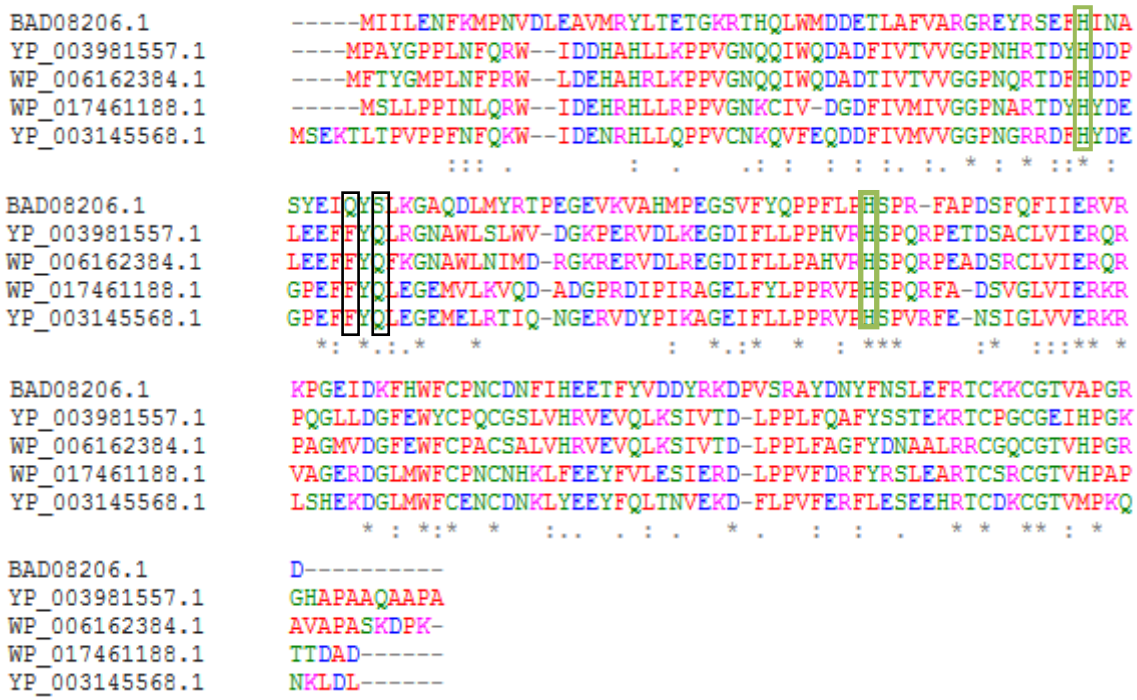

Figure 3: Result of the CLUSTAL Omega alignment of 4-amino-3-hydroxybenzoate 2,3-dioxygenase and 3-hydroxyanthranilate 3,4-dioxygenases (3-HAD's).
4-Amino-3-hydroxybenzoate 2,3-dioxygenase of *Bordetella* sp. 10d (BAD08206.1); 3-Hydroxyanthranilate 3,4-dioxygenase of *Dyella ginsengisoli* (WP_017461188.1); 3-Hydroxyanthranilate 3,4-dioxygenase of *Kangiella koreensis* DSM 16069 (YP_003145568.1); 3-Hydroxyanthranialte 3,4-dioxygenase of *Achromobacter xylosoxidans* A8 (YP_003981557.1); 3-Hydroxyanthranilate 3,4-dioxygenase of *Cupriavidus basilensis* (WP_006162384.1);
The asterisks below the aligned sequences signify that the residues in that column are identical in all five sequences. Highly conserved groups are marked with colons, while weakly conserved one are denoted with full stops. Two histidyl residues, which are essential for catalytic activity, are on the position 52 and 97 of the 4A3HBA23DA protein sequence (BAD08206.1) [54].

3.1 Recloning of Cupin13

Different molecular biological methods were used to reclone the Cupin13 gene into various expression vectors. In the first method, the purchased synthetic Cupin13 gene was successfully amplified using the PCR technique (see 2.2.1) as can be seen in lane 2 (Figure 4) as band at 537 bp, which corresponds to the size of the gene.

The second tested method contains the in vivo amplification of the synthetic pMA_Cupin13 plasmid by *E. coli* TOP10F' cells (2.2.5). A colony of the bacterial lawn was selected for the dilution plating and resulted in nineteen white single opaque colonies (size: approximately 3 mm diameter; the shape: round; surface: smooth), which were visible on the transformation plate. Thereof, four colonies were selected and prepared for plasmid isolation (2.2.6).

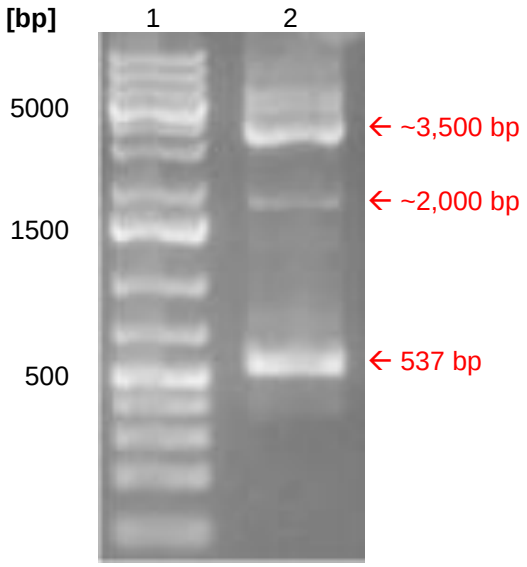

Figure 4 : 1 % Agarose control gel of amplified Cupin13 (using the PCR method)
Lane 1: Standard marker O'GeneRuler™ 1 kb Plus DNA Ladder, **lane 2:** Cupin13 at 537 bp, pMA vector at ~3500 bp with a smear and at ~2000 bp.

After cleavage (by restriction enzymes, Table 15), ligation (with 1:2 and 1:3 vector:insert ratio, Table 16) and transformation in *E. coli* TOP10F' cells, the number of colonies on the LB-agar-plates, which were supplemented with antibiotic (Table 8), were compared with the number of colonies on the LB-agar-control-plate. No colonies were on the LB-agar-control-plate. Due to this result, four *E. coli* colonies of LB-agar-plates of the ligation with 1:2 and 1:3 vector:insert ratio were selected and thereof the plasmid isolation was performed. Afterwards, the plasmids were digested (*Nde*I and

*Hind*III; in 2.2.6) and the resulting DNA fragments were controlled on an agarose gel (Figure 5).

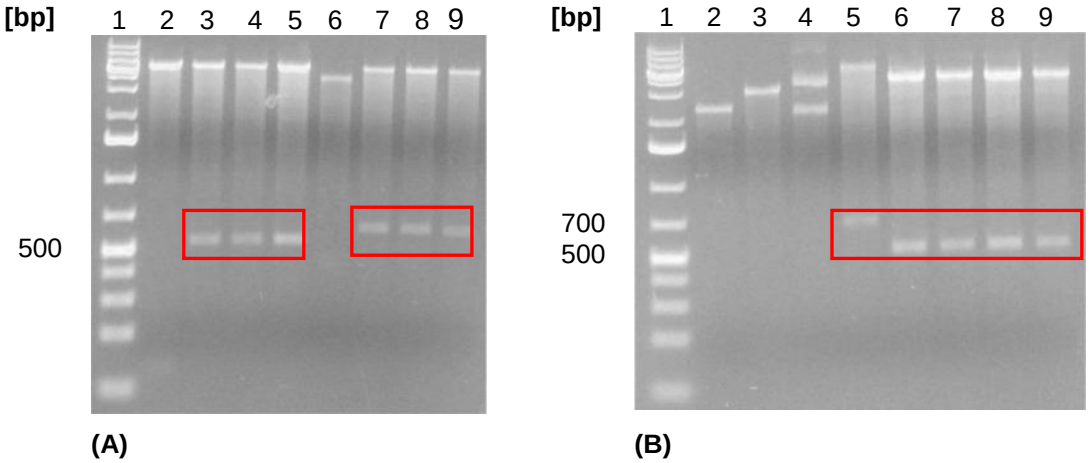

Figure 5: 1 % Agarose control gel of digested pET26-, pEHISTEV-, pESBPTEV- and pMS470-Cupin13 DNA fragments

Lane 1 contains the Standard marker O'GeneRuler™ 1 kb Plus DNA Ladder in both figures (A, B). The Cupin13 (red frame) is visible in gel (A) in the **lanes 3-5** and **7-9.** Additionally, it can be seen in gel (B) in the **lanes 5-9**.

(A) The pET26-Cupin13 was loaded in lanes 2-5 and pEHISTEV-Cupin13 in lanes 6-9. Additionally, the corresponding band of pET26 at approximately 5,000 bp and pEHISTEV at about 5,000 bp as well as in 4,000 bp (lane 6) can be seen. The lanes 2 and 6 contained empty vectors. The Cupin13 is visible at 537 bp in the lanes 3-5. Due to the His-tag and TEV sequence, the Cupin13 can be seen at ~600 bp in the lanes 7-9.

(B) The pESBPTEV-Cupin13 was transferred in lanes 2-5 and pMS470-Cupin13 in lanes 6-9. Furthermore, the band of the pESBPTEV vector was at approximately 2,500 bp (lane 2 and 4), 3,000 bp (lane 3), 4,000 bp (lane 4) and 5,000 bp (lane 5), while the pMS470 vector is only existent at 4,500 bp (lanes 6-9). The Cupin13 is visible at 700 bp (lane 5), based on the SBP-tag and TEV sequence. Moreover, the Cupin13 can be seen at 537 bp in the lanes 6-9.

Due to the bands, which correspond to the size of the Cupin13 gene at 537 bp, and the Cupin13 gene with tag and TEV sequence (~600 bp as well as ~700 bp) in Figure 5, it can be assumed that the ligation was successful.

3.2 Analysis of protein expression

A high quantity of protein was received through protein expression in *E. coli* BL21-Gold (DE3) cells. The 1.76 g, 1.03 g, 2.08 g and 2.00 g harvested *E. coli* cells (with pESBPTEV-, pEHISTEV-, pET26- and pMS470-Cupin13 plasmids) were broken (see

2.3.1) and thereof, the soluble and insoluble fractions were analysed on an SDS-PAGE gel (Figure 6) to identify in which fraction the Cupin13 protein was?

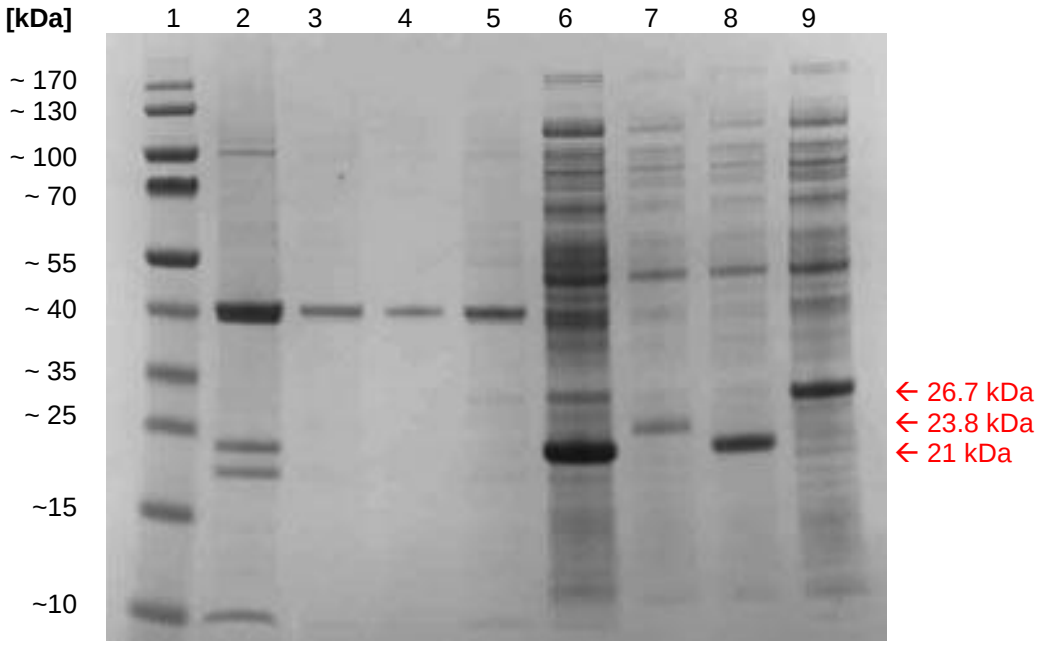

Figure 6: SDS-PAGE gel of the Cupin13 expression in *E. coli* using different vectors
Insoluble fraction was loaded in lanes 2-5 and soluble fraction was transferred in lanes 6-9. **Lane 1:** Standard marker "Page Ruler^{TM} Prestained Protein Ladder", **lane 2, 6:** Cupin13 (pMS470, 21 kDa), **lane 3, 7:** HisTEV-Cupin13 (pEHISTEV, 23.8 kDa), **lane 4, 8:** Cupin13 (pET26, 21 kDa), **lane 5, 9:** SBPTEV-Cupin13 (pESBPTEV, 26.7 kDa)

Bands corresponding to Cupin13 could only be seen in the soluble fractions at 21 kDa (pMS470- and pET26-vector). Furthermore, the bands of HisTEV-Cupin13 at 23.8 kDa and SBPTEV-Cupin13 at 26.7 kDa are also only visible in the soluble fractions. Additionally, the protein sizes of HisTEV- and SBPTEV-Cupin13 were different due to the included tags. The HisTEV-Cupin13 protein size of 23.8 kDa based on the included His-tag (which consisted of six histidines and resulted in 0.84 kDa), TEV cleavage site (0.86 kDa) and the sequence of Cupin13 (20.72 kDa). Moreover, the SBPTEV-Cupin13 protein size of 26.8 kDa contained the SBP-tag (which had a length of 45 amino acids and resulted in 4.90 kDa), TEV cleavage site (0.88 kDa) and the sequence of Cupin13 (20.72 kDa).

Based on this information (Figure 6), it was shown that the Cupin13 protein of the various expression vectors is only visible in the soluble fraction. Furthermore, the Cupin13 protein concentration (in Figure 6) cannot be compared as the same diluted amount of samples was transferred on the SDS-PAGE but not the same concentration.

Further protein analyses were performed with Cupin13 from the pET26-Cupin13 construct.

3.3 Determination of substrate detection limit and layer thickness

Different 4A3HBA substrate concentrations in the range of 0 to 1,000 µM were analysed to determine how much substrate can be used in the reaction before the detection limit of the plate reader is reached and the results were applied for the determination of the layer thickness (described in the section 2.4.1).

Table 24: Result of the substrate detection limit

Name	0 µM	50 µM	100 µM	200 µM	300 µM	400 µM	500 µM	600 µM	700 µM	800 µM	900 µM	1,000 µM
Average of the triplicates	0	0.24 ± 0.00	0.44 ± 0.01	0.81 ± 0.00	1.19 ± 0.03	1.55 ± 0.01	1.90 ± 0.01	2.25 ± 0.04	2.60 ± 0.03	2.88 ± 0.05	3.09 ± 0.02	3.20 ± 0.00

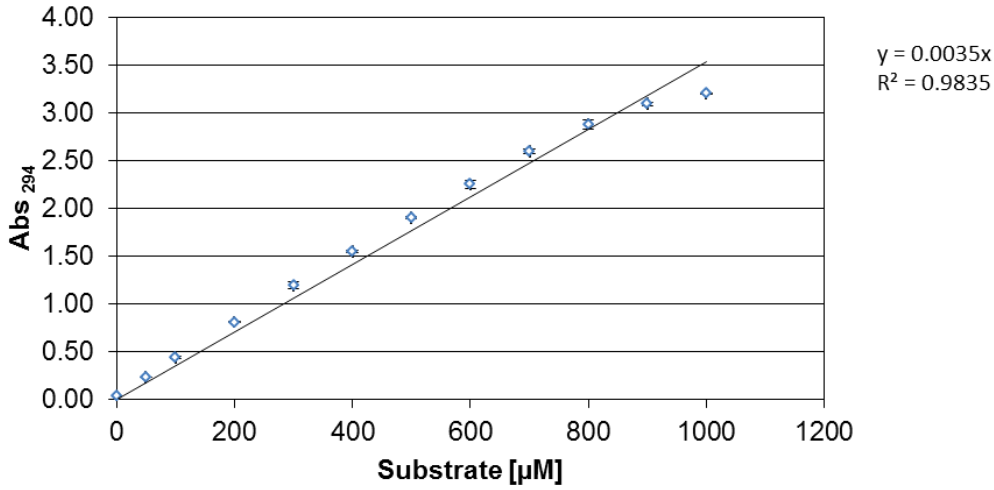

Figure 7: Measurement of various substrate concentrations

The sample (200 µL total volume) contained the corresponding concentration of 4A3HBA (Table 24) in 100 mM $NaPO_4$ buffer at pH 7.5 and was measured at 294 nm (room temperature) in a plate reader. The blank consisted of 100 mM $NaPO_4$ buffer at pH 7.5.

The plate reader can measure the selected substrate concentrations in the range of 0 to 1,000 µM and the absorption range is linear up to 900 µM 4A3HBA (Figure 7). Afterwards, the layer thickness was determined (described in 2.4.1). The average of the measured triplicates of lane A resulted in 0.53 cm, while lane B and C had the same value of 0.52 cm. Due to this information, the layer thickness of 0.52 cm was

used for the kinetic parameters. The tested reaction mixture had a total volume of 200 µL.

3.4 Analysis of Cupin13 activity

The activity of lysate containing Cupin13 from the pET26-Cupin13 construct was tested with 4A3HBA using the enzyme assay from Takenaka et al. (described in 2.4).

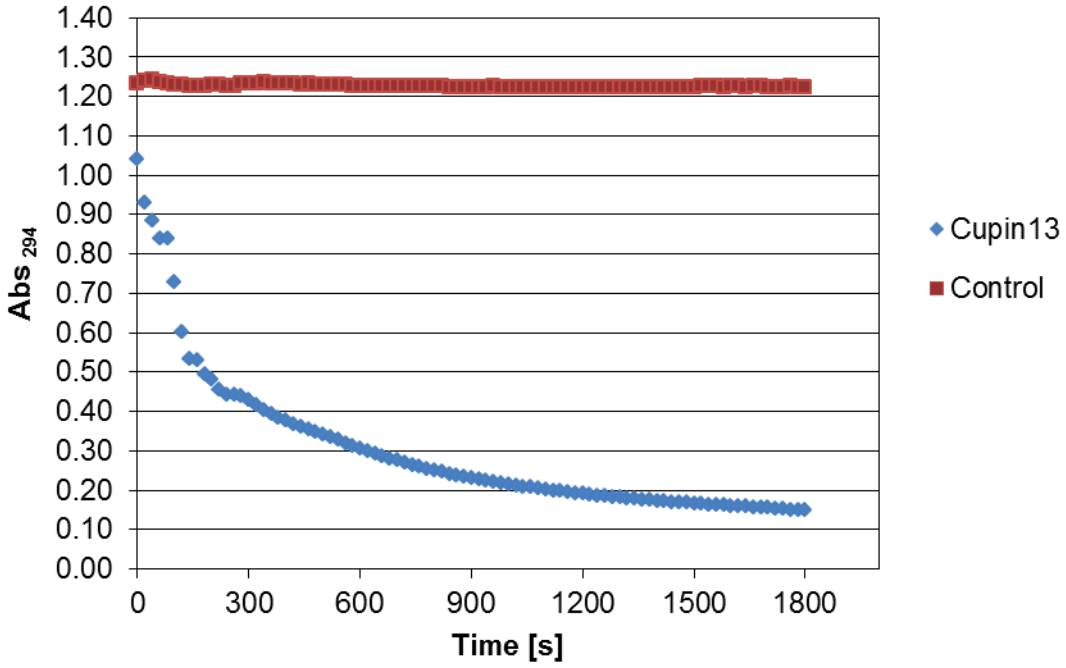

Figure 8: First activity measurement of the lysate containing Cupin13
The sample contained 0.167 mM 4A3HBA and 100 mM $NaPO_4$ buffer at pH 7.5. The reaction was started by adding 0.0099 mg/mL lysate containing Cupin13 and the substrate conversion was monitored for 30 min at 294 nm (room temperature) in a DU 800 Spectrophotometer. The control consisted of 100 mM $NaPO_4$ buffer at pH 7.5 and 0.167 mM 4A3HBA substrate.

The first specific activity of the lysate containing Cupin13 resulted in 24.92 U/mg, while the control showed no activity (Figure 8). Another tested control was *E. coli* harbouring empty pET26b-vector, which had the same activity as the control in Figure 8.
Furthermore, it was determined that the enzyme lost its activity over the time. Due to this result, it was decided that always a freshly cleared lysate (containing Cupin13 protein) has to be prepared. Thereof always 1-2 mL were withdrawn for various tests, while the rest of the lysate was transferred in a reaction tube (where the headspace was purged with gaseous N_2) and kept at 4 °C.

3.4.1 Purification of HisTEV-Cupin13 protein

After the first promising result for the cleared lysate containing Cupin13, the protein was subsequently, tried to purify. Therefore, the HisTEV-Cupin13 protein (4.35 g *E. coli* BL21-Gold (DE3) cells expressed HisTEV-Cupin13 protein) was purified by affinity chromatography, using Ni-agarose beads and afterwards the samples were desalted (described in 2.2.10). The pellet, lysate and fractions of the various purification steps were analysed on an SDS-PAGE gel (Figure 9).

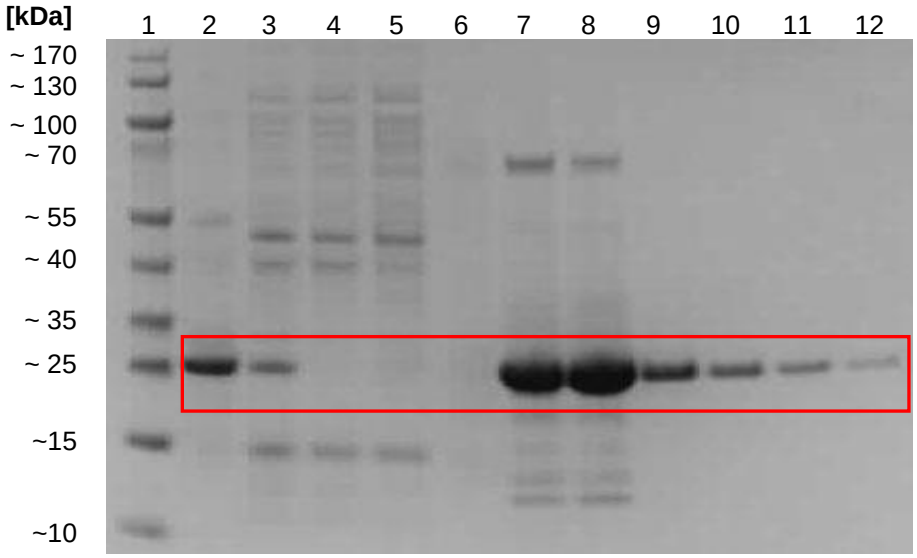

Figure 9: SDS-PAGE gel of the purified HisTEV-Cupin13 protein

HisTEV-Cupin13 (23.8 kDa) is visible in the lanes 2, 3, 7-12 (red frame).

Lane 1: Standard marker "Page Ruler^{TM} Prestained Protein Ladder, **lane 2:** pellet, **lane 3:** lysate, **lane 4:** flow through, **lane 5:** Wash buffer A, **lane 6:** Wash 30 mM imidazole, **lane 7:** Wash 50 mM imidazole, **lane 8:** Wash 100 mM imidazole, **lane 9:** Wash 200 mM imidazole, **lane 10:** Wash 300 mM imidazole, **lane 11-12:** Wash buffer B

The protein was detected in pellet, lysate, eluate with various imidazole concentrations as well as in wash buffer B. Furthermore, Cupin13 protein completely bound to the beads as no protein could be seen at a size of 23.8 kDa in the flow through (lane 4) as well as in lane 5 (wash buffer A) and 6 (30 mM imidazole). In addition, the protein started to eluate at a concentration of 50 mM imidazole.

The protein concentration of HisTEV-Cupin13 (3.5 mL) was determined and aliquots of purified protein were stored at various conditions (described in 2.3.4) for 12 h.

Table 25: Determination of the HisTEV-Cupin13 protein concentration after the storage at various conditions

Name	Protein conc. [mg/mL]
HisTEV-Cupin13 with 100 mM DTT and gaseous N_2, 4 °C	3.1
HisTEV-Cupin13 with gaseous N_2, 4 °C	3.0
HisTEV-Cupin13, 4 °C	3.0
HisTEV-Cupin13, -20 °C	0.4

No difference regarding the protein concentration was detectable between the freshly purified HisTEV-Cupin13 protein (3.0 mg/mL) and the stored aliquots at 4 °C, while at -20 °C the stored protein precipitated (Table 25). Due to this result, the protein was kept at 4 °C in the presence of gaseous N_2 for subsequent activity measurements or further analyses.

The activity of freshly purified HisTEV-Cupin13 protein was measured as described in 2.3.4 and not evaluable (Figure 10). Afterwards, the analysis was repeated and resulted in a similar result.

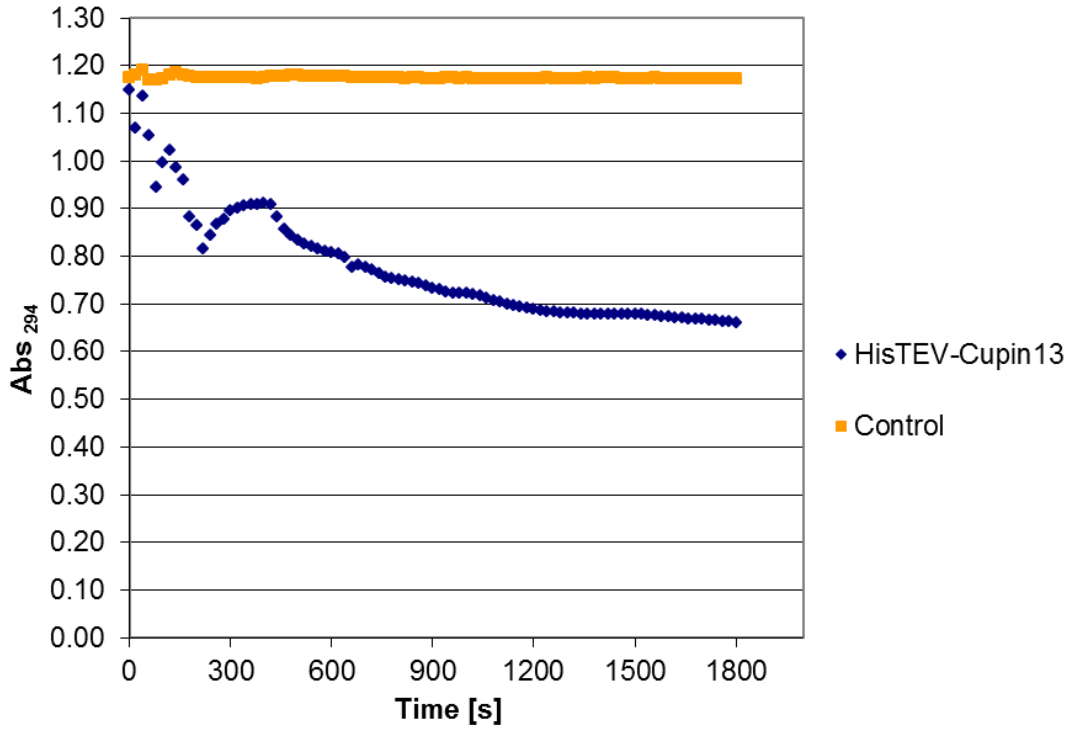

Figure 10: Activity of fresh purified HisTEV-Cupin13 was monitored during the substrate conversion

The sample contained 0.167 mM 4A3HBA in 100 mM $NaPO_4$ buffer at pH 7.4. The reaction started by the addition of 0.03 mg/mL freshly purified HisTEV-Cupin13 protein and

subsequently, the substrate conversion was monitored for 30 min at 294 nm (room temperature) in a DU 800 Spectrophotometer. The control consisted of 0.167 mM 4A3HBA in 100 mM $NaPO_4$ buffer at pH 7.4.

Moreover, it was tried to reactivate the protein by the addition of DTT (1,4-Dithiothreitol), but the activity was lost. Only the HisTEV-Cupin13 protein, which contained gaseous N_2 as well as 100 mM DTT, seems to be slightly active. Due to the results of the purified HisTEV-Cupin13, it was decided, that no purified protein will be used for further tests.

3.4.2 Effect of various metal salts on Cupin13

Takenaka et al. described that the enzyme activity increased in the presence of Fe(II). Based on this knowledge, the activity of Cupin13 (which was expressed in the presence of 10 µM $FeSO_4$ as well as with various bivalent metal salts such as $CuSO_4$, $MnCl_2$ and $NiSO_4$) was tested.

The precultures and main cultures were produced as described in the section 2.3.1. Additionally, 10 µM of the respective metal salt were added in the main culture before the expression was started by the addition of 0.1 mM IPTG. The control contained Cupin13 protein (from pET26-Cupin13 construct) without metal salt and incubated at the same conditions. The harvested cells (Table 27) were broken (described in 2.3.1) and the Cupin13 protein was analysed on an SDS-PAGE gel (Figure 12). The highest protein concentration (compared with the control without metal salt) was determined in the presence of 10 µM $FeSO_4$.

Different BSA concentrations (Table 26) were measured to obtain the calibration curve (Figure 11), which was used for the calculation of the total amount of protein (see 2.3.3).

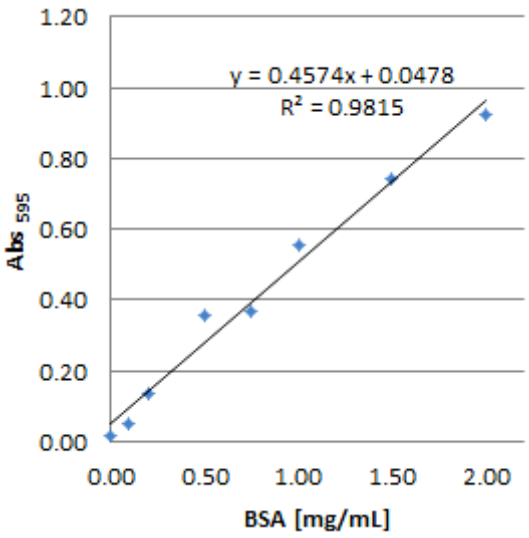

Figure 11: **Calibration curve of BSA assay**

Table 26: Calibration curve of BSA assay

BSA [mg/mL]	Abs $_{595}$
2.0	0.92
1.5	0.74
1.0	0.55
0.75	0.36
0.5	0.35
0.2	0.13
0.1	0.05
0	0.01

Table 27: Cupin13 protein expressed in the presence of various bivalent metal salts

Name	Wet pellet [g]	Protein conc. [mg/mL]
Cupin13 control	1.09	14.75 ± 0.21
Cupin13 with 10 µM $CuSO_4$	1.11	14.77 ± 0.55
Cupin13 with 10 µM $FeSO_4$	1.53	15.45 ± 1.97
Cupin13 with 10 µM $MnCl_2$	1.12	13.74 ± 0.09
Cupin13 with 10 µM $NiSO_4$	1.00	14.89 ± 0.61

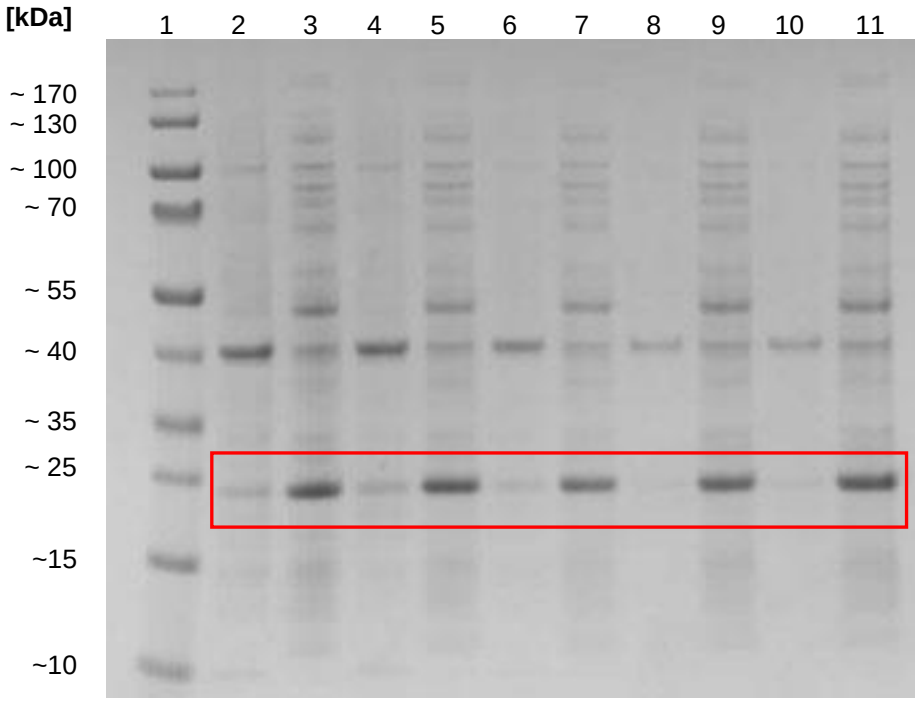

Figure 12: SDS-PAGE gel of Cupin13 expressed in the presence of different metal salts
Cupin13 (in the red frame at 21 kDa) is clearly visible in the soluble fraction (lanes 3, 5, 7, 9, 11), while the protein was almost not visual in the lanes 2, 4, 6, 8 and 10 (insoluble fraction). **Lane 1**: Standard marker "Page Ruler^{TM} Prestained Protein Ladder", **lane 2, 3:** Cupin13-$NiSO_4$, **lane 4, 5:** Cupin13-$FeSO_4$, **lane 6, 7:** Cupin13-$CuSO_4$, **lane 8, 9:** Cupin13-$MnCl_2$, **lane 10, 11:** Cupin13 control (without metal salt; from pET26-Cupin13 construct)

The Cupin13 is clearly visible in the soluble fractions, regardless of whether a metal salt was available or not (Figure 12).

Afterwards, the activity of Cupin13, which was expressed in the presence of various bivalent metal salts, was analysed with the enzyme assay from Takenaka et al., which was modified for 200 µL total volume.

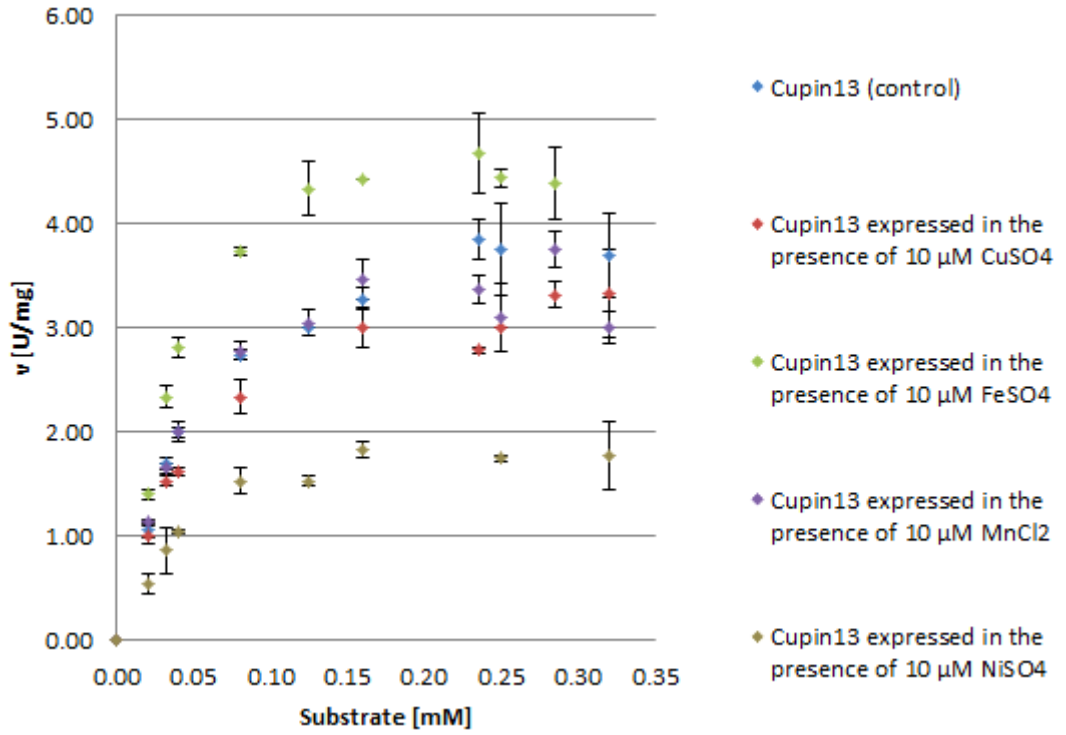

Figure 13: Kinetic of lysate containing Cupin13, which was expressed in the presence of various bivalent metal salts

The enzyme assay contained 0-320 µM 4A3HBA in 100 mM $NaPO_4$ buffer at pH 7.5. The reaction was started by adding 0.01 mg/mL (0.005 mg/mL final conc.) cleared lysate containing Cupin13 protein and the substrate conversion was monitored for 30 min at 294 nm (room temperature) in a plate reader.

Table 28: Analysis of Cupin13 protein expressed in the presence of 10 µM metal salts The sample of the analysis contained the 4A3HBA substrate in the range of 0 to 320 µM in 100 mM $NaPO_4$ buffer at pH 7.5. The reaction was started by adding 0.01 mg/mL (0.005 mg/mL final conc.) cleared lysate containing Cupin13 protein and the substrate conversion was monitored for 30 min at 294 nm (room temperature) in a plate reader.

Name	specific activity [U/mg] of lysate *	K_m [mM]
Cupin13 control	3.85 $^{\#2}$ ± 0.19	0.04
Cupin13 with $CuSO_4$	3.01 $^{\#}$ ± 0.01	0.04
Cupin13 with $FeSO_4$	4.44 $^{\#}$ ± 0.08	0.04
Cupin13 with $MnCl_2$	3.37 $^{\#2}$ ± 0.13	0.04
Cupin13 with $NiSO_4$	1.75 $^{\#}$ ± 0.03	0.04

* containing Cupin13, $^{\#}$ from 0.25 mM 4A3HBA, $^{\#2}$ from 0.24 mM 4A3HBA

The K_m value of the Cupin13 protein samples with various bivalent metal salts was the same compared with the control. Furthermore, the highest and lowest specific activity

was detected in the samples of Cupin13 with 10 µM $FeSO_4$ and Cupin13 with 10 µM $NiSO_4$.

Subsequently, a SDS-PAGE gel was used to quantify the expression level of the Cupin13 in the presence of various bivalent metal salts. The expression levels of Cupin13 protein were compared by gel quantification of the respective bands in the SDS-PAGE; the gel is shown in Figure 14.

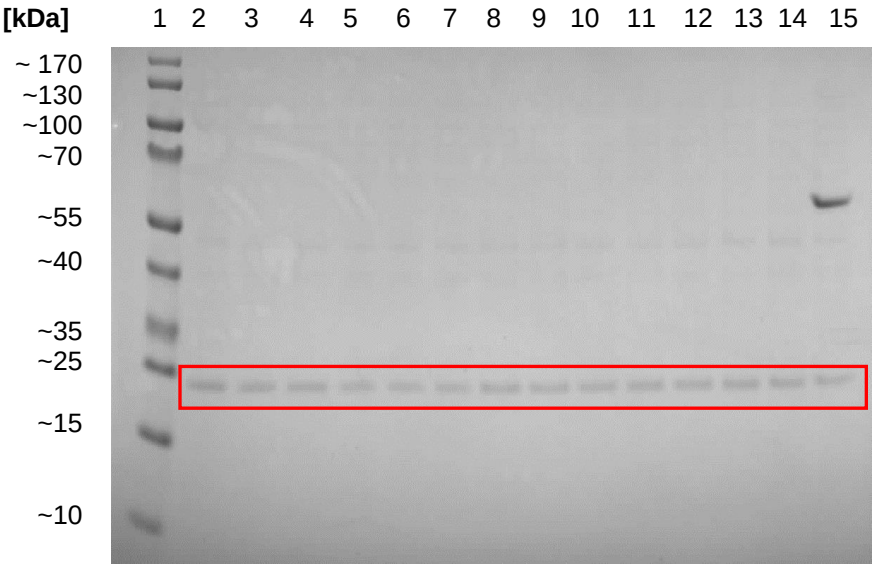

Figure 14: SDS-PAGE gel for the quantification [5 µg] of Cupin13 bands expressed in the presence of various bivalent metal salts
Cupin13 could be seen at 21 kDa (red frame).
Lane 1: Standard marker "Page Ruler^{TM} Prestained Protein Ladder", **lane 2-4:** Cupin13-$FeSO_4$, **lane 5-7:** Cupin13-$NiSO_4$, **lane 8-10:** Cupin13-$CuSO_4$, **lane 11-13:** Cupin13-$MnCl_2$, **lane 14-15:** Cupin13 control without metal salt

A barely protein expression can be seen in all lanes (red frame in Figure 14). Due to this result, the protein concentration was remeasured (Bradford protein assay).

Table 29: Cupin13 protein expressed in the presence of various bivalent metal salts

Name	Wet pellet [g]	Protein conc. [mg/mL]
Cupin13 control	1.09	4.69 ± 0.07
Cupin13 with 10 µM $CuSO_4$	1.11	4.39 ± 0.05
Cupin13 with 10 µM $FeSO_4$	1.53	4.79 ± 0.05
Cupin13 with 10 µM $MnCl_2$	1.12	4.69 ± 0.13
Cupin13 with 10 µM $NiSO_4$	1.00	4.91 ± 0.13

The remeasurement of the protein concentration resulted in a lower protein concentration (Table 30) compared with the concentration in Table 27.

Afterwards, a new SDS-PAGE gel was used to quantify the expression level of the Cupin13 in the presence of various bivalent metal salts. The expression levels of Cupin13 protein were compared by gel quantification of the respective bands in the SDS-PAGE; the gel is visible in Figure 15.

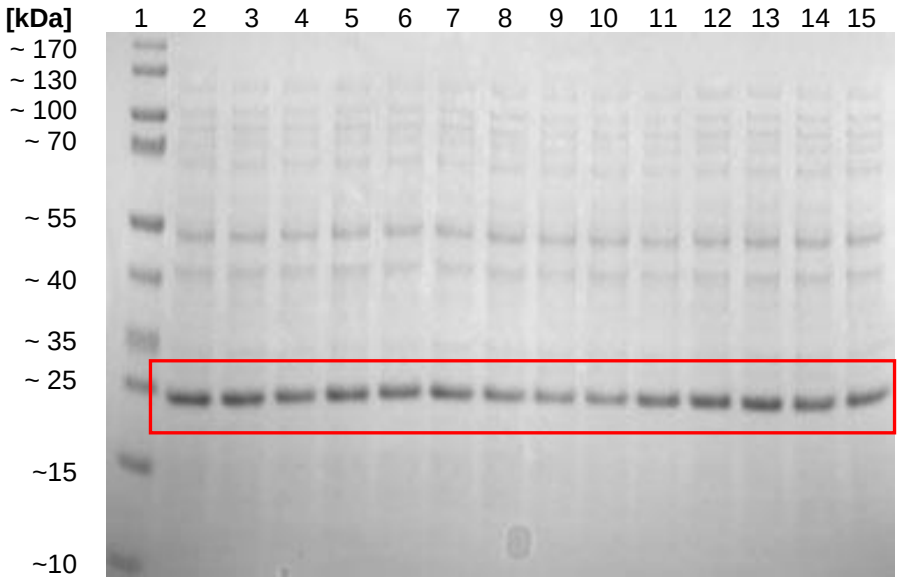

Figure 15: SDS-PAGE gel for the quantification [5 µg] of Cupin13 bands expressed in the presence of various bivalent metal salts

The desired Cupin13 protein can be seen at 21 kDa (red frame).

Lane 1: Standard marker "Page Ruler^{TM} Prestained Protein Ladder", **lane 2-4:** Cupin13-$FeSO_4$, **lane 5-7:** Cupin13-$MnCl_2$, **lane 8-10:** Cupin13-$CuSO_4$, **lane 11-13:** Cupin13-$NiSO_4$, **lane 14-15:** Cupin13 control without metal salt

Table 30: Result of the quantification [5 µg] of Cupin13 protein expressed in the presence of various bivalent metal salts

Lane	2	3	4	5	6	7	8	9	10	11	12	13	14	15
Name	Cupin13-$FeSO_4$			Cupin13-$MnCl_2$			Cupin13-$CuSO_4$			Cupin13-$NiSO_4$			Cupin13 control without metal salt	
Average of triplicates [%]	33.86 ± 1.66			33.14 ± 1.60			24.40 ± 1.74			33.58 ± 2.29			30.24 ± 0.07	

A strong protein expression is visible in nearly all lanes (red frame in Figure 15). The weakest one was detected in the lanes 8-10 (Cupin13-$CuSO_4$, see in Table 30).

Due to the information in Table 29 and Table 30, the enzyme activity (Table 28) was recalculated.

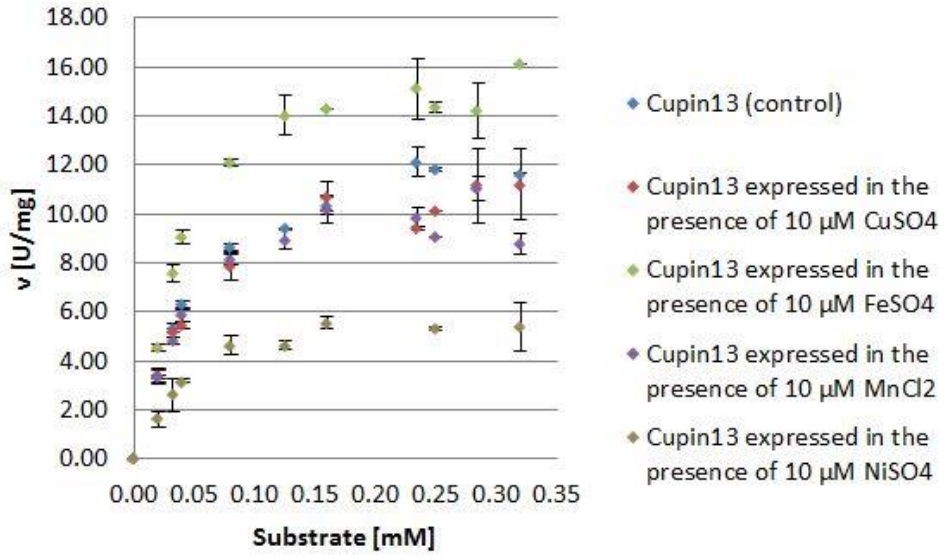

Figure 16: Recalculated Kinetic of lysate containing Cupin13, which was expressed in the presence of various bivalent metal salts

Table 31: Analysis of recalculated Cupin13 protein expressed in the presence of 10 µM metal salts

	specific activity [U/mg] of				
Name	lysate *	Cupin13	K_m [mM]	Cupin13 per well [µg]	k_{cat} of Cupin13 [s^{-1}]
Cupin13 control	12.10 #2 ± 0.60	40.02 #2 ± 1.98	0.04	0.30	13.83
Cupin13 with $CuSO_4$	10.12 # ± 0.01	41.49# ± 0.01	0.04	0.24	15.85
Cupin13 with $FeSO_4$	14.35 # ± 0.24	42.39 # ± 0.24	0.04	0.33	15.42
Cupin13 with $MnCl_2$	9.86 #2 ± 0.39	29.76 #2 ± 1.17	0.04	0.33	11.46
Cupin13 with $NiSO_4$	5.30 # ± 0.08	16.00 # ± 0.23	0.04	0.33	5.79

* containing Cupin13, # from 0.25 mM 4A3HBA, #2 from 0.24 mM 4A3HBA

The K_m value of the Cupin13 protein samples with various bivalent metal salts was the same compared with the control. Furthermore, the highest and lowest specific activity as well as k_{cat} was detected in the samples of Cupin13 with 10 µM $FeSO_4$ and Cupin13 with 10 µM $NiSO_4$. Due to the results in Figure 16 and Table 31, various $FeSO_4$ concentrations were tested to obtain the optimal enzyme activity.

3.4.3 Identification of the optimal $FeSO_4$ concentration for Cupin13

The Figure 13 exemplified that the activity of Cupin13 protein (was expressed in the presence of $FeSO_4$) increased. Based on this information, various $FeSO_4$ concentrations were tested to determine the best concentration for the highest enzyme activity. Additionally, the reproducibility of this enzyme assay was tested and therefore two samples in the presence of 10 µM $FeSO_4$ and controls without metal salt were used. The precultures and main cultures were produced as described in 2.3.1. Additionally, the corresponding amount of ferrous sulphate was added in the main culture before the expression was started by the addition of 0.1 mM IPTG.

Table 32: Cupin13 protein expressed in the presence of different $FeSO_4$ concentrations

Name	x µM $FeSO_4$	Wet pellet [g]	Protein conc. [mg/mL]
Cupin13 control no. 1	0	2.1	6.16 ± 0.21
Cupin13 control no. 2	0	2.1	6.45 ± 0.26
Cupin13 no. 1	10	1.9	5.14 ± 0.08
Cupin13 no. 2	10	2.2	7.35 ± 0.08
Cupin13	50	2.4	7.14 ± 0.09
Cupin13	100	2.3	7.25 ± 0.01
Cupin13	200	2.2	7.24 ± 0.01
Cupin13	500	2.3	7.14 ± 0.22
Cupin13	750	2.5	6.65 ± 0.27
Cupin13	1,000	2.5	8.25 ± 0.25

The *E. coli* cells (Cupin13 control no. 1 and 2) weighed up to 2.1 g and had less weight compared to the other Cupin13 samples with ferrous sulphate except the *E. coli* no. 1 (1.9 g). Furthermore, the protein concentration is higher in the presence of ferrous sulphate, except for the sample of *E. coli* no. 1 (Table 32). Afterwards, the expression

level of the Cupin13 protein (in the presence of various $FeSO_4$ concentrations) was compared by quantification of the band [5 µg] on an SDS-PAGE gel (Figure 17).

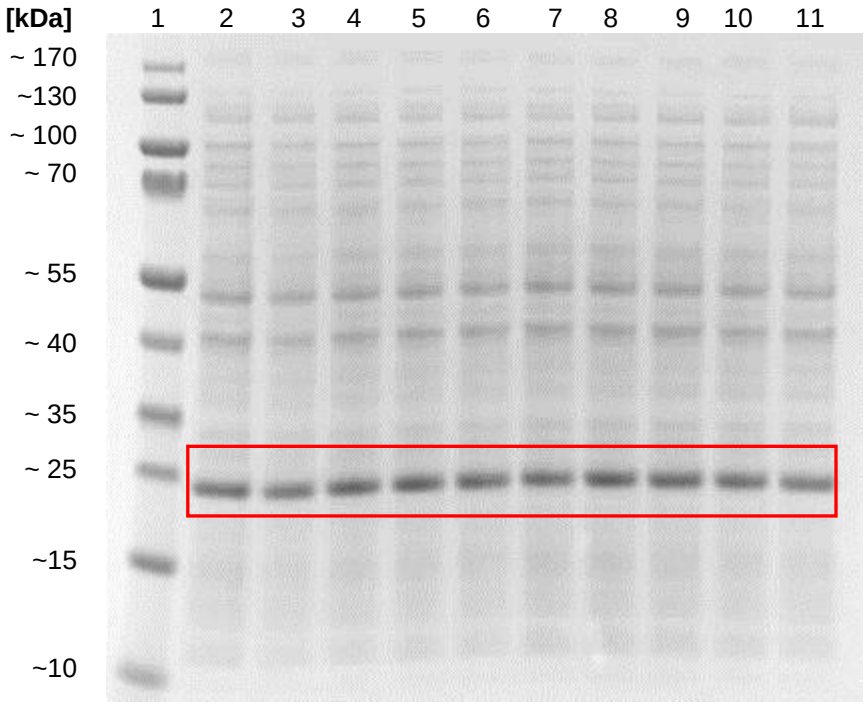

Figure 17: SDS-PAGE gel for the quantification [5 µg] of Cupin13 bands expressed in the presence of various $FeSO_4$ concentrations

Cupin13 could be seen at 21 kDa (red frame).

Lane 1: Standard marker "Page Ruler^{TM} Prestained Protein Ladder", **lane 2:** Cupin13 control no. 1, **lane 3:** Cupin13 with 10 µM $FeSO_4$ no. 1, **lane 4:** Cupin13 with 50 µM $FeSO_4$, **lane 5:** Cupin13 with 100 µM $FeSO_4$, **lane 6:** Cupin13 with 200 µM $FeSO_4$, **lane 7:** Cupin13 control no. 2, **lane 8:** Cupin13 with 10 µM $FeSO_4$ no. 2, **lane 9:** Cupin13 with 500 µM $FeSO_4$, **lane 10:** Cupin13 with 750 µM $FeSO_4$, **lane 11:** Cupin13 with 1,000 µM $FeSO_4$

No differences of the Cupin13 protein expression levels are visible (at 21 kDa, red frame) in the respective lanes (Figure 17).

Table 33: Result of the quantification [5 µg] of Cupin13 protein which was expressed in the presence of various $FeSO_4$ concentrations

Lane	Name	Average of triplicates [%]
2	Cupin13 control no. 1	33.01 ± 2.41
3	Cupin13 with 10 µM $FeSO_4$ no. 1	39.60 ± 4.45
4	Cupin13 with 50 µM $FeSO_4$	35.72 ± 3.02
5	Cupin13 with 100 µM $FeSO_4$	37.54 ± 4.73
6	Cupin13 with 200 µM $FeSO_4$	37.31 ± 3.54
7	Cupin13 control no. 2	30.83 ± 3.59
8	Cupin13 with 10 µM $FeSO_4$ no. 2	34.36 ± 3.14
9	Cupin13 with 500 µM $FeSO_4$	35.10 ± 1.29
10	Cupin13 with 750 µM $FeSO_4$	34.10 ± 3.30
11	Cupin13 with 1,000 µM $FeSO_4$	31.71 ± 4.38

Due to the information in Table 33, it seems that the presence of $FeSO_4$ has a small influence on the expression level. The highest expression level was detected in Cupin13 in the presence of 100 µM $FeSO_4$. Furthermore, Cupin13 in the presence of 1,000 µM $FeSO_4$ had nearly the same expression level as the control no. 2.

Afterwards, the activity of Cupin13 in the presence of various ferrous sulphate concentrations was analysed with the enzyme assay from Takenaka et al., which was modified for a total volume of 200 µL.

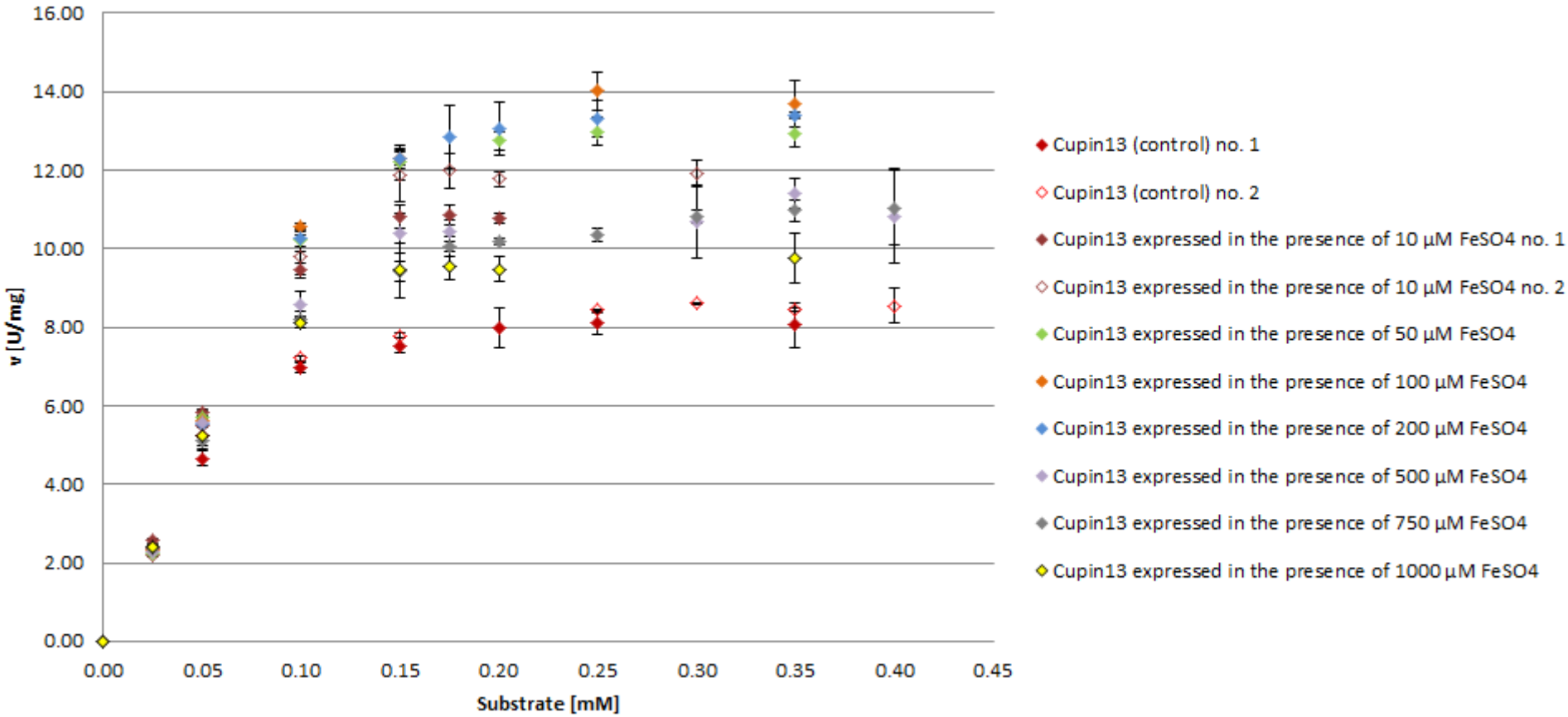

Figure 18: Kinetic of lysate containing Cupin13 protein, which was expressed in the presence of various $FeSO_4$ concentrations

The enzyme assay consisted of 0-400 µM 4A3HBA in 100 mM $NaPO_4$ buffer at pH 7.5. The reaction was started by adding 0.01 mg/mL (0.005 mg/mL final conc.) cleared lysate containing Cupin13 protein. Substrate conversion was monitored for 30 min at room temperature in a plate reader at a wavelength of 294 nm.

Table 34: Analysis of Cupin13 which was expressed in the presence of selected ferrous sulphate concentrations
The analysed samples contained the substrate 4A3HBA in the range of 0 to 400 µM in 100 mM $NaPO_4$ buffer at pH 7.5. The reaction was started by adding 0.01 mg/mL (0.005 mg/mL final conc.) cleared lysate containing Cupin13 protein and the substrate conversion was monitored for 30 min at 294 nm (room temperature) in a plate reader.

	specific activity [U/mg] of				
Name	lysate *	Cupin13	K_m [mM]	Cupin13 per well [µg]	k_{cat} of Cupin13 [s^{-1}]
Cupin13 control no. 1	8.05 # ± 0.58	24.37 # ± 1.75	0.05	0.33	8.47
Cupin13 control no. 2	8.45 # ± 0.05	27.41 # ± 1.09	0.05	0.30	9.64
Cupin13 with 10 µM $FeSO_4$ no. 1	10.77 #2 ± 0.13	27.20 #2 ± 0.32	0.05	0.39	9.47
Cupin13 with 10 µM $FeSO_4$ no. 2	11.77 #2 ± 0.18	34.24 #2 ± 0.52	0.05	0.30	11.97
Cupin13 with 50 µM $FeSO_4$	12.94 # ± 0.35	36.24 # ± 0.99	0.05	0.35	12.55
Cupin13 with 100 µM $FeSO_4$	13.68 # ± 0.58	36.45 # ± 0.40	0.06	0.37	12.90
Cupin13 with 200 µM $FeSO_4$	13.41 # ± 0.06	35.96 # ± 0.17	0.05	0.37	12.33
Cupin13 with 500 µM $FeSO_4$	11.40 # ± 0.37	32.46 # ± 1.07	0.05	0.35	10.65
Cupin13 with 750 µM $FeSO_4$	10.97 # ± 0.27	32.18 # ± 0.79	0.05	0.34	10.96
Cupin13 with 1,000 µM $FeSO_4$	9.76 # ± 0.63	30.79 # ± 1.97	0.04	0.31	10.64

* containing Cupin13, # from 0.35 mM 4A3HBA, #2 from 0.2 mM 4A3HBA

Based on the information in Table 34, it seems that ferrous sulphate had a small influence on the specific activity. The Cupin13 protein, which was expressed in the presence of 100 µM $FeSO_4$, resulted in the optimal enzyme activity (in Table 34 and Figure 18). Additionally, the specific activity of the Cupin13 protein decreased, which was expressed in the presence of more than 100 µM $FeSO_4$ (Table 34).

The difference between the Cupin13 control no. 1 and no. 2 is 4.73 % (specific activity of lysate containing Cupin13), 11.09 % (specific activity of Cupin13) and 12.13 % (k_{cat} of Cupin13). Furthermore, the difference between the Cupin13 with 10 µM $FeSO_4$ no. 1 and no. 2 is 8.49 % (specific activity of lysate containing Cupin13), 20.56 % (specific activity of Cupin13) and 20.88 % (k_{cat} of Cupin13). Due to this information, the process of Cupin13 without and in the presence of 10 µM ferrous sulphate (based on the lysate containing Cupin13 protein) is reproducible as the difference is lower than 10 %.

3.5 Analysis of the Cupin13 mutants

After various tests of Cupin13, mutations were integrated in the putative metal binding site (Cupin13-H52A, -N54A, -E58A, -H97A) as well as in the presumed active site (Cupin13-Q60A, -Q60F, -S62A, -S62Q, -F101A, -F101R, -R144I) by overlap extension PCR technique (described in 2.5). The result can be seen in (Figure 19).

The Cupin13 mutants were screened after colony PCR and the isolated plasmids were examined by control digestion.

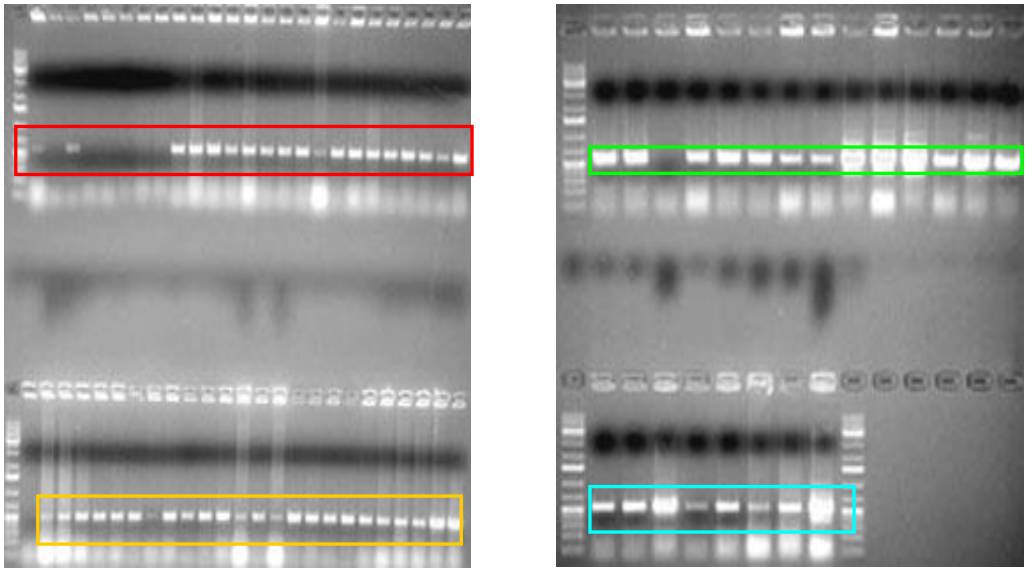

(A) **(B)**

Figure 19: 1 % Agarose control gel of Cupin13 mutants (colony PCR)

The Cupin13 mutants are visible at 537 bp (shown in coloured frames). L**ane 1** contained the standard "O'Gene Ruler 1kb Plus DNA Ladder" in each agarose gel and additionally, in the lower section of **(B)** in **lane 10**.

The agarose control gel **(A)** included the amplified DNA fragment of Cupin13-H52A **(lanes 2-9)**, Cupin13-N54A **(lanes 10-17)**, Cupin13-E58A **(lanes 18-25)** and Cupin13-H97A **(lane 26)** in the upper (red) frame. Additionally, the lower (orange) frame showed Cupin13-H97A **(lanes 2-8)**, Cupin13-S62A **(lanes 9-16)**, Cupin13-S62Q **(lanes 17-24)** and Cupin13-F101A **(lanes 25-26)**.

The agarose control gel **(B)** contained the amplified DNA fragment of Cupin13-F101A **(lanes 2-7)** and Cupin13-F101R **(lanes 8-15)** in the upper (green) frame, while Cupin13-R144I **(lanes 2-9)** is visible in the lower (cyan) frame.

The overlap extension PCR followed by digestion and subsequently, ligation was performed with success, due to the fact that the bands of the Cupin13 including

mutation could be identified by comparison with the standard at a size of 537 bp (Figure 19). Furthermore, the result of the control digestion was that two bands could be identified at 4,069 bp and 1,814 bp and indicated, due to the size of the bands, that Cupin13 was ligated in the pET28-vector. In the case that Cupin13 was not successfully ligated in the pET28-vector, two bands are visible at 1277 bp and 3969 bp.

3.5.1 Analysing the expression level of the Cupin13 variants

The *E. coli* BL21-Gold (DE3) cells, containing the pET28-Cupin13 mutant constructs, were harvested from the main culture and the weight of the respective pellet is listed in Table 35. Afterwards, the *E. coli* cells were broken (described in 2.3.1), moreover, the soluble and insoluble fractions (2.3.2) were analysed on an SDS-PAGE gel (Figure 20).

Table 35: Cupin13 protein variants expressed of *E. coli* BL21-Gold (DE3) cells

Name	Wet pellet [g]	Protein conc. (soluble fraction) [mg/mL]	Protein conc. (insoluble fraction) [mg/mL]
E. coli control (pET26-Cupin13)	1.61	5.78 ± 0.27	1.37 ± 0.15
E. coli (Cupin13-H52A)	1.56	3.77 ± 0.34	1.36 ± 0.30
E. coli (Cupin13-N54A)	1.43	3.69 ± 0.43	0.22 ± 0.24
E. coli (Cupin13-E58A)	1.61	4.87 ± 0.05	1.22 ± 0.18
E. coli (Cupin13-H97A)	1.49	3.61 ± 0.34	1.14 ± 0.21
E. coli (Cupin13-Q60A)	1.68	6.02 ± 0.36	0.21 ± 0.15
E. coli (Cupin13-Q60F)	1.61	4.75 ± 0.47	0.12 ± 0.05
E. coli (Cupin13-S62A)	1.92	6.13 ± 0.09	2.19 ± 0.05
E. coli (Cupin13-S62Q)	1.62	5.18 ± 0.10	0.99 ± 0.17
E. coli (Cupin13-F101A)	1.72	6.13 ± 0.21	2.30 ± 0.14
E. coli (Cupin13-F101R)	1.82	4.76 ± 0.32	1.59 ± 0.29
E. coli (Cupin13-R144I)	1.82	5.50 ± 0.30	2.57 ± 0.15

Based on these results, which are shown in Table 35, it can be seen that the protein concentration is higher in the soluble fraction than in the insoluble fraction. Additionally, the highest protein concentration of the soluble fraction was detected in *E. coli* (Cupin13-S62A) as well as in (Cupin13-F101A), while the lowest protein concentration was detected in the Cupin13-H97A (Table 35).

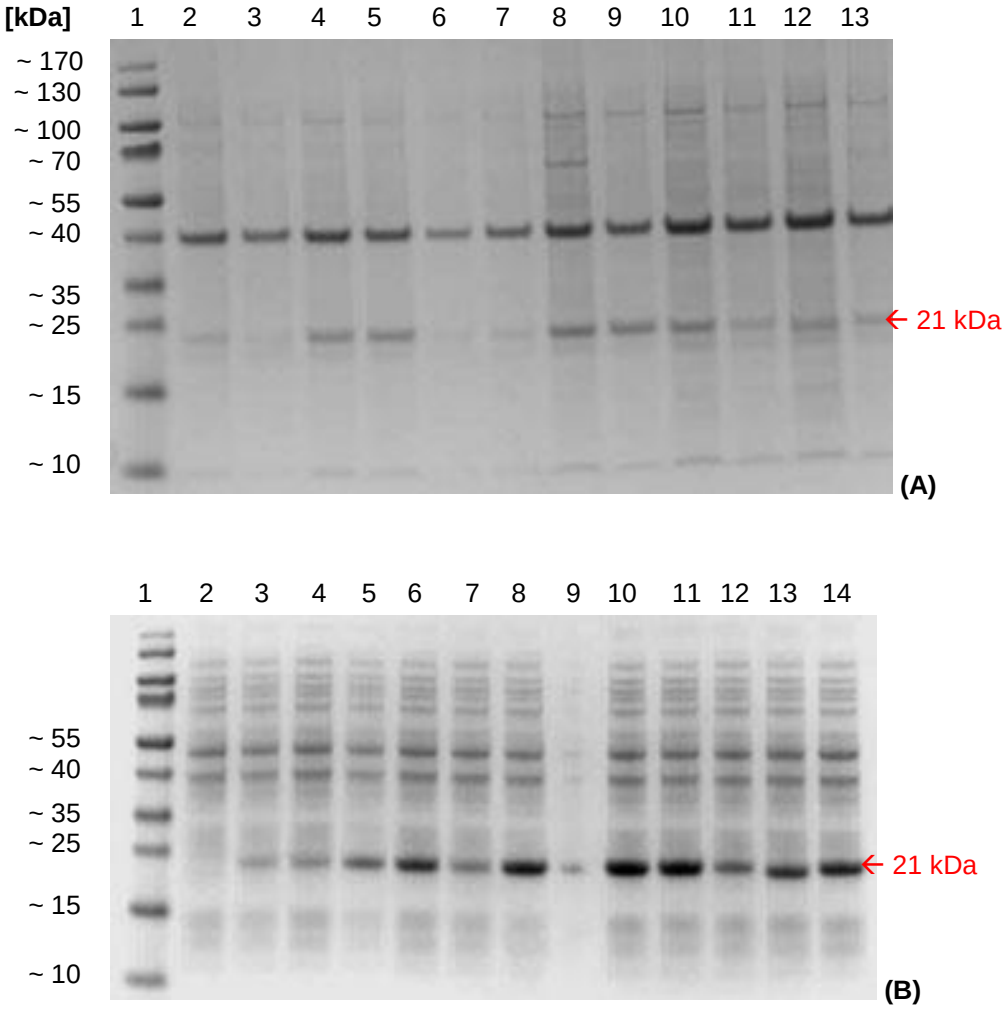

Figure 20: SDS-PAGE gel of the expression of mutated Cupin13 protein in *E. coli*
The Cupin13 protein is visible at 21 kDa in the insoluble fractions **(A)** and soluble fraction **(B)**. **Lane 1**: standard marker "Page Ruler™ Prestained Protein Ladder" (in A and B).
(A) and **(B)** included Cupin13-H52A **(lane 2)**, Cupin13-N54A **(lane 3)**, Cupin13-E58A **(lane 4)**, Cupin13-H97A **(lane 5)**, Cupin13-Q60A **(lane 6)**, Cupin13-Q60F **(lane 7)**, Cupin13-S62A **(lane 8 and in (B) lane 8 + 9)**, Cupin13-S62Q **(lane 9 and in (B) lane 10)**, Cupin13-F101A **(lane 10 and in (B) lane 11)**, Cupin13-F101R **(lane 11 and in (B) lane 12)**, Cupin13-R144I **(lane 12 and in (B) lane 13)**, Cupin13 control without mutation (**lane 13 and in (B) lane 14)**

The Cupin13 protein variants are clearly visible at 21 kDa in the soluble fraction and less in the insoluble fraction (Figure 20). Furthermore, no protein (Cupin13-H52A) can be seen in the gel (B) in the lane 2. Subsequently, the amount of protein was determined and calculated (described in 2.3.3). The results are listed in Table 35.

3.5.2 Detecting the enzyme activity of the mutated Cupin13 protein

The activity of the cleared lysates, containing the Cupin13 protein variants (from pET28-Cupin13 mutant constructs) was tested with the substrate 4A3HBA using the enzyme assay based on Takenaka et al.

From the eleven tested mutated Cupin13 proteins only five were active (Cupin13-Q60A, -Q60F, -S62A, -S62Q, -R144I) and the results are listed in Table 36.

Table 36: Determination of the activity of the Cupin13 mutants
The enzyme assay was modified and included 10 µM 4A3HBA substrate in 100 mM $NaPO_4$ buffer at pH 7.5. The reaction was started by adding 0.01 mg/mL (0.005 mg/mL final conc.) cleared lysate containing Cupin13 (including mutations). The substrate conversion was monitored for 30 min at room temperature in a plate reader at a wavelength of 294 nm. The total protein amount was 1 µg per well.

Cupin13 mutants	Amino acid exchange	Activity [U/mL]
1	H52A	n.d.
2	N54A	n.d.
3	E58A	n.d.
4	H97A	n.d.
5	Q60A	0.61
6	Q60F	0.49
7	S62A	6.50
8	S62Q	0.10
9	F101A	n.d.
10	F101R	n.d.
11	R144I	4.26
Cupin13 control *	---	5.35

n.d. = not determinable, * pET26-Cupin13 construct

Interestingly, the Cupin13-S62A was more active than the control (Table 36).

3.5.3 Analysis of the mutated Cupin13-Q60A, -R144I and -S62A without and in the presence of ferrous sulphate

Due to this information, the most active Cupin13 protein variants (Cupin13-Q60A, -S62A and -R144I) were tested with and without the addition of 100 µM $FeSO_4$ into the main culture. Moreover, they were compared with the wild type Cupin13 protein, which was used as control. The precultures and main cultures were produced as described in

2.3.1. Additionally, 100 µM $FeSO_4$ was optionally added in the main culture before the expression was started by adding 0.1 mM IPTG and the results are shown in Table 37.

Table 37: Mutated Cupin13 proteins expressed without and with the addition of 100 µM $FeSO_4$

Name	Wet pellet [g]	Protein conc. [mg/mL]
E. coli control no. 1 (pET26-Cupin13)	2.0	5.25 ± 0.05
E. coli control no. 2 (pET26-Cupin13) *	1.8	5.68 ±0.04
E. coli no. 1 (Cupin13-Q60A)	1.8	5.19 ± 0.13
E. coli no. 2 (Cupin13-Q60A) *	1.9	5.65 ± 0.07
E. coli no. 1 (Cupin13-S62A)	2.0	7.02 ± 0.04
E. coli no. 2 (Cupin13-S62A) *	1.9	7.35 ± 0.06
E. coli no. 1 (Cupin13-R144I)	1.8	5.89 ± 0.06
E. coli no. 2 (Cupin13-R144I) *	1.8	5.88 ± 0.10

* 100 µM $FeSO_4$ was added in the media of the main culture

The protein concentration (without and in the presence of 100 µM $FeSO_4$ supplemented in the main culture) of the controls was lower than the Cupin13-S62A and higher in comparison to Cupin13-Q60A as well as Cupin13-R144I (Table 37).
Afterwards, the expression levels of the Cupin13 mutants with and without the addition of ferrous sulphate were determined. Therefore, the bands [5 µg] were compared to each other on the SDS-PAGE gel (Figure 21).

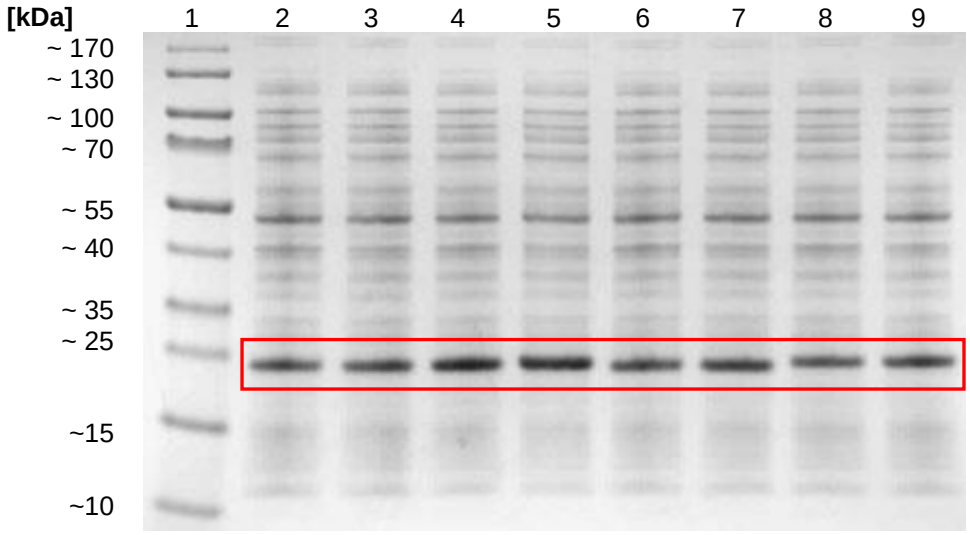

Figure 21: SDS-PAGE gel for the quantification [5 µg] of the bands of Cupin13 protein mutants, which were expressed in the presence or absence of 100 µM $FeSO_4$

The expressed mutated Cupin13 proteins with and without the addition of 100 µM $FeSO_4$ are visible at 21 kDa (red frame). Furthermore, the mutated Cupin13 proteins without metal salt can be seen in the lanes 2, 4, 6 and 8, whereas the mutated Cupin13 proteins with 100 µM $FeSO_4$ are loaded in the lanes 3, 5, 7 and 9.

Lane 1: Standard marker „Page Ruler^{TM} Prestained Protein Ladder", **lanes 2, 3:** Cupin13-Q60A, **lanes 4, 5:** Cupin13-S62A, **lanes 6, 7:** Cupin13-R144I, **lanes 8, 9:** Cupin13 control (from pET26-Cupin13 construct)

Table 38: Result of the quantification [5 µg] of mutated Cupin13 proteins, which were expressed in the presence or absence of 100 µM $FeSO_4$

Lane	Name	Average of triplicates [%]
2	Cupin13-Q60A	28.92 ± 1.22
3	Cupin13-Q60A with 100 µM $FeSO_4$	29.49 ± 2.45
4	Cupin13-S62A	37.39 ± 0.52
5	Cupin13-S62A with 100 µM $FeSO_4$	40.07 ± 1.32
6	Cupin13-R144I	28.88 ± 0.79
7	Cupin13-R144I with 100 µM $FeSO_4$	32.52 ± 1.28
8	Cupin13 control	28.01 ± 1.02
9	Cupin13 control with 100 µM $FeSO_4$	32.66 ± 0.85

The protein expression level of the modified protein Cupin13-S62A (lanes 4, 5) is higher than the one of the Cupin13 control (lanes 8, 9). Furthermore, the Cupin13

control, Cupin13-Q60A and Cupin13-R144I seem to be visually similar (Figure 21 and Table 38).

Afterwards, the activity of the lysate containing mutated Cupin13 protein was tested with 4A3HBA using the enzyme assay based on Takenaka et al.

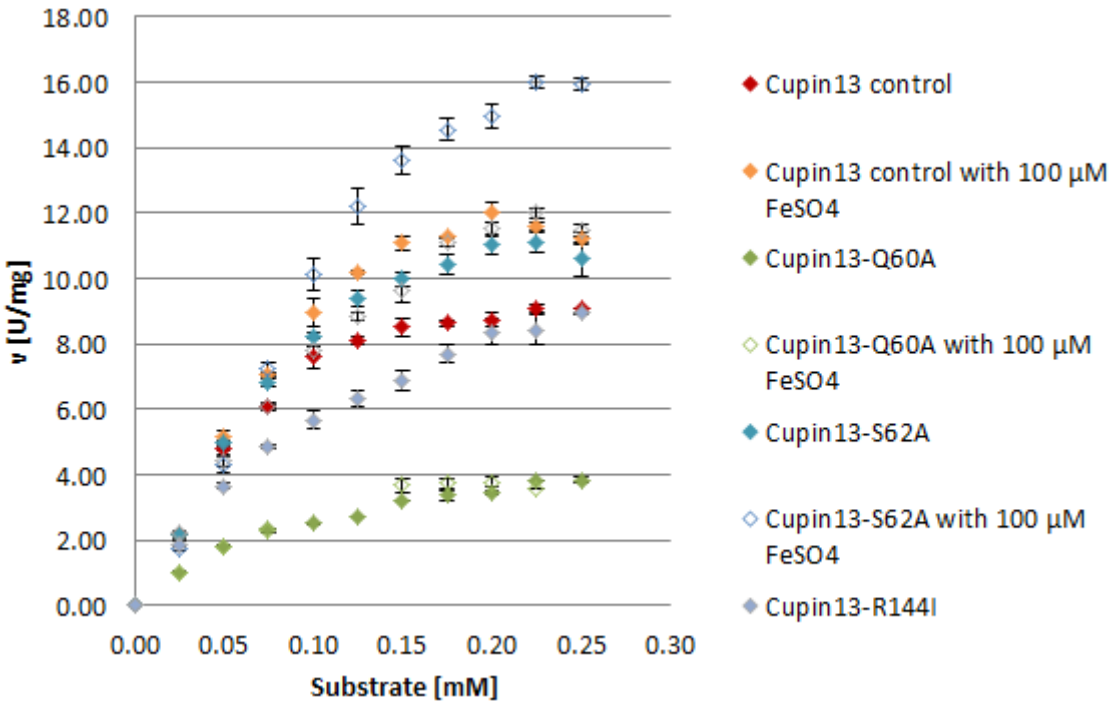

Figure 22: Activity of lysate containing Cupin13 protein mutants in the presence or absence of 100 µM $FeSO_4$

The enzyme assay contained of 0-250 µM 4A3HBA in 100 mM $NaPO_4$ buffer at pH 7.5. The reaction was started by adding 0.01 mg/mL (0.005 mg/mL final conc.) cleared lysate, which contained the mutated Cupin13 proteins. The substrate conversion was monitored for 30 min at room temperature in a plate reader at a wavelength of 294 nm.

Table 39: Analysis of Cupin13 variant proteins in the presence or absence of 100 µM $FeSO_4$
The enzyme assay was modified and the tested samples included the substrate 4A3HBA in the range of 0 to 250 µM, dissolved in 100 mM $NaPO_4$ buffer at pH 7.5. The reaction was started by the addition of 0.01 mg/mL (0.005 mg/mL final conc.) cleared lysate containing mutated Cupin13 protein. Moreover, the substrate conversion was monitored for 30 min at room temperature in a plate reader at a wavelength of 294 nm.

	specific activity [U/mg] of				
Name	lysate *[2]	Cupin13	K_m [mM]	Cupin13 per well [µg]	k_{cat} of Cupin13 [s^{-1}]
Cupin13 control	9.07 [#2] ± 0.13	32.39 [#2] ± 0.45	0.04	0.28	10.77
Cupin13 control *	11.61 [#2] ± 0.11	35.56 [#2] ± 0.33	0.05	0.32	11.88
Cupin13-Q60A	3.45 [#] ± 0.05	11.93 [#] ± 0.17	0.05	0.28	4.02
Cupin13-Q60A *	3.79 [#] ± 0.18	12.84 [#] ± 0.61	0.05	0.29	4.44
Cupin13-S62A	11.13 [#2] ± 0.31	29.76 [#2] ± 0.84	0.05	0.37	10.28
Cupin13-S62A *	16.01 [#2] ± 0.18	39.95 [#2] ± 0.44	0.07	0.40	13.80
Cupin13-R144I	8.43 [#2] ± 0.51	29.20 [#2] ± 1.78	0.05	0.28	10.09
Cupin13-R144I *	12.00 [#2] ± 0.13	36.90 [#2] ± 0.39	0.05	0.32	12.75

* with 100 µM $FeSO_4$, *[2] containing Cupin13 mutants, [#] of 0.20 mM 4A3HBA, [#2] of 0.23 mM 4A3HBA,

The specific activity and k_{cat} are higher in the samples, which contained 100 µm $FeSO_4$. Additionally, the best specific activity of lysate containing Cupin13 was received from Cupin13-S62A without and in the presence of ferrous sulphate. The weakest specific activity and k_{cat} were detected in Cupin13-Q60A (Table 39).

Afterwards, the stability of the Cupin13 protein variants was tested. Therefore, the results of the specific activity of freshly cleared lysates (containing Cupin13 proteins with mutation) were compared with the specific activity of the same lysates, which were stored for one week at 4 °C and the headspace of the reaction tube was purged with gaseous nitrogen.

Table 40: Stability testing of mutated Cupin13 proteins

	specific activity [U/mg] of				stability difference of	
Name	lysate fresh *4	lysate *4, *3	Cupin13 fresh	Cupin13 *3	lysate *4 [%]	Cupin13 [%]
Cupin13 control *	9.07 *6 ± 0.13	9.00 *6 ± 0.12	32.39 *6 ± 0.45	32.15 *6 ± 0.45	0.78	0.75
Cupin13 control *,*2	11.61 *6 ± 0.11	11.98 *6 ± 0.29	35.56 *6 ± 0.33	36.69 *6 ± 0.89	3.09	3.08
Cupin13-Q60A	3.45 *5 ± 0.05	3.01 *5 ± 0.01	11.93 *5 ± 0.17	10.42 *5 ± 0.01	14.62	14.49
Cupin13-Q60A *2	3.79 *5 ± 0.18	3.47 *5 ± 0.10	12.84 *5 ± 0.61	11.79 *5 ± 0.35	9.22	8.91
Cupin13-S62A	11.13 *6 ± 0.31	11.82 *6 ± 0.33	29.76 *6 ± 0.84	31.60 *6 ± 0.88	5.84	5.82
Cupin13-S62A *2	16.01 *6 ± 0.18	13.75 *6 ± 0.45	39.95 *6 ± 0.44	34.32 *6 ± 1.13	16.44	16.40
Cupin13-R144I	8.43 *6 ± 0.45	7.42 *6 ± 0.10	29.20 *6 ± 1.57	25.70 *6 ± 0.35	13.61	13.62
Cupin13-R144I *2	12.00 *6 ± 0.13	10.84 *6 ± 0.50	36.90 *6 ± 0.39	33.33 *6 ± 1.55	10.70	10.26

* pET26-Cupin13 construct, *2 with 100 µM $FeSO_4$ in the main culture, *3 kept at 4 °C for one week and the headspace of the reaction tube was purged with the N_2 (gas), *4 containing Cupin13 protein variants, *5 of 20 mM 4A3HBA, *6 of 0.23 mM 4A3HBA

The specific enzyme activity was tested of the mutated enzymes and its lysate to determine the enzyme stability after storage. The difference of the detected activity of the Cupin13 control (0.78 % and 0.75 %) as well as the Cupin13-S62A (5.84 % and 5.82 %) in the absence of ferrous sulphate was lower than 10 %. Additionally, the Cupin13 control and the Cupin13-Q60A in the presence of 100 µM $FeSO_4$ had lower than 10 % activity difference (Table 40). Consequently, the stored proteins could be considered as stable.

3.5.4 Analysis of inactive and low active mutants in the presence of $FeSO_4$

Due to the results, which are shown in Table 36, the inactive and less active mutants were tested with 100 µM $FeSO_4$, which was added into the expression medium. The precultures and main cultures were produced as described in 2.3.1. Additionally,

100 µM $FeSO_4$ were added in the main culture before the expression was started by the addition of 0.1 mM IPTG and the results can be seen in Table 41.

Table 41: Determination of the protein concentration of Cupin13 protein variants

Name	Wet pellet [g]	Protein conc. [mg/mL]
E. coli control (pET26-Cupin13 contstruct) *	1.6	4.38 ± 0.04
E. coli (Cupin13-N54A) *	1.6	3.84 ± 0.06
E. coli (Cupin13-E58A) *	1.8	4.15 ± 0.19
E. coli (Cupin13-H97A) *	1.8	4.83 ± 0.07
E. coli (Cupin13-Q60F) *	1.7	4.08 ± 0.03
E. coli (Cupin13-S62Q) *	1.8	6.25 ± 1.01
E. coli (Cupin13-F101A) *	1.7	5.61 ± 0.17
E. coli (Cupin13-F101R) *	1.7	4.97 ± 0.05

* 100 µM $FeSO_4$ added in the main culture

The *E. coli* cells of the Cupin13 control as well as the one which contained the modified Cupin13-N54A had nearly the same weight, but both were lighter in comparison to the other tested pellets. Furthermore, the highest and lowest protein concentration was detected in the mutated Cupin13-F101A and Cupin13-N54A protein (Table 41).

Afterwards, the expression levels of the Cupin13 mutants with 100 µM $FeSO_4$ were compared by gel quantification [5 µg] of the bands on an SDS-PAGE gel (Figure 23).

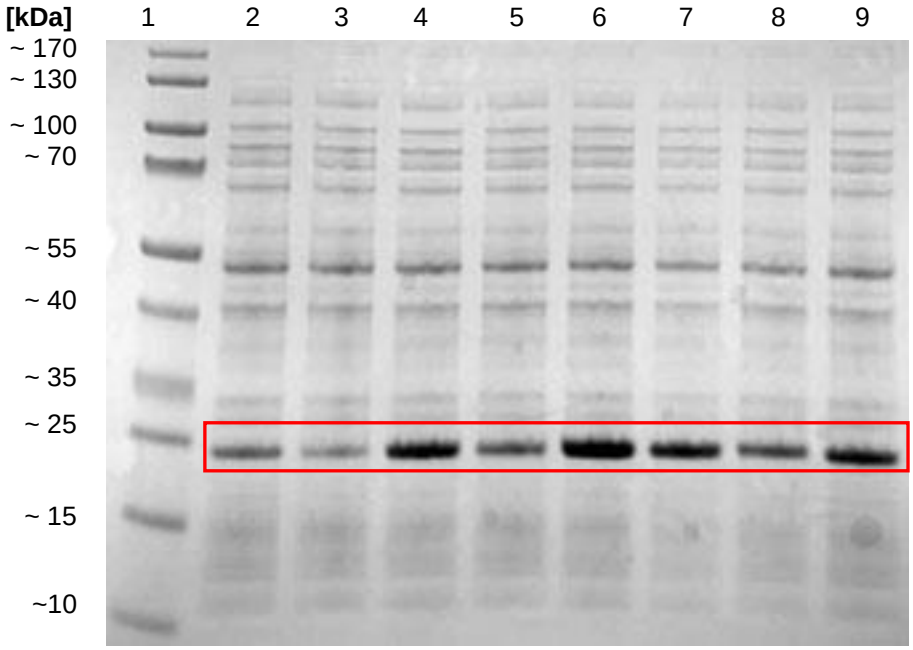

Figure 23: SDS-PAGE gel for the quantification [5 µg] of low active and inactive Cupin13 mutants bands expressed in the presence of 100 µM $FeSO_4$

The band (of the Cupin13, which is from pET28-Cupin13 construct) was visible in all tested samples, which contained the mutated proteins at a molecular mass of 21 kDa (red frame). **Lane 1:** Standard marker "Page Ruler^{TM} Prestained Protein Ladder", **lane 2:** Cupin13-N54A, **lane 3:** Cupin13-E58A, **lane 4:** Cupin13-H97A, **lane 5:** Cupin13-Q60F, **lane 6:** Cupin13-S62Q, **lane 7:** Cupin13-F101A, **lane 8:** Cupin13-F101R, **lane 9:** Cupin13 (pET26-Cupin13 construct)

Table 42: Results of the gel quantification [5 µg] of less active and inactive mutated Cupin13 proteins in the presence of 100 µM $FeSO_4$

Name	Average of triplicates [%]
Cupin13 control (pET26-Cupin13 construct) [1]	40.50 ± 1.31
Cupin13-N54A [1,2]	24.65 ± 1.11
Cupin13-E58A [1,2]	16.89 ± 0.90
Cupin13-H97A [1,2]	42.96 ± 1.67
Cupin13-Q60F [1,2]	28.51 ± 0.65
Cupin13-S62Q [1,2]	52.13 ± 1.56
Cupin13-F101A [1,2]	49.18 ± 1.56
Cupin13-F101R [1,2]	34.83 ± 0.66

[1] 100 µM $FeSO_4$ (added to the expression medium), [2] pET28-Cupin13 variants construct

The protein expression of the control was on the one hand lower than Cupin13-S62Q, -F101A and -H97A and on the other hand higher than Cupin13-F101R, -Q60F and -E58A (Table 42 and Figure 23). Furthermore, the highest and lowest protein

expression level was detected in the modified samples Cupin13-S62A and Cupin13-E58A.

Afterwards, the activity of the lysates was tested with 4A3HBA using the enzyme assay based on Takenaka et al. in the presence of 100 µM $FeSO_4$, which was added in the main culture.

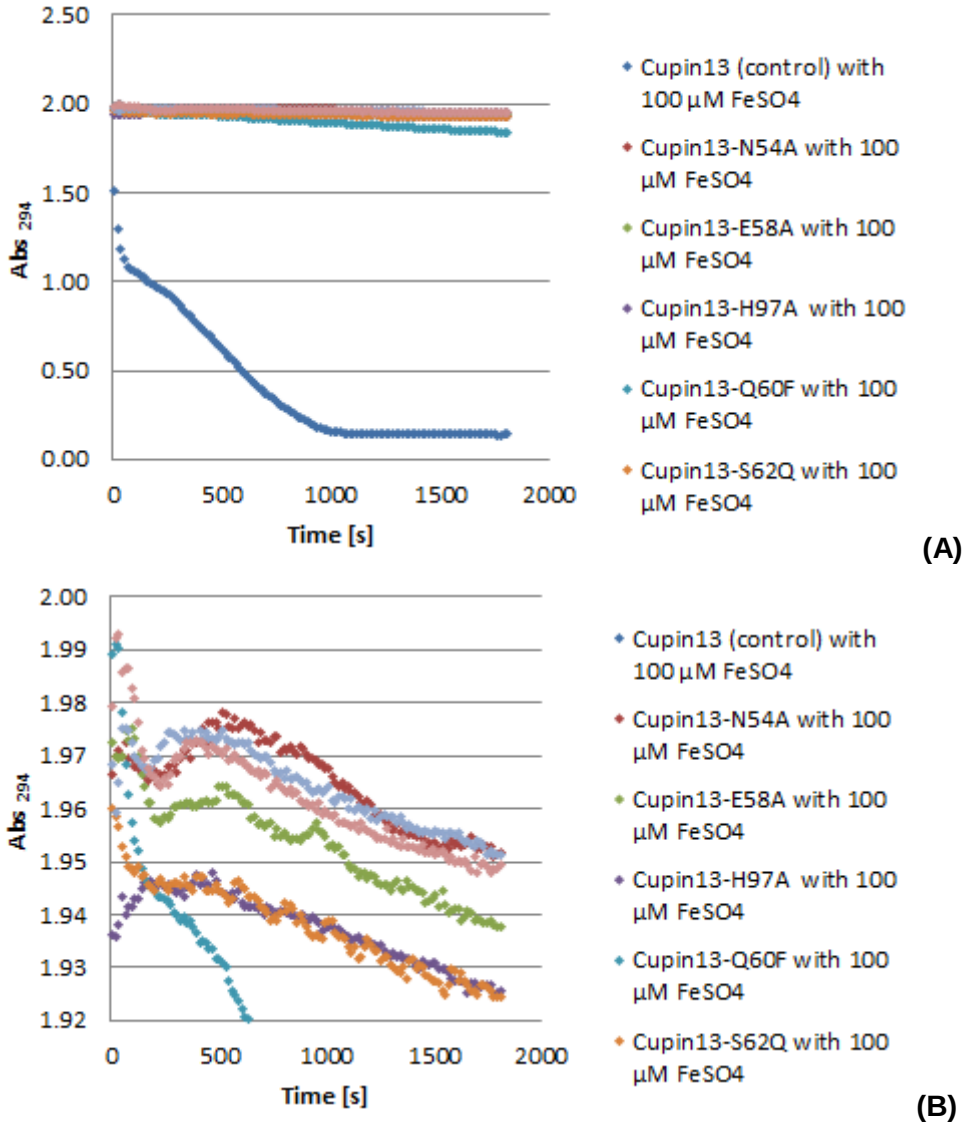

Figure 24: Monitoring the activity of the lysate containing Cupin13 mutants with low or no activity in the presence of 100 µM $FeSO_4$ (A) all samples are shown (B) some selected samples are shown in detail (zoomed)

The samples of the analyses contained the 500 µM 4A3HBA substrate (in 100 mM $NaPO_4$ buffer at pH 7.5) as well as 0.01 mg/mL (0.005 mg/mL final conc.) cleared lysate including mutated Cupin13 proteins in the presence of 100 µM $FeSO_4$. The substrate conversion was monitored for 30 min at room temperature in a plate reader at a wavelength of 294 nm.

The pET26-Cupin13 construct, which was used as control, was active and moreover, a very low activity could be detected for Cupin13-Q60F, while the other Cupin13 mutants were inactive (Figure 24, (A). Due to this information, the Figure 24 (A) was zoomed for better analysis and hence, a slightly activity could be determined for the Cupin13-Q60F and -S62Q mutants (Figure 24, (B).

3.5.5 Comparison of the Cupin13-H52A with the wild type protein

The modified protein Cupin13-H52A was not visible on the gel of the soluble fraction (Figure 20, (B)) and signifies that the protein was not expressed. Due to this information, the analysis of this protein was repeated with and without the presence of 100 µM $FeSO_4$ to find out whether ferrous sulphate influences the protein expression. Precultures and main cultures were produced as described in 2.3.1. Moreover, 100 µM $FeSO_4$ were optionally added in the main culture before the expression was started by the addition of 0.1 mM IPTG and the results are listed in Table 43.

Table 43: Determination of the protein concentration of the Cupin13-H52A protein

Name	Wet pellet [g]	Protein conc. [mg/mL]
E. coli control (pET26-Cupin13)	1.7	2.97 ± 0.08
E. coli control (pET26-Cupin13) *	1.8	2.98 ± 0.17
E. coli (Cupin13-H52A)	1.7	2.50 ± 0.10
E. coli (Cupin13-H52A) *	1.8	2.57 ± 0.05

* 100 µM $FeSO_4$ was added in the main culture

The same weight of the pellet with and without adding 100 µM $FeSO_4$ showed the control as well as the modified Cupin13-H52A mutant (Table 43). Furthermore, the protein concentration of the controls was higher than the one of the modified Cupin13-H52A protein (Table 43).

Afterwards, the expression level of Cupin13 in the presence and absence of 100 µM $FeSO_4$ was compared by gel quantification [5 µg] with the bands of a previously performed SDS-PAGE (Figure 25).

The results shown in the Figure 25 were the same as shown in Figure 20 (B). Consequently, no Cupin13-H52A protein was expressed with and without adding 100 µM $FeSO_4$ in the main culture.

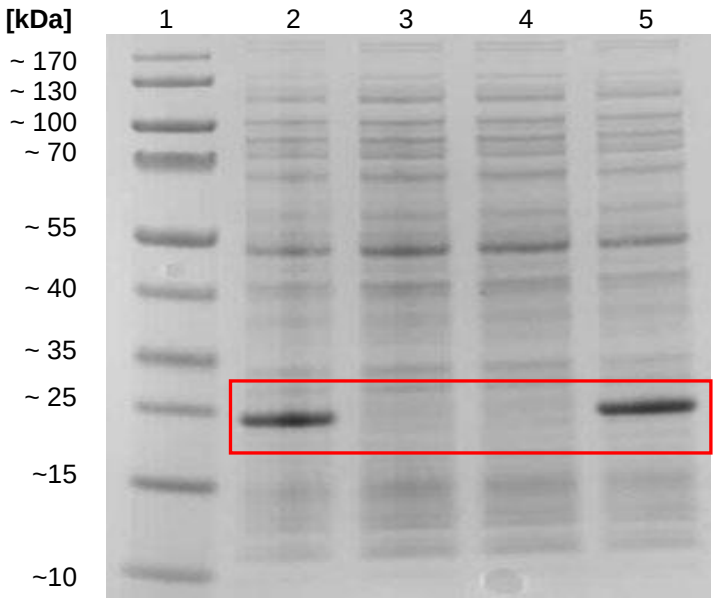

Figure 25: SDS-PAGE gel for quantification [5 µg] of the Cupin13-H52A protein bands

Only the band of Cupin13 protein control (pET26-Cupin13 construct) was visible at 21 kDa (red frame). The 100 µM $FeSO_4$ was available in the expression medium of Cupin13-H52A (lane 3) and Cupin13 control (lane 5).

Lane 1: Standard marker "Page Ruler^{TM} Prestained Protein Ladder", **lanes 2, 5:** Cupin13 (pET26-Cupin13 construct), **lanes 3, 4:** Cupin13-H52A (pET28-Cupin13-H52A construct).

3.6 Activity testing of the whole intact *E. coli* BL21-Gold (DE3) cells

The whole intact *E. coli* BL21-Gold (DE3) cells were always broken to receive the Cupin13 protein with or without mutation. Until now it is still unknown if these cells, which contained the pET26-Cupin13 construct, possess the ability to converse the substrate 4A3HBA (described in 2.4.2). The amount of whole intact *E. coli* BL21-Gold (DE3) cells and the substrate 4A3HBA have to be determined, which can be used for the plate reader (until the detection limit was reached). At first, the selected whole intact cell concentration in the range of 0 to 10 mg cells/mL was measured in the absence of the substrate (4A3HBA).

Table 44: Determination of the amount of whole intact *E. coli* BL21-Gold (DE3) cells

Name	0 mg cells/mL	0.01 mg cells/mL	0.5 mg cells/mL	1 mg cells/mL	5 mg cells/mL	10 mg cells/mL
Average of the tested triplicates	0.06 ± 0.00	0.07 ± 0.00	0.58 ± 0.01	0.99 ± 0.01	2.27 ± 0.02	3.26 ± 0.02

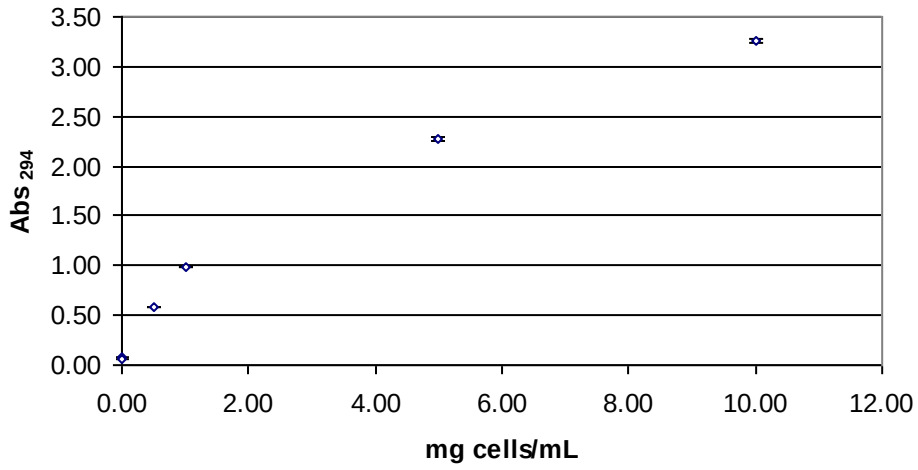

Figure 26: Determination of the amount of whole intact *E. coli* BL21-Gold (DE3) cells
The well (of the UV-Star Microplate 96-well, F-bottom) contained the respective concentration of mg cells/mL (Table 44) in 100 mM $NaPO_4$ buffer at pH 7.5 in a total volume of 200 µL per well. Afterwards, the samples, which contained the *E. coli* cells as well as $NaPO_4$ buffer, were measured at room temperature in a plate reader at a wavelength of 294 nm.

Based on the obtained information, which is depicted in Figure 26, it is only possible to work with concentrations up to 10 mg cells/mL. In the next step, the plate reader was tested with the same cell concentrations (Table 44) and with 1,000 µM of the substrate 4A3HBA.

Table 45: Determination of the amount of whole intact *E. coli* BL21-Gold (DE3) cells in the presence of 4A3HBA

Name	0 mg cells/mL	0.01 mg cells/mL	0.5 mg cells/mL	1 mg cells/mL	5 mg cells/mL	10 mg cells/mL
Average of the tested triplicates	1.50 ± 0.38	1.60 ± 0.42	1.93 ± 0.43	2.18 ± 0.39	3.08 ± 0.33	3.33 ± 0.32

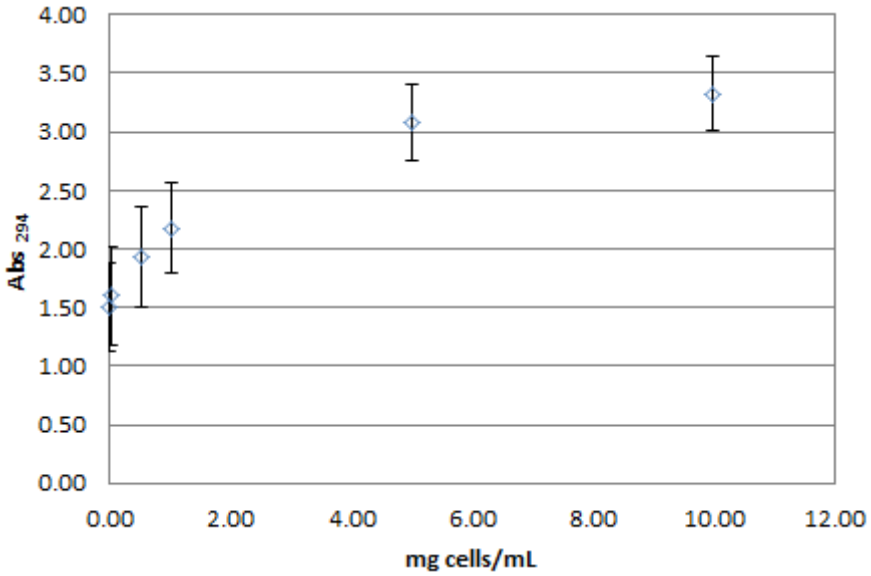

Figure 27: Determination of the amount of whole intact *E. coli* BL21-Gold (DE3) cells in the presence of 4A3HBA

The well (of the UV-Star Microplate 96-well, F-bottom) contained the respective concentration of mg cells/mL (Table 45) in 100 mM $NaPO_4$ buffer at pH 7.5 and 1,000 µM 4A3HBA in a total volume of 200 µL per well. Afterwards, the samples, which contained the *E. coli* cells as well as $NaPO_4$ buffer, were measured at room temperature in a plate reader at a wavelength of 294 nm.

Due to the results, which are depicted in Figure 27 in comparison to the one shown in Figure 26, it can be seen that the slope decreased at a concentration of approximately 5 mg cells/mL, which showed a detected absorption of 3.24. Therefore, the linear range of the concentration 0 to 3.5 mg cells/mL was tested again without and in the presence of 1,000 µM substrate (4A3HBA).

Table 46: Determination of the linear detection range of the plate reader testing whole intact *E. coli* BL21-Gold (DE3) cells in the concentration range of 0 to 3.5 mg cells/mL

Name	0 mg cells/ mL	0.5 mg cells/ mL	1.0 mg cells/ mL	1.5 mg cells/ mL	2.0 mg cells/ mL	2.5 mg cells /mL	3.0 mg cells/ mL	3.5 mg cells/ mL
Average of the tested triplicates	0.07 ± 0.01	0.60 ± 0.01	0.98 ± 0.02	1.36 ± 0.01	1.54 ± 0.01	1.71 ± 0.01	1.87 ± 0.01	1.99 ± 0.01

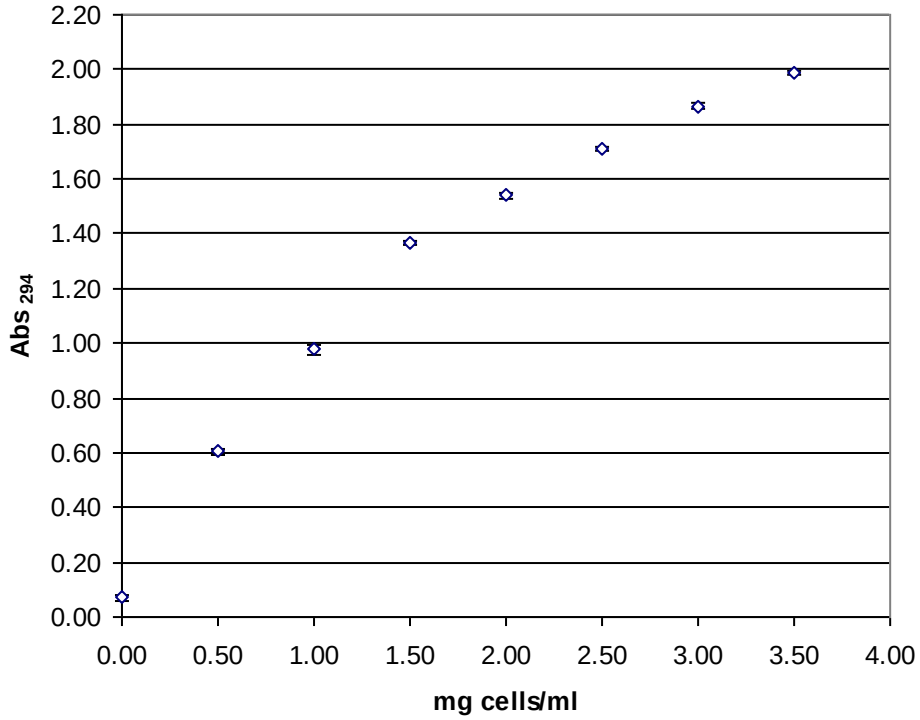

Figure 28: Determination of the linear detection range of the plate reader testing whole intact *E. coli* BL21-Gold (DE3) cells in the range of 0 to 3.5 mg cells/mL

The well (of the UV-Star Microplate 96-well, F-bottom) contained the respective concentration of mg cells/mL (Table 46) in 100 mM $NaPO_4$ buffer at pH 7.5 in a total volume of 200 µL per well. Afterwards, the samples, which contained the *E. coli* cells as well as $NaPO_4$ buffer, were measured at room temperature in a plate reader at a wavelength of 294 nm.

The linear range was determined for concentrations up to 1.50 mg cells/mL and had an absorption value of 1.36 (Figure 28). Due to this performed testing, the next measurement contained the same cell concentration (Table 46) and 1,000 µM of the substrate 4A3HBA.

Table 47: Determination of the linear detection range of the plate reader testing whole intact *E. coli* BL21-Gold (DE3) cells in the concentration range of 0 to 3.5 mg cells/mL in the presence of 1,000 µM 4A3HBA

Name	0 mg cells/ mL	0.5 mg cells/ mL	1.0 mg cells/ mL	1.5 mg cells/ mL	2.0 mg cells/ mL	2.5 mg cells/ mL	3.0 mg cells/ mL	3.5 mg cells/ mL
Average of the tested	0.05	0.30	2.47	2.72	2.85	3.00	3.10	0.09
triplicates	±	±	±	±	±	±	±	±
	0.00	0.01	0.00	0.02	0.00	0.02	0.01	0.05

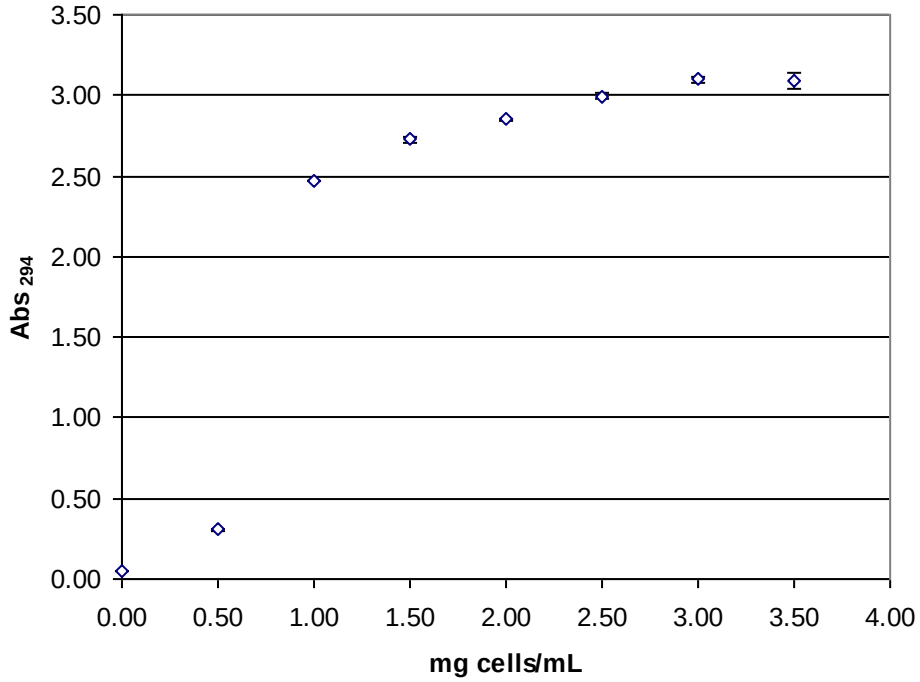

Figure 29: Determination of the linear detection range of the plate reader testing whole intact *E. coli* BL21-Gold (DE3) cells in the concentration range of 0 to 3.5 mg cells/mL in the presence of 1,000 µM 4A3HBA

The well (of the UV-Star Microplate 96-well, F-bottom) contained the respective concentration of mg cells/mL (Table 47) in 100 mM $NaPO_4$ buffer at pH 7.5 in a total volume of 200 µL per well. Afterwards, the samples, which contained the *E. coli* cells as well as $NaPO_4$ buffer were measured at room temperature in a plate reader at a wavelength of 294 nm.

The linear range in Figure 29 cannot be seen hence there are no values in the range of 0.50 to 2.00 mg cells/mL. Based on this result and by comparing them with the results of the Figure 28, it was decided that the range of 0 to 0.75 mg cells/mL had to be remeasured.

Table 48: Determination of the linear detection range of the plate reader testing whole intact *E. coli* BL21-Gold (DE3) cells in the concentration range of 0 to 0.75 mg cells/mL

Name	0 mg cells/ mL	0.10 mg cells/ mL	0.20 mg cells/ mL	0.30 mg cells/ mL	0.40 mg cells/ mL	0.50 mg cells/ mL	0.60 mg cells/ mL	0.75 mg cells/ mL
Average of the tested triplicates	0.04 ± 0.00	0.12 ± 0.00	0.21 ± 0.00	0.38 ± 0.00	0.48 ± 0.00	0.60 ± 0.01	0.72 ± 0.03	0.90 ± 0.00

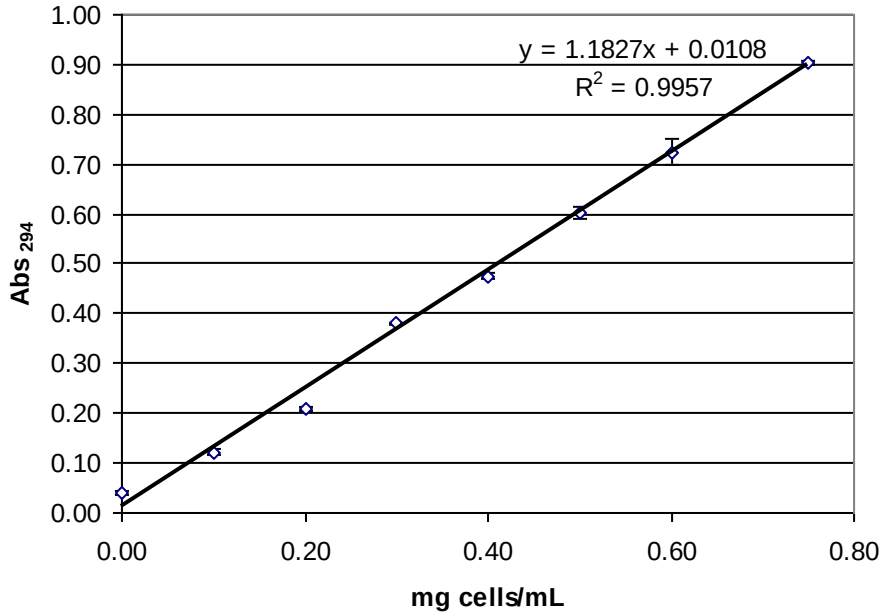

Figure 30: Determination of the linear detection range of the plate reader testing whole intact *E. coli* BL21-Gold (DE3) cells in the concentration range of 0 to 0.75 mg cells/mL

The well (of the UV-Star Microplate 96-well, F-bottom) contained the respective concentration of mg cells/mL (Table 48) in 100 mM $NaPO_4$ buffer at pH 7.5 in a total volume of 200 µL per well. Afterwards, the samples, which contained the *E. coli* cells as well as $NaPO_4$ buffer, were measured at room temperature in a plate reader at a wavelength of 294 nm.

The concentration range of 0 to 0.75 mg cells/mL of whole intact *E. coli* BL21-Gold (DE3) cells showed a linear progression. Based on this result, the same cell concentration (Table 48) was measured in the presence of 1,000 µM 4A3HBA.

Table 49: Determination of the linear detection range of the plate reader testing whole intact *E. coli* BL21-Gold (DE3) cells in the concentration range of 0 to 0.75 mg cells/mL in the presence of 1,000 µM 4A3HBA

Name	0 mg cells/ mL	0.10 mg cells/ mL	0.20 mg cells/ mL	0.30 mg cells/ mL	0.40 mg cells/ mL	0.50 mg cells/ mL	0.60 mg cells/ mL	0.75 mg cells/ mL
Average of the tested triplicates	1.78 ± 0.03	1.84 ± 0.01	1.96 ± 0.02	2.05 ± 0.03	2.14 ± 0.02	2.29 ± 0.03	2.32 ± 0.02	2.44 ± 0.03

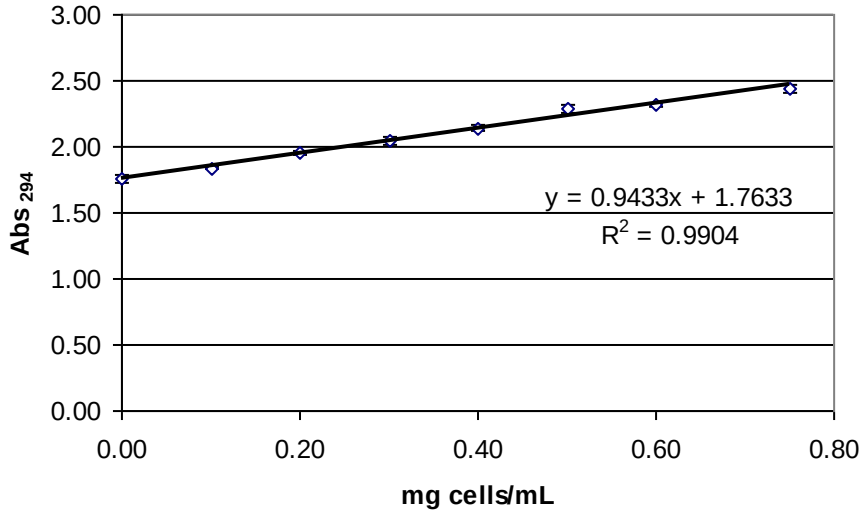

Figure 31: Determination of the linear detection range of the plate reader testing whole intact *E. coli* BL21-Gold (DE3) cells in the concentration range of 0 to 0.75 mg cells/mL in the presence of 1,000 µM 4A3HBA

The well (of the UV-Star Microplate 96-well, F-bottom) contained the respective concentration of mg cells/mL (Table 49) in 100 mM $NaPO_4$ buffer at pH 7.5 and 1,000 µM 4A3HBA in a total volume of 200 µL per well. Afterwards, the samples, which contained the *E. coli* cells as well as $NaPO_4$ buffer, were measured at room temperature in a plate reader at a wavelength of 294 nm.

The linear range was detected in the concentrations of 0 to 0.75 mg cells/mL of whole intact *E. coli* BL21-Gold (DE3) cells, which were tested with 4A3HBA. Based on these figures (Figure 30 and Figure 31), the range of cell concentration [0-0.75 mg cells/mL] with 4A3HBA can be used for measuring the enzyme activity.

New whole intact *E. coli* BL21-Gold (DE3) cells, including the pET26-Cupin13 construct, were produced without and in the presence of 100 µM $FeSO_4$ (described in the section 2.3.1 until the step of sonication) and were tested with 1,000 µM of the substrate 4A3HBA for monitoring the conversion (see in 2.4.2). The performed measurement resulted in no detectable enzyme activity. Afterwards, new whole intact *E. coli* BL21-Gold (DE3) cells, containing the pET26-Cupin13 construct, were produced and the pellets were separated for two different testings. On the one hand the whole intact cells were analysed regarding their activity as well as their enzyme activity, on the other hand, they were broken (described in 2.3.1) and the activity of the desired enzymes were tested to demonstrate that the enzymes are active within the whole cells.

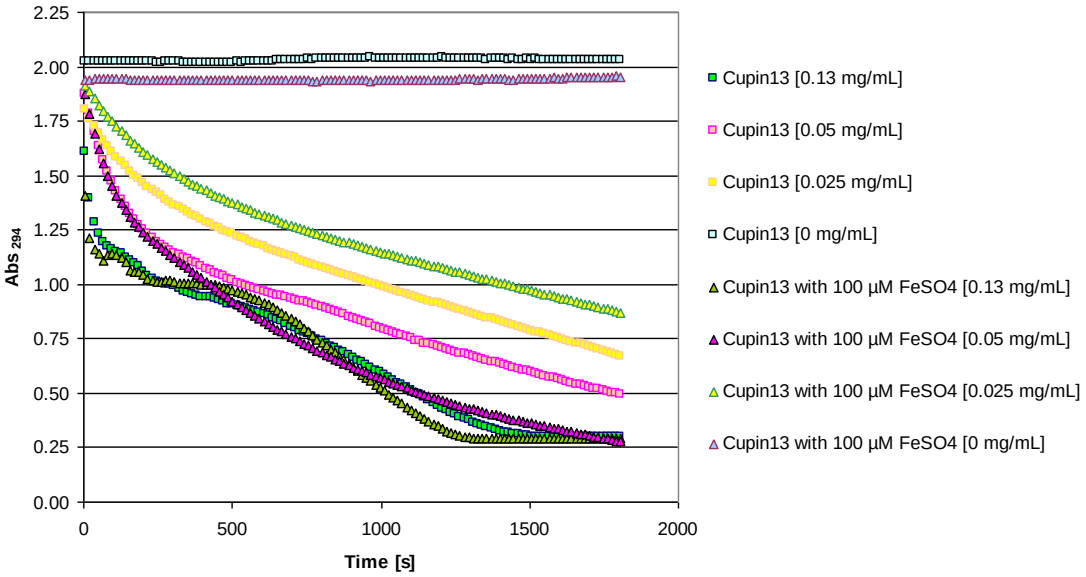

Figure 32: Determination of the desired enzyme activity of broken *E. coli* cells
Each sample contained 1,000 µM of the substrate 4A3HBA in 100 mM $NaPO_4$ pH 7.4. The reaction was started by the addition of the respective concentration of Cupin13 (see in Figure 32). The substrate conversion was monitored for 30 min at room temperature in a plate reader at a wavelength of 294 nm.

At first, the whole intact *E. coli* cells were tested and resulted in no detectable activity and consequently, they could be compared with the activity of the Cupin13 [0 mg/mL] in Figure 32. Afterwards, the Cupin13 protein from the broken cells was examined and they showed that the enzymes within the whole intact cells were active (Figure 32).

3.7 Determination of the transformation efficiency and detection of potential contamination of the electrocompetent *E. coli* TOP10F' cells

The electrocompetent *E. coli* TOP10F' cells were tested regarding their transformation efficiency, additionally, to detect potential contamination risks. The LB-agar plate was supplemented with ampicillin and 50 µL of the electrocompetent *E. coli* TOP10F' cells were streaked out. This resulted in 169 single opaque colonies and consequently, the cells had a calculated transformation efficiency of 2.9 * 10^8 cfu/µg. Furthermore, the second LB-agar plate with ampicillin, where 100 µL electrocompetent *E. coli* TOP10F' cells were streaked out, resulted in 376 single opaque colonies and a calculated transformation efficiency of 3.3 * 10^8 cfu/µg. Additionally, the controls (LB-agar plate with ampicillin and another one with kanamycin) showed no visible colonies, which

signifies that there were no contaminations in the reaction tubes of electrocompetent *E. coli* TOP10F' cells.

4. DISCUSSION

The first aim of the master thesis was to characterise the 4-amino-3-hydroxybenzoate 2,3-dioxygenase, which was called Cupin13. Therefore, a purchased synthetic gene was amplified via PCR and resulted in three DNA bands (Figure 4) at 537, about 2,000 and 3,500 bp. The amplification was successful because the first band at 537 bp contained the desired enzyme Cupin13. It can be assumed that the second band comprised a part of the template (~ 2,000 bp) and that the third band (~3,500 bp) was the synthetic pMA_Cupin13 plasmid. A possible explanation for the second and third band could be that a too high amount of template (50 ng/µL) was amplified by using the PCR.

The amplified Cupin13 and the expression vectors (Table 15) were digested for ligation and control (result of control digestion is shown in Figure 5). The lanes 2 and 6 (A) as well as 2 to 4 (B) in Figure 5 included empty vectors. It can be supposed that the empty pET26 and pEHISTEV-Cupin13 vector (in Figure 5 (A)) resulted from re-ligation of the plasmid without the previous performed integration of a DNA fragment in the polylinker region.

Furthermore, it can be assumed that the empty pESBPTEV vector was presented in several conformations such as linear (lane 2, at 2,500 bp), circular (lane 3, at 3,000 bp) and a mixture of both (linear and circular vector, lane 4) in Figure 5 (B). Possible reason for the vectors without insert might be that the digestion of the vector pESBPTEV or the ligation was performed with suboptimal conditions.

After recloning of the synthetic gene, the protein expression of the Cupin13 was analysed. The harvested *E. coli* TOP10F' cells, including recombinant plasmids, resulted in different weights of the wet pellets (in the section 3.2). A possible explanation for the different weights could be that beside the wet pellet a remaining liquid was measured.

Afterwards, the Cupin13 protein was analysed by SDS-PAGE and Bradford protein assay. The Cupin13 protein band of the soluble fraction was clearly visible at 21 kDa in the SDS-PAGE gel (Figure 6) and this protein size corresponds to the finding of Takenaka et al. [55] and Murakami et al. [54]. Additionally, the Cupin13 protein was detected at 23.8 kDa (HisTEV-Cupin13 protein) and 26.8 kDa (SBPTEV-Cupin13 protein) due to the included tags (Figure 6). The details of the Cupin13 protein contained tag and TEV sequences are listed in the Appendix.

Further protein analyses were performed with the pET26-Cupin13 protein. The first measurement of Cupin13 resulted in a specific activity of 24.92 U/mg, while the $NaPO_4$ buffer and *E. coli* harbouring empty pET26b-vector, had no detectable activity. As a consequence, only the Cupin13 (4A3HBA23DA) possesses the ability to degrade the substrate 4A3HBA. The results of the testing were consisted with the ones of Takenaka et al. who detected that this enzyme (the purified enzyme had a K_m value of 35 µM and specific activity of 12 U/mg) had a high substrate specificity for 4A3HBA [55]. Furthermore, the K_m value of Takenaka et al. are nearly the same (K_m value of 0.04 mM and 0.05 mM) compared with the results of the lysate containing only Cupin13 (control) without the addition of ferrous sulphate (shown in Table 34 and Table 39). However, the specific activity of these controls (8.05 U/mg ± 0.58; 8.45 U/mg ± 0.05 and 9.07 U/mg ± 0.13) are lower in comparison with the purified enzyme (12 U/mg) of Takenaka et al. A possible explanation could be that the 4A3HBA23DA protein of *Bordetella* sp. strain 10d (which Takenaka et al. used) was better expressed than the one of the *E. coli* BL21-Gold (DE3) cells.

For further studies, it would be interesting to study if this enzyme possesses the ability to degrade other similar substrates such as 4-amino-3-methoxybenzoic acid (which differs from the 4A3HBA in one position and includes instead of a hydroxyl group a methoxy group) and 3-hydroxy-4-nitrobenzoic acid (which includes instead of an amino group a nitro group). The details of the numerated substrates are listed in the Appendix.

4.1 Purification of the Cupin13 protein

After the first testings of the cleared lysate containing the Cupin13 protein, it was decided to purify the Cupin13 protein by affinity chromatography. The purified Cupin13 protein (4.35 g *E. coli* BL21-Gold (DE3) cells expressing HisTEV-Cupin13 protein) with His_6-tags was detected by SDS-PAGE gel (Figure 9) and the band of the Cupin13 protein (23.8 kDa) was clearly visible in the pellet as well as barely in the lysate (Figure 9). As a consequence, it can be expected that the protein might be an insoluble protein. Furthermore, the Cupin13 protein was completely bound to Ni-agarose beads. As a result, no protein was visible at 21 kDa in the flow through (lane 4) as well as in the wash buffer A (lane 5, Figure 9).

Afterwards, the protein concentration of the purified HisTEV-Cupin13 (3.5 mL) was analysed and resulted in 3.0 mg/mL. It can be assumed that the low protein

concentration was measured due to the low expression level (Figure 6) and the insoluble protein in the pellet (lane 2 in Figure 9).

Subsequently, the activity of the freshly purified HisTEV-Cupin13 was measured and not evaluable based on the strong fluctuations (Figure 10). A possible reason for this result could be that a small amount of ethanol (used for cleaning the cuvettes) was still present and disturbed the substrate conversion.

Afterwards, the freshly purified HisTEV-Cupin13 protein was stored at various conditions for 12 h and then remeasured to determine the enzyme activity. The enzyme showed no detectable activity except in the presence of gaseous nitrogen, stored at 4 °C. Based on the information of Takenaka et al. that the enzyme contained 1.9 mol Fe(II) per mol protein [55], it can be assumed that on the one hand the Fe(II) is sensitive to oxygen and perhaps oxidised to Fe(III), which on the other hand influenced the activity of the enzyme.

4.2 Analysis of the Cupin13 protein in the presence of various metal salts

The Cupin13 protein (of pET26-Cupin13 construct) was expressed in the presence of various bivalent metal salts such as $CuSO_4$, $MnCl_2$, $NiSO_4$ and $FeSO_4$. Due to the information of Takenaka et al., that the enzyme activity increased in the presence of Fe(II), completely inhibited with $CuSO_4$ and that other metal salts have no effect to the enzyme activity [55]. Different weights of the wet pellets were obtained (see Table 27), which can be assumed that beside the wet pellet a small amount of the main culture was measured. Based on the results of the protein concentration (listed in Table 27), it can be expected that the presence of bivalent metal salts influence minimal the protein expression. Moreover, it was detected that in the presence of $NiSO_4$, $FeSO_4$ and $MnCl_2$ the protein expression slightly increased (compared with the control). But less Cupin13 protein was expressed in the presence of the metal salt $CuSO_4$ (Figure 15). Furthermore, the band of the Cupin13 protein in the soluble fraction was clearly visible at 21 kDa (Figure 12) and barely in the insoluble fraction and signifies that in the presence or absence of bivalent metal salt the Cupin13 protein is available in the soluble fraction (supernatant of broken and centrifuged *E. coli* cells.

After the Cupin13 protein, which was expressed in the presence of metal salts, was analysed, the enzyme activity was determined. The highest and lowest specific activities as well as k_{cat} were obtained of Cupin13 with $FeSO_4$ and $NiSO_4$ (Table 31). It can be assumed that $FeSO_4$ and $NiSO_4$ had an influence on the enzyme activity

contrary to the $CuSO_4$ and the $MnCl_2$. The enzyme activity (the Cupin13 protein was expressed in the presence of bivalent metal salt) increased by the addition of ferric sulphate and decreased in the presence of $NiSO_4$.

4.3 Optimisation of the enzyme activity

Due to the results (in Table 31), ferrous sulphate was added to the main culture at various concentrations, before the expression was started, to optimise enzyme activity. Different weights of the wet pellets were obtained (listed in Table 32); these fluctuations can be explained based on the reason that the wet pellet, which was measured, contained a small amount of the main culture.

The highest specific enzyme activity and k_{cat} were received for the Cupin13 protein in the presence of 100 µM $FeSO_4$. Due to the results in Table 34, it seems that higher metal salt concentrations decreased the specific activity as well as the k_{cat}. A possible explanation could be that concentrations above 100 µM $FeSO_4$ showed a negative effect on the Cupin13 protein expression, especially on the specific enzyme activity based on the lower specific activity and k_{cat} value compared to the results of the Cupin13 in the presence of 100 µM $FeSO_4$.

For further studies, possible future objectives can be to test the Fe(II) in combination with other metal ions or to find a possibility to use higher bivalent metal salt concentrations and to avoid inhibition.

4.4 Analysis of the mutated Cupin13 proteins

Regions of local similarity between protein sequences were determined with the computer program BLAST search of NCBI. The 3-hydroxyanthranilate 3,4-dioxygenase resulted in the best alignment with the lowest E-value of $2*10^{-30}$ (Table 23).

Both enzymes (4A3HBA23DA and 3-HAD) have some common feature for example they belong to the extradiol dioxygenases, possess a cupin fold and are homodimer [55,59]. The subunit size of 4A3HBA23DA is 21 kDa, while the 3-HAD had a molecular weight of 22 kDa per monomer [55,59]. Takenaka et al. determined that the 4A3HBA23DA only cleaves the 4A3HBA [55]. In addition, Murakami et al. detected that this enzyme did not cleave the ring of 3-hydroxyanthranilate, which differs from 4A3HBA in the position of an amino group [54]. Due to the unknown protein structure as well as the substrate specificity of the 4A3HBA23DA protein and the high sequence

similarity with 3-hydroxyanthranilate 3,4-dioxygenase, the mutations were integrated in the putative active site of the 4A3HBA23DA protein to determine the important amino acids for the activity as well as the stability.

The Cupin13-Q60A, -Q60F, -S62A, -S62Q, -F101A, -F101R and -R144I protein variants contain mutations in the putative active site of 4A3HBA23DA. In addition, the Cupin13-H52A, -N54A, -E58A, and -H97A of the 4A3HBA23DA contain mutations in the supposed metal binding site, which is part of the active site.

This is the first report of Cupin13 protein variants, which have a mutation in putative metal binding site or presumed active site.

4.4.1 Cupin13 protein with mutations in the putative metal binding site

Cupin13-H52A

From eleven mutated Cupin13 proteins only four proteins have their mutation in the presumed metal binding site (in the active site) and thereof three Cupin13 proteins were inactive, which are expressed in the *E. coli* BL21-Gold (DE3) cells (Figure 20).

The Cupin13-H52A protein was not expressed in the presence or absence of 100 µM $FeSO_4$ (Figure 25). The most members of the cupin superfamily have a cupin domain, which included two different motifs [10]. Based on the information of Fetzner et al. the first motif contained two histidine residues as well as one glutamate residue and together with the motif two (included a histidine residue) are both in the position to perform as ligands for the binding of a bivalent metal ion [10]. It can be expected that this histidine (a basic, charged amino acid with an Imidazole ring) on position 52 is important for the protein expression and metal binding of a bivalent metal ion. Due to its exchange through alanine (a non-polar and small amino acid with a methylgroup) the Cupin13 protein was not produced and detected at a mass of 21 kDa (Figure 25).

Cupin13-N54A, -E58A and -H97A

Furthermore, a weak protein expression of Cupin13-N54A and -E58A as well as a strong protein expression of Cupin13-H97A in the presence of 100 µM $FeSO_4$ was determined and compared with the wild type (Figure 23 and Table 42). It can be assumed that a polar amino acid with an NH_2 group (asparagine) on position 54 or a charged and acidic reacting amino acid (glutamic acid) on position 58 is required instead of a non-polar amino acid (alanine) for a good protein expression.

Afterwards, these Cupin13 protein variants were tested for their activity. None of them was active, if expressed in the presence or absence of 100 µM $FeSO_4$, (Table 37 and

Figure 24). It can be assumed that the metal binding site is important for the Cupin13 protein expression, stability as well as for the activity. Furthermore, it can be expected that the metal binding site had an indirect influence on the activity, due to the fact that in the absence of ferrous sulphate or another metal salt the activity was decreased.

4.4.2 Cupin13 proteins with a mutation in the supposed active site

Eleven modified Cupin13 proteins were tested, where only one amino acid was exchanged. Of these only seven proteins showed a mutation in the active site (Figure 21). Furthermore, of these mutations only five were active (Table 36) and were analysed.

Cupin13-Q60A and -Q60F

The expression levels of Cupin13-Q60A and -Q60F were approximately the same (Table 39 and Table 42). It can be assumed that the amino acid exchange of glutamine (polar amino acid) to alanine (non-polar amino acid with an alkyl-substituent) or phenylalanine (unpolar amino acid with a hydrophobic side chain) on position 60 of Cupin13 protein showed no detectable influence in the protein expression.

Afterwards, the enzyme activity of these modified Cupin13 proteins was tested. The enzyme activity was higher in the wild type than in Cupin13-Q60A as well as in -Q60F (Table 36). Due to this result it can be expected that alanine on position 60 is a too small molecule for an efficient substrate (4A3HBA) binding and that phenylalanine, due to its hydrophobic side chain required too much space in the active site.

Cupin13-S62A and -S62Q

The expression level of Cupin13-S62A and -S62Q was higher in comparison to the wild type enzyme, which was used as control (Table 39 and Table 42). Additionally, these two modified Cupin13 proteins compared to each other resulted in higher expression levels of Cupin13-S62Q compared to Cupin13-S62 protein. A possible explanation could be that a polar amino acid with a NH_2-group (glutamine) on position 62 might have a better influence in the protein expression than alanine or serine (a polar amino acid with a hydroxyl group). However, the highest enzyme activity was obtained from the Cupin13-S62A, which was better than the wild type or any of the other active Cupin13 protein variants (Figure 22 and Table 39). A possible explanation could be that replacement of serine (a polar amino acid with a hydroxyl group) or glutamine (a polar amino acid with a NH_2-group) by alanine (a small and unpolar

amino acid) the substrate (4A3HBA) fits better in the active site and the affinity as well as the k_{cat} were increased.

Cupin13-F101A and -F101R

Both expression levels of the Cupin13-F101A and Cupin13-F101R were analysed and compared to each other as well as with the wild type. The Cupin13-F101A had a higher expression level than the wild type or Cupin13-F101R (Table 42). It can be assumed that alanine, due to its small size and non-polar property, resulted in an increased translation velocity of the protein than the phenylalanine (an unpolar amino acid with a benzene ring) or arginine (a basic, charged, big amino acid). Both mutated Cupin13 proteins had no detectable enzyme activity, which were expressed in the presence or absence of 100 µM $FeSO_4$.

A possible explanation could be that on position 101 a non-polar amino acid with a benzene ring (phenylalanine) is required instead of alanine, which is also an unpolar amino acid, but it contains a methyl group as side chain or arginine which is a basic, charged, big amino acid with a long side chain. Furthermore, it can be assumed that the size of arginine prevented the binding of the substrate (4A3HBA) to the active site.

Cupin13-R144I

The protein expression level of Cupin13-R144I is nearly the same than of the wild type (Table 39). It can be supposed that the exchange of arginine to isoleucine (belongs to the non-polar group of amino acids) on position 144 has a small effect on the protein translation (Table 39). However, the enzyme activity of this mutated Cupin13 protein was lower in the comparison to the control (wild type). It can be expected that on position 144 the isoleucine was too small compared with arginine to bind with a high efficiency to the substrate (4A3HBA).

4.4.3 Comparison of the most active mutants in the presence and absence of 100 µM $FeSO_4$ as well as a stability test

Due to the information of Takenaka et al. and the results of the mutated Cupin13 proteins in the presence of 100 µM $FeSO_4$, the most active Cupin13 protein variants were tested with this metal salt concentration, which resulted in a higher specific activity, k_{cat} and expression level.

Afterwards, the stored mutated Cupin13 protein was tested in the presence or absence of 100 µM $FeSO_4$. The protein of the wild type and Cupin13-Q60A (expressed in the

presence of ferrous sulphate) as well as the wild type and Cupin13-S62A (expressed in the absence of this metal salt) lost less than 10 % of activity during one week of storage at 4 °C (Table 40). Based on the results in Table 40, it can be assumed that the 100 mM $NaPO_4$ buffer is not optimal for the storage. Moreover, a possible explanation could be that due to the information that Cupin13 protein contained 1.9 mol Fe(II) per mol protein [55], the protein is sensitive in the presence of oxygen as Fe(II) can oxidise to Fe(III). As a result a decrease of the enzyme activity could be detected. Therefore, the mutations for best enzyme activity as well as expression level could be combined and compared with the wild type. In addition, other mutation(s) can be integrated by site specific mutagenesis (by overlap extension PCR) or random mutagenesis (e.g. by error prone PCR) in the Cupin13 gene, followed by screening and at the end the sequencing of the DNA.

4.5 Activity testing of the whole intact *E. coli* cells

After various experiments with the wild type and the mutated Cupin13 proteins, the whole intact *E. coli* BL21-Gold (DE3) cells, which contained the Cupin13 protein of the pET26-Cupin13 construct, were monitored during the substrate (4A3HBA) conversion. It was determined that these whole intact cells have no detectable activity, but the Cupin13 enzymes within the cells were tested to be active. A possible explanation could be that the substrate is too big for the transport system through the cell membrane, consequently the cells were not able to degrade the substrate without a previous cell disruption.

CONCLUSION

The major aim of the thesis was to characterise a 4-amino-3-hydroxybenzoate 2,3-dioxygenase (4A3HBA23DA) from *Bordetella* sp. 10d, a protein with Cupin fold. For this purpose the purchased synthetic Cupin13 was recloned in various expression vectors by molecular biological methods. The pET26-Cupin13 construct (wild type) as well as the modified proteins were analysed by protein biochemical techniques.

It was demonstrated that *E. coli* cells (harbouring empty pET26-vectors) and $NaPO_4$ buffer do not possess the ability to degrade the substrate 4-amino-3-hydroxybenzoic acid (4A3HBA), but only the intracellular produced Cupin13 protein. Furthermore, the Cupin13 protein was purified, which resulted in 3.0 mg/mL and stored under different conditions. The purified Cupin13 protein can be kept at 4 °C and purged head space with gaseous nitrogen, while the protein in the presence of oxygen was inactive and at -20 °C precipitated. Thus, it was decided that all further experiments should be performed with *E. coli* lysate.

Afterwards, the protein was analysed in the presence of various bivalent metal salts in the expression medium, which resulted in that the maximal enzyme activity was obtained with 100 µM ferrous sulphates, while higher concentrations thereof showed a decreased of the enzyme activity.

A further focus was on the comparison of the wild type and modified Cupin13 proteins, which had mutations in the putative active site (Cupin13-Q60A, -Q60F, -S62A, -S62Q, -R144I) as well as therein possibly presumed metal binding site (Cupin13-H52A, -N54A, -E58A, -H97A) of the Cupin13 protein. The evaluation of the modified proteins resulted in that the Cupin13-H52A was not expressed due to the mutation, while the other proteins containing mutations in the putative metal binding site were produced, but the enzymes showed no activity. It can be expected that the metal binding site is important for the activity and stability of the protein. Furthermore, of eleven Cupin13 protein muteins only five were active (Cupin13-Q60A, -Q60F, -S62A, -S62Q, -R144I). Only, Cupin13-S62A protein was more active than the wild type.

Afterwards, the activity of the whole intact *E. coli* BL21-Gold (DE3) cells was tested by monitoring the substrate (4A3HBA) conversion. The result was no detectable activity, but it was proven that the enzyme in the cells is active.

It can be summarised that the performed mutation study was successful. Due to the fact that the enzyme activity could be enhanced and that important positions of the

amino acids were detected, which are necessary for the protein expression or enzyme activity.

REFERENCES

[1] Bugg TDH: **Dioxygenase Enzymes and Oxidative Cleavage Pathways**. 2010.

[2] Loh K-C, Chua S-S: **Ortho pathway of benzoate degradation in Pseudomonas putida: induction of meta pathway at high substrate concentrations**. *Enzyme Microb Technol* 2002,**30**:620–6.

[3] Zhang J, Zheng H, Groce SL, Lipscomb JD: **Basis for specificity in methane monooxygenase and related non-heme iron-containing biological oxidation catalysts**. *J Mol Catal A Chem* 2006,**251**:54–65.

[4] Guzik U, Greń I, Hupert-Kocurek K, Wojcieszyńska D: **Catechol 1,2-dioxygenase from the new aromatic compounds – Degrading Pseudomonas putida strain N6**. *Int Biodeterior Biodegradation* 2011,**65**(**3**):504–12.

[5] Jun S-Y, Fushinobu S, Nojiri H, Omori T, Shoun H, Wakagi T: **Improving the catalytic efficiency of a meta-cleavage product hydrolase (CumD) from Pseudomonas fluorescens IP01**. *Biochim Biophys Acta* 2006,**1764**(**7**):1159–66.

[6] Suenaga H, Koyama Y, Miyakoshi M, Miyazaki R, Yano H, Sota M, Ohtsubo Y, Tsuda M, Miyazaki K: **Novel organization of aromatic degradation pathway genes in a microbial community as revealed by metagenomic analysis.** *ISME J* 2009,**3**(**12**):1335–48.

[7] Dou J, Liu X, Hu Z: **Anaerobic BTEX degradation in soil bioaugmented with mixed consortia under nitrate reducing conditions.** *J Environ Sci (China)* 2008,**20**(**5**):585–92.

[8] Kitayama A, Achioku T, Yanagawa T, Kanou K, Kikuchi M, Suzuki E, Nishimura H, Nagamun-e T: **Cloning and Characterization of Extradiol Aromatic Ring-Cleavage Dioxygenases of Pseudomonas aeruginosa JI104**. *J Ferment Bioeng* 1996,**82**(**3**):217–23.

[9] Seo J-S, Keum Y-S, Li QX: **Bacterial degradation of aromatic compounds.** *Int J Environ Res Public Health* 2009,**6**:278–309.

[10] Fetzner S: **Ring-cleaving dioxygenases with a cupin fold**. *Appl Environ Microbiol* 2012,**78**(**8**):2505–14.

[11] Vaillancourt FH, Bolin JT, Eltis LD: **The ins and outs of ring-cleaving dioxygenases**. *Crit Rev Biochem Mol Biol* 2006,**41**(**4**):241–67.

[12] Bugg TDH: **Dioxygenase enzymes: catalytic mechanisms and chemical models**. *Tetrahedron* 2003,**59**(**36**):7075–101.

[13] Ferraroni M, Matera I, Steimer L, Bürger S, Scozzafava A, Stolz A, Briganti F: **Crystal structures of salicylate 1,2-dioxygenase-substrates adducts: A step towards the comprehension of the structural basis for substrate selection in class III ring cleaving dioxygenases.** *J Struct Biol* 2012,**177**(**2**):431–8.

[14] Buongiorno D, Straganz GD: **Structure and function of atypically coordinated enzymatic mononuclear non-heme-Fe(II) centers**. *Coord Chem Rev* 2013,**257**(**2**):541–63.

[15] Ferraroni M, Steimer L, Matera I, Bürger S, Scozzafava A, Stolz A, Briganti F: **The generation of a 1-hydroxy-2-naphthoate 1,2-dioxygenase by single point mutations of salicylate 1,2-dioxygenase -Rational design of mutants and the crystal structures of the A85H and W104Y variants**. *J Struct Biol* 2012,**180**(**3**):563–71.

[16] Wang C-H, Lu J-W, Wei H-H, Takeda M: **Functional model for intradiol-cleaving catechol 1,2-dioxygenase: Synthesis, structure, spectra, and catalytic activity of iron(III) complexes with substituted salicylaldimine ligands**. *Inorganica Chim Acta* 2007,**360**(**9**):2944–52.

[17] Bugg TDH, Ramaswamy S: **Non-heme iron-dependent dioxygenases: unravelling catalytic mechanisms for complex enzymatic oxidations.** *Curr Opin Chem Biol* 2008,**12**(**2**):134–40.

[18] Emerson JP, Kovaleva EG, Farquhar ER, Lipscomb JD, Que L: **Swapping metals in Fe- and Mn-dependent dioxygenases: evidence for oxygen activation without a change in metal redox state.** *Proc Natl Acad Sci U S A* 2008,**105**(**21**):7347–52.

[19] Kovaleva EG, Neibergall MB, Chakrabarty S, Lipscomb JD: **Finding intermediates in the O2 activation pathways of non-heme iron oxygenases**. *Acc Chem Res* 2007,**40**(**7**):475–83.

[20] Vetting MW, Wackett LP, Que L, Lipscomb JD, Ohlendorf DH: **Crystallographic Comparison of Manganese- and Iron-Dependent Homoprotocatechuate 2,3-Dioxygenase**. *J Bacteriol* 2004,**186**(**7**):1945–58.

[21] Anon: **Quercetinase, a dioxygenase containing copper**. *Biochem Biophys Res Commun* 1971,**43**(**1**):1–5.

[22] Fusetti F, Schröter KH, Steiner R a, van Noort PI, Pijning T, Rozeboom HJ, Kalk KH, Egmond MR, Dijkstra BW: **Crystal structure of the copper-containing quercetin 2,3-dioxygenase from Aspergillus japonicus**. *Structure* 2002,**10**(**2**):259–68.

[23] Ragsdale SW: **Nickel-based Enzyme Systems**. *J Biol Chem* 2009,**284**(**28**):18571–5.

[24] He P, Moran GR: **Structural and mechanistic comparisons of the metal-binding members of the vicinal oxygen chelate (VOC) superfamily**. *J Inorg Biochem* 2011,**105**(**10**):1259–72.

[25] Agarwal G, Rajavel M, Gopal B, Srinivasan N: **Structure-based phylogeny as a diagnostic for functional characterization of proteins with a cupin fold**. *PLoS One* 2009,**4**(**5**):e5736.

[26] Rocha CS, Luz DF, Oliveira ML, Baracat-Pereira MC, Medrano FJ, Fontes EPB: **Expression of the sucrose binding protein from soybean: renaturation and stability of the recombinant protein**. *Phytochemistry* 2007,**68**(**6**):802–10.

[27] Adams M a, Singh VK, Keller BO, Jia Z: **Structural and biochemical characterization of gentisate 1,2-dioxygenase from Escherichia coli O157:H7**. *Mol Microbiol* 2006,**61**(**6**):1469–84.

[28] Castillo J, Genovés A, Franco L, Rodrigo MI: **A multifunctional bicupin serves as precursor for a chromosomal protein of Pisum sativum seeds**. *J Exp Bot* 2005,**56**(**422**):3159–69.

[29] Radauer C, Breiteneder H: **Evolutionary biology of plant food allergens**. *J Allergy Clin Immunol* 2007,**120**(**3**):518–25.

[30] Cechin AL, Sinigaglia M, Lemke N, Echeverrigaray S, Cabrera OG, Pereira G a G, Mombach JCM: **Cupin: a candidate molecular structure for the Nep1-like protein family**. *BMC Plant Biol* 2008,**8**:50.

[31] Dunwell JM, Purvis A, Khuri S: **Cupins: the most functionally diverse protein superfamily?** *Phytochemistry* 2004,**65**(**1**):7–17.

[32] Straganz GD, Egger S, Aquino G, Auria SD, Nidetzky B: **Exploring the cupin-type metal-coordinating signature of acetylacetone dioxygenase Dke1 with site-directed mutagenesis: Catalytic reaction profile and Fe2+ binding stability of Glu-69 → Gln mutant**. *J Mol Catal B Enzym* 2006,**39**:171–8.

[33] Simmons CR, Liu Q, Huang Q, Hao Q, Begley TP, Karplus PA, Stipanuk MH: **Crystal structure of mammalian cysteine dioxygenase: A novel mononuclear iron center for cysteine thiol oxidation**. *J Biol Chem* 2006,**281**(**27**):18723–33.

[34] Stipanuk MH, Simmons CR, Karplus PA, Dominy JE: **Thiol dioxygenases: unique families of cupin proteins.** *Amino Acids* 2011,**41**(**1**):91–102.

[35] Miyauchi K, Adachi Y, Nagata Y, Takagi M: **Cloning and sequencing of a novel meta-cleavage dioxygenase gene whose product is involved in degradation of gamma-hexachlorocyclohexane in Sphingomonas paucimobilis.** *J Bacteriol* 1999,**181**(**21**):6712–9.

[36] Carmona M, Zamarro MT, Blázquez B, Durante-Rodríguez G, Juárez JF, Valderrama JA, Barragán MJL, García JL, Díaz E: **Anaerobic catabolism of aromatic compounds: a genetic and genomic view**. *Microbiol Mol Biol Rev* 2009,**73**(**1**):71–133.

[37] Wang C-L, You S-L, Wang S-L: **Purification and characterization of a novel catechol 1,2-dioxygenase from Pseudomonas aeruginosa with benzoic acid as a carbon source**. *Process Biochem* 2006,**41**(**7**):1594–601.

[38] Táncsics A, Farkas M, Szoboszlay S, Szabó I, Kukolya J, Vajna B, Kovács B, Benedek T, Kriszt B: **One-year monitoring of meta-cleavage dioxygenase gene expression and microbial community dynamics reveals the relevance of subfamily I.2.C extradiol dioxygenases in hypoxic, BTEX-contaminated groundwater**. *Syst Appl Microbiol* 2013,**36**(**5**):339–50.

[39] Tuan NN, Hsieh H-C, Lin Y-W, Huang S-L: **Analysis of bacterial degradation pathways for long-chain alkylphenols involving phenol hydroxylase, alkylphenol monooxygenase and catechol dioxygenase genes**. *Bioresour Technol* 2011,**102**(**5**):4232–40.

[40] Wojcieszyńska D, Hupert-Kocurek K, Jankowska A, Guzik U: **Properties of catechol 2,3-dioxygenase from crude extract of Stenotrophomonas maltophilia strain KB2 immobilized in calcium alginate hydrogels**. *Biochem Eng J* 2012,**66**:1–7.

[41] Engineering G, Applications T, Burg-elarab N: **Detection of meta- and ortho-cleavage dioxygenases in bacterial phenol-degraders**. *J Appl Sci Environ Mgt* 2006,**10**(**3**):75–81.

[42] Mahiudddin M, Fakhruddin a NM, Abdullah-Al-Mahin: **Degradation of Phenol via Meta Cleavage Pathway by Pseudomonas fluorescens PU1**. *ISRN Microbiol* 2012,**2012**.

[43] Pérez-Pantoja D, Donoso R, Agulló L, Córdova M, Seeger M, Pieper DH, González B: **Genomic analysis of the potential for aromatic compounds biodegradation in Burkholderiales**. *Environ Microbiol* 2012,**14**(**5**):1091–117.

[44] Sha LUO: **Molecular Cloning and Biochemical Characterization of Protocatechuate 3,4-dioxygenase in Burkholderia sp . NCIMB 10467**. *Microbiology* 2008,**35**(**5**):712–9.

[45] Romero-Silva MJ, Méndez V, Agulló L, Seeger M: **Genomic and functional analyses of the gentisate and protocatechuate ring-cleavage pathways and related 3-hydroxybenzoate and 4-hydroxybenzoate peripheral pathways in Burkholderia xenovorans LB400**. *PLoS One* 2013,**8**(**2**):e56038.

[46] Masai E, Katayama Y, Fukuda M: **Genetic and Biochemical Investigations on Bacterial Catabolic Pathways for Lignin-Derived Aromatic Compounds**. *Biosci Biotechnol Biochem* 2007,**71**(**1**):1–15.

[47] Kasai D, Fujinami T, Abe T, Mase K, Katayama Y, Fukuda M, Masai E: **Uncovering the protocatechuate 2,3-cleavage pathway genes**. *J Bacteriol* 2009,**191**(**21**):6758–68.

[48] Liu D, Zhu T, Fan L, Quan J, Guo H, Ni J: **Identification of a novel gentisate 1,2-dioxygenase from Silicibacter pomeroyi**. *Biotechnol Lett* 2007,**29**(**10**):1529–35.

[49] Luo S, Liu DQ, Liu H, Zhou NY: **Site-directed mutagenesis of gentisate 1,2-dioxygenases from Klebsiella pneumoniae M5a1 and Ralstonia sp. strain U2**. *Microbiol Res* 2006,**161**(**2**):138–44.

[50] Kolvenbach B a, Lenz M, Benndorf D, Rapp E, Fousek J, Vlcek C, Schäffer A, Gabriel FL, Kohler H-PE, Corvini PF: **Purification and characterization of hydroquinone dioxygenase from Sphingomonas sp. strain TTNP3.** *AMB Express* 2011,**1**(**1**):8.

[51] Moonen MJH, Synowsky S a, van den Berg W a M, Westphal AH, Heck AJR, van den Heuvel RHH, Fraaije MW, van Berkel WJH: **Hydroquinone dioxygenase from Pseudomonas fluorescens ACB: a novel member of the family of nonheme-iron(II)-dependent dioxygenases**. *J Bacteriol* 2008,**190**(**15**):5199–209.

[52] Kulkarni M, Chaudhari A: **Microbial remediation of nitro-aromatic compounds: an overview.** *J Environ Manage* 2007,**85**(**2**):496–512.

[53] Kovaleva EG, Lipscomb JD: **Intermediate in the O-O bond cleavage reaction of an extradiol dioxygenase**. *Biochemistry* 2008,**47**(**43**):11168–70.

[54] Murakami S, Sawami Y, Takenaka S, Aoki K: **Cloning of a gene encoding 4-amino-3-hydroxybenzoate 2,3-dioxygenase from Bordetella sp. 10d**. *Biochem Biophys Res Commun* 2004,**314**(**2**):489–94.

[55] Takenaka S, Asami T, Orii C, Murakami S, Aoki K: **A novel meta-cleavage dioxygenase that cleaves a carboxyl-group-substituted 2-aminophenol**. *Eur J Biochem* 2002,**269**(**23**):5871–7.

[56] Orii C, Takenaka S, Murakami S, Aoki K: **A novel coupled enzyme assay reveals an enzyme responsible for the deamination of a chemically unstable intermediate in the metabolic pathway of 4-amino-3-hydroxybenzoic acid in Bordetella sp. strain 10d**. *Eur J Biochem* 2004,**271**(**15**):3248–54.

[57] Lendenmann U, Spain JC: **2-aminophenol 1,6-dioxygenase: a novel aromatic ring cleavage enzyme purified from Pseudomonas pseudoalcaligenes JS45**. *J Bacteriol* 1996,**178**(**21**):6227–32.

[58] He Z, Davis JK: **Purification , Characterization and Sequence Analysis of 2-Aminomuconic 6-Semialdehyde Dehydrogenase from Pseudomonas pseudoalcaligenes JS45**. *J Bacteriol* 1998,**180**(**17**):4591–5.

[59] Zhang Y, Colabroy KL, Begley TP, Ealick SE: **Structural studies on 3-hydroxyanthranilate-3,4-dioxygenase: the catalytic mechanism of a complex oxidation involved in NAD biosynthesis**. *Biochemistry* 2005,**44**(**21**):7632–43.

[60] Li X, Guo MIN, Fan JUN, Tang W, Wang D, Ge H, Rong HUI, Teng M, Niu L, Liu QUN, Hao Q: **Crystal structure of 3-hydroxyanthranilic acid 3,4-dioxygenase from Saccharomyces cerevisiae: A special subgroup of the type III extradiol dioxygenases**. *Protein Sci* 2006,**15**:761–73.

[61] Orii C, Takenaka S, Murakami S, Aoki K: **Metabolism of 4-Amino-3-hydroxybenzoic Acid by Bordetella sp. Strain 10d: A Different Modified Meta-Cleavage Pathway for 2-Aminophenols**. *Biosci Biotechnol Biochem* 2006,**70**(**11**):2653–61.

[62] Chung LW, Li X, Sugimoto H, Shiro Y, Morokuma K: **ONIOM study on a missing piece in our understanding of heme chemistry: bacterial tryptophan 2,3-dioxygenase with dual oxidants**. *J Am Chem Soc* 2010,**132**(**34**):11993–2005.

[63] Rafice S a, Chauhan N, Efimov I, Basran J, Raven EL: **Oxidation of L-tryptophan in biology: a comparison between tryptophan 2,3-dioxygenase and indoleamine 2,3-dioxygenase**. *Biochem Soc Trans* 2009,**37**(**Pt 2**):408–12.

[64] Forouhar F, Anderson JLR, Mowat CG, Vorobiev SM, Hussain A, Abashidze M, Bruckmann C, Thackray SJ, Seetharaman J, Tucker T, Xiao R, Ma L, Zhao L, Acton TB, Montelione GT, Chapman SK, Tong L: **Molecular insights into substrate recognition and catalysis by tryptophan 2,3-dioxygenase**. *Natl Acad Sci USA* 2007,**104**(**2**):473–8.

[65] Hirata F, Ohnishi T, Hayaishi O: **Indoleamine 2,3-Dioxygenase**. *J Biol Chem* 1977,**252**(**13**):4637–42.

[66] Hirata F, Hayaishi O: **New degradative routes of 5-hydroxytryptophan and serotonin by intestinal tryptophan 2,3-dioxygenase**. *Biochem Biophys Res Commun* 1972,**47**(**5**):1112–9.

[67] Zhang Y, Kang S a, Mukherjee T, Bale S, Crane BR, Begley TP, Ealick SE: **Crystal structure and mechanism of tryptophan 2,3-dioxygenase, a heme enzyme involved in tryptophan catabolism and in quinolinate biosynthesis**. *Biochemistry* 2007,**46**(**1**):145–55.

[68] Shimizu T, Nomiyama S, Hirata F, Hayaishi O: **Indoleamine 2,3-dioxygenase. Purification and some properties**. *J Biol Chem* 1978,**253**(**13**):4700–6.

[69] Liu H, Naismith JH: **A simple and efficient expression and purification system using two newly constructed vectors**. *Protein Expr Purif* 2009,**63**(**2**):102–11.

[70] Balzer D, Ziegelin G, Pansegrau W, Kruft V, Lanka E: **KorB protein of promiscuous plasmid RP4 recognizes inverted sequence repetitions in regions essential for conjugative plasmid transfer**. *Nucleic Acids Res* 1992,**20**(**8**):1851–8.

[71] Spektralphotometer N, Kurzanleitung V: **NanoDrop 2000/2000c Spektralphotometer V1.0 Kurzanleitung**. 2000.

[72] Lichty JJ, Malecki JL, Agnew HD, Michelson-Horowitz DJ, Tan S: **Reprint of: Comparison of affinity tags for protein purification**. *Protein Expr Purif* 2011,**41**:98–105.

[73] Andersen KR, Leksa NC, Schwartz TU: **Optimized E. coli expression strain LOBSTR eliminates common contaminants from His-tag purification**. *Proteins* 2013,**81**(**11**):1857–61.

[74] Hoffmann a, Roeder RG: **Purification of his-tagged proteins in non-denaturing conditions suggests a convenient method for protein interaction studies**. *Nucleic Acids Res* 1991,**19**(**22**):6337–8.

[75] Scheich C, Sievert V, Büssow K: **An automated method for high-throughput protein purification applied to a comparison of His-tag and GST-tag affinity chromatography.** *BMC Biotechnol* 2003,**3**:12.

[76] Zhao C, Hellman LM, Zhan X, Bowman WS, Whiteheart SW, Fried MG: **Hexahistidine-tag-specific optical probes for analyses of proteins and their interactions**. *Anal Biochem* 2010,**399**(**2**):237–45.

[77] Ho SN, Hunt HD, Horton RM, Pullen JK, Pease LR: **Site-directed mutagenesis by overlap extension using the polymerase chain reaction**. *Gene* 1989,**77**(**1**):51–9.

APPENDIX

Plasmids

The plasmids were created by using the computer program “PhotoDraw”.

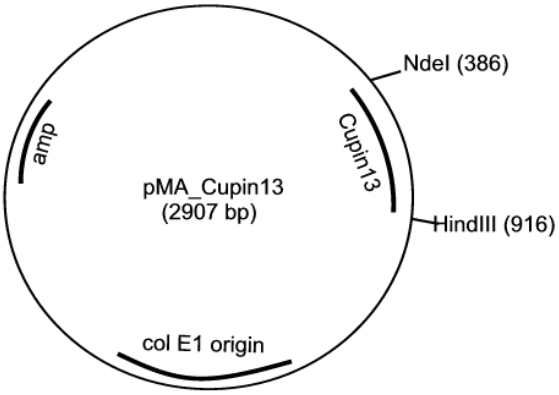

Figure 33: synthetic pMA_Cupin13

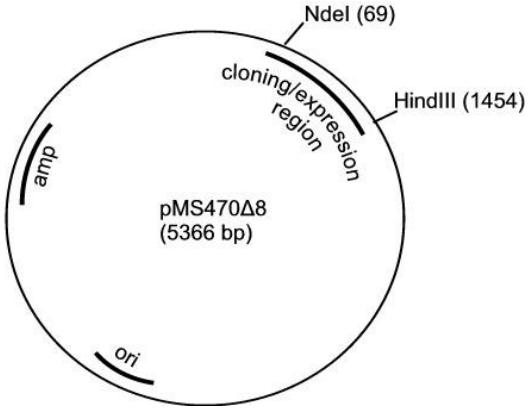

Figure 34: pMS470Δ8

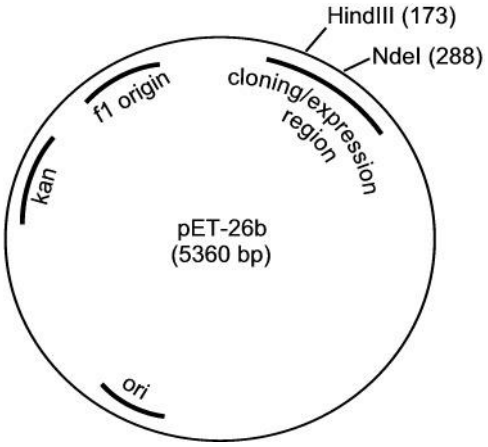

Figure 35: pET26b

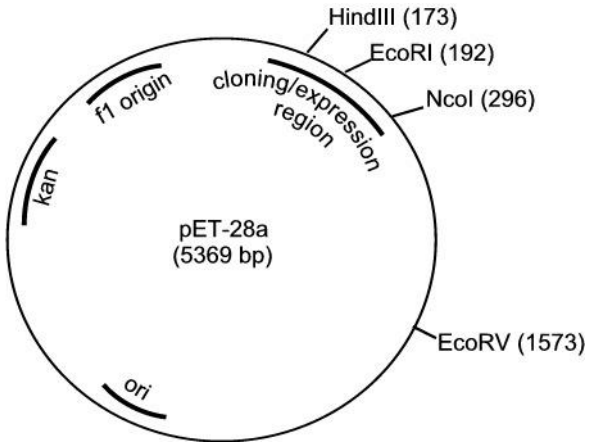

Figure 36: pET28a

Protein sequence of 4-amino-3-hydroxygenzoate 2,3-dioxygenase (4A3HBA23DA)

The protein sequence of 4A3HBA23DA was searched in NCBI (National Center for Biotechnology Information) and the molecular weight was calculated via computer programme ExPASy.

1 miilenfkmp nvdleavmry ltetgkrthq lwmddetlaf vargreyrse fhinasyeiq
61 yslkgaqdlm yrtpegevkv ahmpegsvfy qppflphspr fapdsfqfii ervrkpgeid
121 kfhwfcpncd nfiheetfyv ddyrkdpvsr aydnyfnsle frtckkcgtv apgrd

Amino acid exchange:
H52A, N54A, E58A, H97A, Q60A, Q60F, S62A, S62Q, F101A, F101R, R144I

Number of amino acids:...175
Molecular weight:.....20728.4 Dalton

Extinction coefficients:
Extinction coefficients are in units of M^{-1} cm^{-1}, at 280 nm measured in water.

Ext. coefficient: 26150
Abs 0.1% (=1 g/l) 1.262, assuming all pairs of Cys residues form cystines

Ext. coefficient: 25900
Abs 0.1% (=1 g/l) 1.249, assuming all Cys residues are reduced

---

HISTEV-Cupin13 protein sequence calculated via computer programme ExPASy

ProtParam
User-provided sequence:

```
        10         20         30         40         50         60
MSYYHHHHHH DYDIPTTENL YFQGAMIILE NFKMPNVDLE AVMRYLTETG KRTHQLWMDD

        70         80         90        100        110        120
ETLAFVARGR EYRSEFHINA SYEIQYSLKG AQDLMYRTPE GEVKVAHMPE GSVFYQPPFL

       130        140        150        160        170        180
PHSPRFAPDS FQFIIERVRK PGEIDKFHWF CPNCDNFIHE ETFYVDDYRK DPVSRAYDNY

       190        200
FNSLEFRTCK KCGTVAPGRD
```

The His-tag, TEV cleavage site and 4A3HBA23DA protein sequence are tagged in orange, green and pink.

Number of amino acids:..... 200
Molecular weight:..... 23824.7 Dalton

Extinction coefficients:
Extinction coefficients are in units of M^{-1} cm^{-1}, at 280 nm measured in water.

Ext. coefficient: 32110
Abs 0.1% (=1 g/l) 1.348, assuming all pairs of Cys residues form cystines

Ext. coefficient: 31860
Abs 0.1% (=1 g/l) 1.337, assuming all Cys residues are reduced

The TEV cleavage site: ENLYFQG
Number of amino acids:..... 7
Molecular weight:..... 869.9 Dalton

SBPTEV-Cupin13 protein sequence calculated via computer programme ExPASy

ProtParam
User-provided sequence:

```
        10         20         30         40         50         60
MDEKTTGWRG GHVVEGLAGE LEQLRARLEH HPQGQREPSG GCKLGLGTEN LYFQSMIILE

        70         80         90        100        110        120
NFKMPNVDLE AVMRYLTETG KRTHQLWMDD ETLAFVARGR EYRSEFHINA SYEIQYSLKG

       130        140        150        160        170        180
AQDLMYRTPE GEVKVAHMPE GSVFYQPPFL PHSPRFAPDS FQFIIERVRK PGEIDKFHWF

       190        200        210        220        230
CPNCDNFIHE ETFYVDDYRK DPVSRAYDNY FNSLEFRTCK KCGTVAPGRD
```

The SBP-tag, TEV cleavage site and 4A3HBA23DA protein sequence are tagged in orange, green and pink.

Number of amino acids:..... 230
Molecular weight:..... 26772.1

Extinction coefficients:
Extinction coefficients are in units of M^{-1} cm^{-1}, at 280 nm measured in water.

Ext. coefficient: 33140
Abs 0.1% (=1 g/l) 1.238, assuming all pairs of Cys residues form cystines

Ext. coefficient: 32890
Abs 0.1% (=1 g/l) 1.229, assuming all Cys residues are reduced

The TEV cleavage site: ENLYFQS
Number of amino acids:..... 7
Molecular weight:..... 899.9 Dalton

Different substrates for 4A3HBA23DA

The substrate information's are from the Sigma-Aldrich Company.

Used substrate:

4-Amino-3-hydroxybenzoic acid (4A3HBA)

Chemical formula: ..... $C_7H_7NO_3$

Linear formula: ..... $H_2NC_6H_3(OH)CO_2H$

Molecular weight: ..... 153.14 g/mol

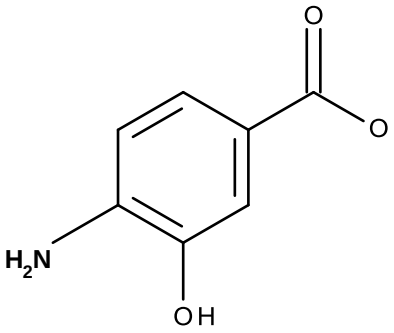

Figure 37: 4-amino-3-hydroxy-benzoic acid
This Figure was drawn by using the program Accelrys Draw 4.1.

Suggested substrates:

4-Amino-3-methoxybenzoic acid

Chemical formula: .... $C_8H_9NO_3$

Linear formula:..... $H_2NC_6H_3(OCH_3)CO_2H$

Molecular weight:..... 167.16 g/mol

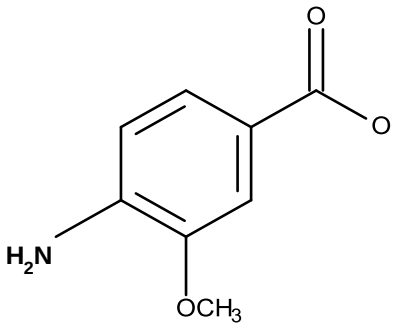

Figure 38: 4-Amino-3-methoxybenzoic acid
This Figure was created by using the program Accelrys Draw 4.1.

3-Hydroxy-4-nitrobenzoic acid

Chemical formula:..... $C_7H_5NO_5$

Linear formula:..... $HOC_6H_3(NO_2)CO_2H$

Molecular weight:..... 183.12 g/mol

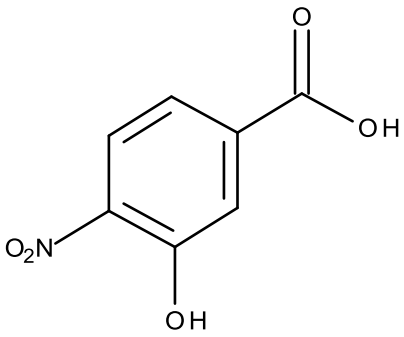

Figure 39: 3-Hydroxy-4-nitrobenzoic acid
This Figure was drawn by using the program Accelrys Draw 4.1.

Alignment of 4A3HBA23DA with different dioxygenases

The results of the BLAST search and protein sequence alignment are from NCBI.

Name:	**3-Hydroxyanthranilate 3,4-dioxygenase [*Dyella ginsengisoli*]**				
Sequence ID:	WP_017461188.1				
Range 1:	30 to 108				
Score	**Expect**	**Method**	**Identities**	**Positives**	**Gaps**
99.0 bits(245)	$2 * 10^{-30}$	Compositional matrix adjust.	50/141 (35 %)	78/141 (55 %)	2/141 (1 %)

```
Query  33   MDDETLAFVARGREYRSEFHINASYEIQYSLKGAQDLMYRTPEGEVKVAHMPEGSVFYQP  92
            +D + +  +  G   R+++H +   E  Y L+G   L  +  +G   +  +  G +FY P
Sbjct  30   VDGDFIVMIVGGPNARTDYHYDEGPEFFYQLEGEMVLKVQDADGPRDIP-IRAGELFYLP  88

Query  93   PFLPHSPRFAPDSFQFIIERVRKPGEIDKFHWFCPNCDNFIHEETFYVDDYRKDPVSRAY  152
            P +PHSP+   DS   +IER R  GE D   WFCPNC++ + EE F ++   +D +   +
Sbjct  89   PRVPHSPQRFADSVGLVIERKRVAGERDGLMWFCPNCNHKLFEEYFVLESIERD-LPPVF  147

Query  153  DNYFNSLEFRTCKKCGTVAPG  173
            D ++ SLE RTC +CGTV P
Sbjct  148  DRFYRSLEARTCSRCGTVHPA  168
```

Name:	**3-Hydroxyanthranilate 3,4-dioxygenase [*Kangiella koreensis* DSM 16069]**				
Sequence ID:	YP_003145568.1				
Range 1:	22 to 176				
Score	**Expect**	**Method**	**Identities**	**Positives**	**Gaps**
92.0 bits(227)	$6 * 10^{-28}$	Compositional matrix adjust.	54/158 (34 %)	83/158 (52 %)	4/158 (2 %)

```
Query  19   RYLTETGKRTHQLWMDDETLAFVARGREYRSEFHINASYEIQYSLKGAQDLMYRTPEGEV  78
            R+L +      Q++  D+ +  V  G   R +FH +   E  Y L+G  +L  RT +
Sbjct  22   RHLLQPPVCNKQVFEQDDFIVMVVGGPNGRRDFHYDEGPEFFYQLEGEMEL--RTIQNGE  79

Query  79   KVAH-MPEGSVFYQPPFLPHSPRFAPDSFQFIIERVRKPGEIDKFHWFCPNCDNFIHEET  137
            +V + +  G +F  PP +PHSP    +S   ++ER R   E D   WFC NCDN ++EE
Sbjct  80   RVDYPIKAGEIFLLPPRVPHSPVRFENSIGLVVERKRLSHEKDGLMWFCENCDNKLYEEY  139

Query  138  FYVDDYRKDPVSRAYDNYFNSLEFRTCKKCGTVAPGRD  175
            F + +  KD +   ++ +  S E RTC KCGTV P ++
Sbjct  140  FQLTNVEKDFLP-VFERFLESEEHRTCDKCGTVMPKQN  176
```

Name:	**3-Hydroxyanthranilate 3,4-dioxygenase [*Achromobacter xylosoxidans* A8]**				
Sequence ID:	YP_003981557.1				
Range 1:	19 to 172				
Score	**Expect**	**Method**	**Identities**	**Positives**	**Gaps**
85.5 bits(210)	$2 * 10^{-25}$	Compositional matrix adjust.	47/156 (30 %)	77/156 (49 %)	3/156 (1 %)

```
Query  20   YLTETGKRTHQLWMDDETLAFVARGREYRSEFHINASYEIQYSLKGAQDLMYRTPEGEVK  79
            +L +      Q+W D + +  V  G  +R+++H +   E  Y L+G   L      +G+ +
Sbjct  19   HLLKPPVGNQQIWQDADFIVTVVGGPNHRTDYHDDPLEEFFYQLRGNAWLSLWV-DGKPE  77

Query  80   VAHMPEGSVFYQPPFLPHSP-RFAPDSFQFIIERVRKPGEIDKFHWFCPNCDNFIHEETF  138
               + EG +F   PP + HSP R   DS   +IER R  G +D F W+CP C + +H
Sbjct  78   RVDLKEGDIFLLPPHVRHSPQRPETDSACLVIERQRPQGLLDGFEWYCPQCGSLVHRVEV  137

Query  139  YVDDYRKDPVSRAYDNYFNSLEFRTCKKCGTVAPGR  174
             +     D +   +  +++S E RTC  CG + PG+
Sbjct  138  QLKSIVTD-LPPLFQAFYSSTEKRTCPGCGEIHPGK  172
```

Name:	3-Hydroxyanthranilate 3,4-dioxygenase [*Cupriavidus basilensis*]				
Sequence ID:	WP_006162384.1				
Range 1:	12 to 172				
Score	Expect	Method	Identities	Positives	Gaps
86.3 bits(212)	$9 * 10^{-26}$	Compositional matrix adjust.	53/165 (32 %)	78/165 (47 %)	13/165 (7 %)

```
Query  19   RYLTETGKR------THQLWMDDETLAFVARGREYRSEFHINASYEIQYSLKGAQ--DLM  70
            R+L E   R        Q+W D +T+  V  G   R++FH +   E  Y  KG    ++M
Sbjct  12   RWLDEHAHRLKPPVGNQQIWQDADTIVTVVGGPNQRTDFHDDPLEEFFYQFKGNAWLNIM  71

Query  71   YRTPEGEVKVAHMPEGSVFYQPPFLPHSP-RFAPDSFQFIIERVRKPGEIDKFHWFCPNC  129
             R   G+ +   + EG +F  P  + HSP R   DS   +IER R  G +D F WFCP C
Sbjct  72   DR---GKRERVDLREGDIFLLPAHVRHSPQRPEADSRCLVIERQRPAGMVDGFEWFCPAC  128

Query  130  DNFIHEETFYVDDYRKDPVSRAYDNYFNSLEFRTCKKCGTVAPGR  174
              +H     +     D +   +  ++++   R C +CGTV PGR
Sbjct  129  SALVHRVEVQLKSIVTD-LPPLFAGFYDNAALRRCGQCGTVHPGR  172
```

Input of CLUSTAL Omega:

>BAD08206.1 (4-Amino-3-hydroxybenzoate 2,3-dioxygenase [*Bordetella* sp. 10d])
MIILENFKMPNVDLEAVMRYLTETGKRTHQLWMDDETLAFVARGREYRSEFHINASYEIQYSLK
GAQDLMYRTPEGEVKVAHMPEGSVFYQPPFLPHSPRFAPDSFQFIIERVRKPGEIDKFHWFCPN
CDNFIHEETFYVDDYRKDPVSRAYDNYFNSLEFRTCKKCGTVAPGRD

>WP_017461188.1 (3-Hydroxyanthranilate 3,4-dioxygenase [*Dyella ginsengisoli*])
MSLLPPINLQRWIDEHRHLLRPPVGNKCIVDGDFIVMIVGGPNARTDYHYDEGPEFFYQLEGEM
VLKVQDADGPRDIPIRAGELFYLPPRVPHSPQRFADSVGLVIERKRVAGERDGLMWFCPNCNHK
LFEEYFVLESIERDLPPVFDRFYRSLEARTCSRCGTVHPAPTTDAD

>YP_003145568.1 (3-Hydroxyanthranilate 3,4-dioxygenase [*Kangiella koreensis DSM 16069*])
MSEKTLTPVPPFNFQKWIDENRHLLQPPVCNKQVFEQDDFIVMVVGGPNGRRDFHYDEGPEFFY
QLEGEMELRTIQNGERVDYPIKAGEIFLLPPRVPHSPVRFENSIGLVVERKRLSHEKDGLMWFC
ENCDNKLYEEYFQLTNVEKDFLPVFERFLESEEHRTCDKCGTVMPKQNKLDL

>YP_003981557.1 (3-Hydroxyanthranilate 3,4-dioxygenase [*Achromobacter xylosoxidans* A8])
MPAYGPPLNFQRWIDDHAHLLKPPVGNQQIWQDADFIVTVVGGPNHRTDYHDDPLEEFFYQLRG
NAWLSLWVDGKPERVDLKEGDIFLLPPHVRHSPQRPETDSACLVIERQRPQGLLDGFEWYCPQC
GSLVHRVEVQLKSIVTDLPPLFQAFYSSTEKRTCPGCGEIHPGKGHAPAAQA
APA

>WP_006162384.1 (3-Hydroxyanthranilate 3,4-dioxygenase [*Cupriavidus basilensis*])
MFTYGMPLNFPRWLDEHAHRLKPPVGNQQIWQDADTIVTVVGGPNQRTDFHDDPLEEFFYQFKG
NAWLNIMDRGKRERVDLREGDIFLLPAHVRHSPQRPEADSRCLVIERQRPAGMVDGFEWFCPAC
SALVHRVEVQLKSIVTDLPPLFAGFYDNAALRRCGQCGTVHPGRAVAPASKD
PK